BAYESIAN MODELLING OF INTEGRATED DATA AND ITS APPLICATION TO SEABIRD POPULATIONS

Toby J. Reynolds

A Thesis Submitted for the Degree of PhD
at the
University of St. Andrews

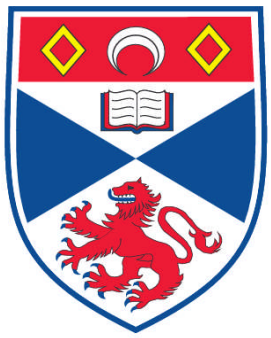

2010

Bayesian Modelling of Integrated Data and its Application to Seabird Populations

Toby J. Reynolds

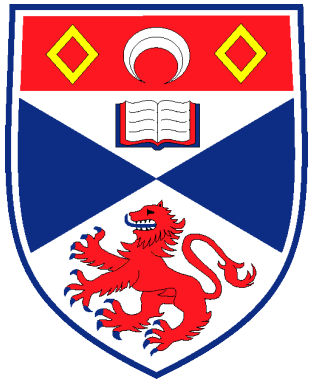

Thesis submitted for the degree of
Doctor of Philosophy
in the School of Mathematics and Statistics
University of St Andrews

June 2010

Declaration

I, Toby John Reynolds, hereby certify that this thesis, which is approximately 48,000 words in length, has been written by me, that it is the record of work carried out by me and that it has not been submitted in any previous application for a higher degree.

I was admitted as a research student in October 2005 and as a candidate for the degree of Doctor of Philosophy in Statistics in October 2006; the higher study for which this is a record was carried out in the University of St Andrews between 2005 and 2009.

date: _____ signature of candidate: _____

I hereby certify that the candidate has fulfilled the conditions of the Resolution and Regulations appropriate for the degree of Doctor of Philosophy in Statistics in the University of St Andrews and that the candidate is qualified to submit this thesis in application for that degree.

date: _____ signature of supervisor: _____

In submitting this thesis to the University of St Andrews we understand that we are giving permission for it to be made available for use in accordance with the regulations of the University Library for the time being in force, subject to any copyright vested in the work not being affected thereby. We also understand that the title and the abstract will be published, and that a copy of the work may be made and supplied to any bona fide library or research worker, that my thesis will be electronically accessible for personal or research use unless exempt by award of an embargo as requested below, and that the library has the right to migrate my thesis into new electronic forms as required to ensure continued access to the thesis. We have obtained any third-party copyright permissions that may be required in order to allow such access and migration, or have requested the appropriate embargo below.

The following is an agreed request by candidate and supervisor regarding the electronic publication of this thesis:

Access to Printed copy and electronic publication of thesis through the University of St Andrews.

date: _____ signature of candidate: _____

date: _____ signature of supervisor: _____

Abstract

Integrated data analyses are becoming increasingly popular in studies of wild animal populations where two or more separate sources of data contain information about common parameters. Here we develop an integrated population model using abundance and demographic data from a study of common guillemots *Uria aalge* on the Isle of May, southeast Scotland. A state-space model for the count data is supplemented by three demographic time series (productivity and two mark-recapture-recovery (MRR)), enabling the estimation of prebreeder emigration rate—a parameter for which there is no direct observational data, and which is unidentifiable in the separate analysis of MRR data. A Bayesian approach using MCMC provides a flexible and powerful analysis framework.

This model is extended to provide predictions of future population trajectories. Adopting random effects models for the survival and productivity parameters, we implement the MCMC algorithm to obtain a posterior sample of the underlying process means and variances (and population sizes) within the study period. Given this sample, we predict future demographic parameters, which in turn allows us to predict future population sizes and obtain the corresponding posterior distribution. Under the assumption that recent, unfavourable conditions persist in the future, we obtain a posterior probability of 70% that there is a population decline of $> 25\%$ over a 10-year period.

Lastly, using MRR data we test for spatial, temporal and age-related correlations in guillemot survival among three widely separated Scottish colonies that have varying overlap in nonbreeding distribution. We show that survival is highly correlated over time for colonies/age classes sharing wintering areas, and essentially uncorrelated for those with separate wintering areas. These results strongly suggest that one or more aspects of winter environment are responsible for spatiotemporal variation in survival of British guillemots, and provide insight into the factors driving multi-population dynamics of the species.

Acknowledgements

First and foremost, I gratefully acknowledge the input of my 'panel' of supervisors and collaborators, without whom this thesis would not have been possible. My primary supervisor, Ruth King, provided superb support and guidance throughout, devoting countless hours to meetings, answering queries, editing and proof-reading my writing, and generally attempting to make me into a good Bayesian. John Harwood helped to cast light on my findings and provide new avenues for investigation with his tremendous all round knowledge. Last, but by no means least, Morten Frederiksen, Mike Harris and Sarah Wanless of the Centre for Ecology and Hydrology conceived the project, provided the all-important Isle of May data, gave invaluable biological input, and were instrumental in keeping the project moving in new and interesting directions.

My research benefitted greatly from discussions with many other excellent scientists, including Takis Besbeas, Vanessa Cave, Stephen Freeman, Catriona Harris, Jason Matthiopoulos, Rachel McCrea, Rob Robinson and Sophie Smout, to name but a few. I also recognise the input of an associate editor for *JABES* and two anonymous referees, whose valuable comments on a submitted paper improved the content of Chapter 3. The entire thesis was meticulously scrutinised by my two examiners, Len Thomas and Stephen Baillie, and their thoughtful insights resulted in a number of beneficial changes and additions to the manuscript. I gratefully acknowledge their contribution and thank them for their time.

I thank the many people who collected field data on guillemots over the years, making this study possible. Scottish Natural Heritage permitted studies on the Isle of May National Nature Reserve and made the recent annual counts of guillemots. The fieldwork was funded in part by the Natural Environment Research Council and the Joint Nature Conservation Committee's integrated Seabird Monitoring Programme. Mark Newell kindly gave me the opportunity to spend several weeks on the Isle of May, to observe and carry out fieldwork first-hand. I thank the British Trust for Ornithology for supplying ring-recovery

data. The BTO Ringing Scheme is funded by a partnership of the British Trust for Ornithology, the Joint Nature Conservation Committee (on behalf of Natural England, Scottish Natural Heritage and the Countryside Council for Wales, and also on behalf of the Environment and Heritage Service in Northern Ireland), The National Parks and Wildlife Service (Ireland) and the ringers themselves. The Canna and Colonsay data used in Chapter 5 were provided by Bob Swann and David Jardine, respectively, who also contributed some thoughts and discussion towards this chapter.

I acknowledge generous funding from the National Centre for Statistical Ecology through an EPSRC Mathematics Interdisciplinary Critical Mass Award.

Finally, special thanks must go to Sally, who shared with me my PhD highs and helped me through my lows.

Contents

List of Figures

List of Tables

Chapter 1

Introduction

1.1 Justification

How and why populations change over time are two of the central questions in population ecology (Turchin 2003). The 'how' concerns the quantification of changes in population size in terms of the key demographic parameters of productivity, survival and movement. The 'why' attempts to identify the factors driving changes in these primary population processes. Knowledge of population ecology can help us understand why some populations are decreasing rapidly while others are increasing and expanding their range; why some species' populations cycle or crash and others do not; and whether changes in demographic rates and/or population size are related to intrinsic factors (e.g. density dependence), extrinsic factors (e.g. weather variables, habitat changes), or both.

In this time of dramatic losses of global biodiversity and ever greater demands placed on wild living resources by an increasing human population, such knowledge is essential for conservation biologists, wildlife managers, and resource biologists alike (Rockwood 2006). Therefore, as King et al. (2009) note, 'it is clearly a very important time for the study of population ecology, for the precise estimation of demographic rates, and application of the best methods for statistical inference and forecasting'. Two important recent advances that help to fulfil these criteria are the development of integrated population modelling, and the growth of Bayesian methods for statistical ecology. These topics are the focus of this thesis.

In this introductory chapter, we give a brief overview of some of the models encountered in population ecology, along with the essentials of Bayesian inference, before applying the methods to real data in the remainder of the thesis.

1.2 Models for population data

Long-term monitoring schemes for wildlife populations may generate numerous types of data, each containing information on different aspects of the population, for example its size, survival rates, productivity parameters, movement rates, measurements of the size/weight of individuals, behavioural observations, etc. In this section, we provide a brief introduction to some of the data types encountered in the remainder of the thesis, including discussion of the associated models that are typically fitted to these data. We note here that all the modelling approaches used in the thesis are based on a discrete time-scale with yearly intervals, which is highly appropriate for annually reproducing organisms in a seasonal environment, such as seabirds.

1.2.1 Modelling survival

Survival is an important driver of population growth rate (Heppell et al. 2000, Sæther & Bakke 2000, Oli & Dobson 2003), and is thus a key parameter of population dynamics models. Estimates of survival are most commonly obtained using mark-recapture and/or ring-recovery data, known collectively as mark-recapture-recovery (MRR) data. We first outline separately the two types of data and their associated models, before considering how they may analysed simultaneously.

Mark-recapture data

The collection of mark-recapture data for survival estimation begins with marking a sample of animals using unique individual marks—these are commonly either man-made marks such as rings or tags, or natural physical features of the animal such as pelage colouration or fin shape—and these 'marked' animals may then be identified at subsequent recapture occasions. Identification may be through physical recapture or, if the mark is identifiable from a distance, through resighting; however, due to the nature of wild animals, it is rare for them to be seen on every occasion. It is also typical for there to be additional releases of newly-marked animals at each occasion. This process results in a unique capture history for each animal, consisting of a series of ones and zeros indicating whether that individual was caught or not caught, respectively, at each recapture occasion; see Section 2.3.2 for an example capture history and further explanation.

Modelling the recapture process requires two sets of parameters: survival

rates, commonly denoted by ϕ, give the probability of survival for an individual from one capture occasion to the next, and recapture probabilities, denoted p, give the probability that an individual, alive during a particular capture occasion, is recaptured or resighted at that time (Lebreton et al. 1992). With these parameters, the probability of the various possible capture histories can be calculated and the likelihood formed as the product of the probabilities associated with each capture history, conditional on first release, resulting in a product-multinomial likelihood (see King et al. 2009, section 2.3.2). It is important to note that the survival parameter ϕ estimated using mark-recapture data is actually a product of two biologically interpretable parameters: the probability of surviving between capture occasions, and the probability of remaining in the study area (fidelity). Because these two parameters are confounded, ϕ essentially represents 'apparent survival' (Burnham 1993). We return to this issue below.

The standard model for analysing mark-recapture data is the Cormack-Jolly-Seber (CJS) model (Cormack 1964, Jolly 1965, Seber 1965), which considers time-dependent survival and recapture rates, denoted ϕ_t and p_t, respectively. Reduced forms of the CJS model exist, allowing ϕ, p, or both, to be constant over time (Lebreton et al. 1992). These models are often too simplistic to realistically capture biological processes, and thus a number of extensions have been proposed over the years. Lebreton et al. (1992) considered modelling of survival and capture rates as functions of time, age, environmental covariates and categorical variables characterising the individuals (e.g. gender, location), as well as accounting for previous capture history effects (e.g. trap dependence). Individual fixed covariates (e.g. size or weight at birth) can also be handled (e.g. Skalski et al. 1993), and more recent developments allow for the modelling of time-varying individual covariates (Bonner & Schwarz 2004, King et al. 2006, 2008a). Random effects can be introduced to allow for additional variability not accounted for by any of the covariates (King et al. 2009) and may provide a parsimonious compromise between constant and completely time-dependent models (Royle & Link 2002). Data from several populations can be analysed simultaneously to gain further insight into spatiotemporal patterns of variation in survival (e.g. Harris et al. 2005, Schaub et al. 2005, Grosbois et al. 2006). Numerous other approaches and applications are discussed in reviews by Schwarz & Seber (1999) and Grosbois et al. (2008), for example. A comprehensive coverage of the topic is provided by Williams et al. (2002, chapter 17), and King et al. (2009) give many up-to-date examples featuring use of the latest methodology.

Ring-recovery data

The structure of ring-recovery data is very similar to that of mark-recapture data, as are the statistical methods involved. The major difference is that, instead of animals being recaptured/resighted on multiple recapture occasions, they may only be recorded once (after initial capture and marking) and that is upon their death. Thus, instead of a recapture probability we have a recovery probability, commonly denoted by λ, which is the combined probability that a dead animal is found and has its mark reported. The full likelihood is again the product of separate multinomial likelihoods, one for each cohort of marked animals (see King et al. 2009, section 2.3.1).

A classic reference for recovery data is Brownie et al. (1985), in which the basic modelling framework is summarised, including models to allow for dependence of survival and recovery on time, age, sex and geographic area. Many of the same extensions applied to mark-recapture data are possible, for example the effects of covariates (Catchpole et al. 1999), and the inclusion of random effects (Royle & Link 2002, Barry et al. 2003). See Schwarz & Seber (1999) and Williams et al. (2002, chapter 16) for further details and alternative models.

Combining mark-recapture and ring-recovery data

Many studies generate both live recaptures and ring recoveries for the same individuals, and in such cases it is natural to consider a fusion of the two modelling approaches. Burnham (1993) developed a theory for the combined analysis of 'mark-recapture-recovery' data for the time-dependent case and showed that this enables the separate estimation of survival and fidelity, which are confounded in the standard mark-recapture model. Catchpole et al. (1998) generalised this approach to allow both age- and time-dependence of the model parameters, and showed that it allows more realistic models to be fitted and increases precision of parameter estimates compared with separate analyses. Further details, including Catchpole et al.'s efficient form for the likelihood and the associated sufficient statistics required, are provided in Sections 3.2.2 and 3.2.3.

1.2.2 State-space models for abundance data

Abundance data, or count data, come in many forms, from complete national censuses to site-specific indices of abundance. These estimates of abundance are rarely without error, and state-space models provide a means to account for this 'observation error' separately to the noise in the underlying demographic

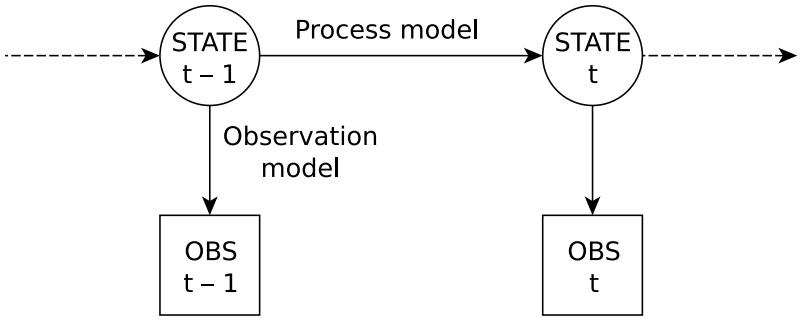

Figure 1.1 Schematic diagram of a state-space model. The process model describes the evolution of the true but unknown state of the population over time, which may involve intermediate subprocesses. The observations are connected to the states by an observation model.

process, or 'process uncertainty' (e.g. Newman 1998, Millar & Meyer 2000, de Valpine & Hastings 2002, Buckland et al. 2004, Jamieson & Brooks 2004). They thereby provide a framework for linking observations on the size of a wildlife population to a population dynamics model.

In essence, a state-space model describes the evolution of two time series running in parallel, referred to as the observations and the states: for count data, the observations correspond to estimates of population size, whereas the state(s) correspond to the true, underlying number of animals in one or more age/size classes, regions, etc. These time series are linked by an observation model, while the population dynamics model, or process model, describes the transition of the underlying states between consecutive time points (Figure 1.1). It is possible in the state-space approach to obtain estimates of the number of individuals in each state without having observed them all directly (Thomas et al. 2005).

The process model may be parameterised by, for example, growth rates and density dependence structures (e.g. Jamieson & Brooks 2004), or birth, survival and movement rates (e.g. Buckland et al. 2004). The state-space framework readily incorporates additional information relating to these population processes: this may be in the form of prior distributions in a Bayesian analysis, reflecting expert opinion (Thomas et al. 2005) or the results of previous analyses (Harrison et al. 2006); alternatively, additional datasets may be incorporated, to be analysed simultaneously in an integrated population model.

1.2.3 Integrated population modelling

Abundance and demographic data are often collected on the same population of animals, and the integration of these data within a single, consistent framework has been the focus of a number of recent studies (e.g. Besbeas et al. 2002, Brooks

et al. 2004, Schaub et al. 2007, Borysiewicz et al. 2008). This methodology is termed 'integrated population modelling' and it underlies much of the work in this thesis. The backbone of the approach is a state-space model describing the population counts, and additional likelihoods for other datasets may be simply 'bolted on'; more formally, assuming independence between datasets, a joint likelihood may be formed by multiplying the likelihood resulting from the count data and the likelihoods for the demographic data. (In cases where the separate likelihoods are not independent, it may be possible to split the data into two (or more) subsets that are independent and use each one to derive a different likelihood; see Cave et al. 2009.)

By combining data from different sources, we obtain more robust (and self-consistent) parameter estimates that fully reflect the information available (King et al. 2009). The approach also has great potential for estimating parameters that were not originally monitored in the field and cannot be estimated from the individual data alone. These are termed 'hidden' parameters by Tavecchia et al. (2009), and an example is the estimation of productivity using abundance and ring-recovery data (Besbeas et al. 2002). Integrated population modelling may be especially relevant in conservation biology, where the available data for a particular species of concern are often sparse or incomplete. Here, the improved population estimates and demographic rates from an integrated population model may be crucial for assessing a species' endangered status and devising conservation actions (Schaub et al. 2007, Véran & Lebreton 2008).

Previous studies have considered the integration of abundance data with various types of demographic data, including ring-recoveries (Besbeas et al. 2002, Brooks et al. 2004, Besbeas & Freeman 2006), mark-recaptures (Goodman 2004, Schaub et al. 2007), mark-recapture and productivity data (Gauthier et al. 2007) and multi-site mark-recapture-recovery data (Borysiewicz et al. 2008). But in theory it is possible to combine and analyse simultaneously any two (or more) sources of data containing information about the same parameters.

1.3 Bayesian inference

The use of Bayesian techniques for the statistical analysis of ecological data has become increasingly common in recent years, with a wide variety of applications especially in population and community ecology (Wade 2000, Ellison 2004, Royle & Dorazio 2008, King et al. 2009, Link & Barker 2009). There are a number of reasons for this, not least that the Bayesian approach pro-

vides 'a far more powerful and flexible framework for the analysis of complex stochastic processes than the corresponding [classical approach]' (King et al. 2009). We leave discussion of the differences between Bayesian and classical statistical inference, along with their respective advantages and disadvantages for population data analysis, to later chapters, and we also refer the reader to the references given above (also Ellison 1996) for more detailed comparisons. In the following sections, we provide a brief overview of some of the important concepts in Bayesian inference that are relevant to the material in this thesis.

1.3.1 Bayes' Theorem

Bayesian inference is based upon what is known as Bayes' Theorem: a simple mathematical formula used for calculating conditional probabilities, first proposed by the Rev. Thomas Bayes (Bayes 1763). Suppose we have a set of parameters $\boldsymbol{\theta} = \{\theta_1, \ldots, \theta_m\}$ on which we wish to make inference. We then observe data $\boldsymbol{x} = \{x_1, \ldots, x_n\}$ from some known probability density function $f(\boldsymbol{x}|\boldsymbol{\theta})$, which determines the probability of observing different data under different parameter values. Then, by Bayes' Theorem, the (joint) posterior distribution for $\boldsymbol{\theta}$ is given by

$$\pi(\boldsymbol{\theta}|\boldsymbol{x}) = \frac{f(\boldsymbol{x}|\boldsymbol{\theta})p(\boldsymbol{\theta})}{f(\boldsymbol{x})}. \tag{1.1}$$

Here the term $p(\boldsymbol{\theta})$ is referred to as the prior distribution and $\pi(\boldsymbol{\theta}|\boldsymbol{x})$ the posterior distribution: the prior represents the initial beliefs about the parameters prior to observing any data; the posterior represents an update of these beliefs, following the data $\boldsymbol{x}$ being observed. The denominator $f(\boldsymbol{x})$ is independent of the parameters $\boldsymbol{\theta}$, being a function only of the observed data, and is simply equal to some constant; it is typically omitted from the calculation, and Bayes' Theorem is more often quoted in the form

$$\pi(\boldsymbol{\theta}|\boldsymbol{x}) \propto f(\boldsymbol{x}|\boldsymbol{\theta})p(\boldsymbol{\theta}). \tag{1.2}$$

The resulting posterior distribution is multi-dimensional and often complex, but in most cases we are interested in the marginal posterior distributions of individual parameters. For example, suppose we are only interested in θ_1, then

$$\pi(\theta_1|\boldsymbol{x}) = \int \pi(\boldsymbol{\theta}|\boldsymbol{x}) d\theta_2, \ldots, d\theta_m. \tag{1.3}$$

Alternatively, we might be interested in summary inferences such as point estimates and uncertainty intervals, which, as Gimenez et al. (2008) note, are often

more interpretable (see King et al. 2009, section 4.4, for an overview of different ways to summarise the posterior). The integrals involved in calculating marginal distributions or summary statistics are typically too complex to calculate analytically. However, the Markov chain Monte Carlo (MCMC) algorithm provides an alternative approach, whereby we sample from the posterior and obtain sample estimates of the quantaties of interest (Brooks 1998). Before we present details of the MCMC algorithm, we first discuss the issue of prior specification.

1.3.2 Prior distributions

As noted above, the prior distribution represents an analyst's beliefs about the parameter values before observing any data. In ecological applications, the prior is a useful means of incorporating expert opinion or information from previous studies, particularly in situations where the data are sparse and inference on certain parameters would otherwise be impossible (King et al. 2009). Conversely, the subjectivity involved in specifying priors is one of the criticisms that Bayesian methods often face (Dennis 1996). In general throughout this thesis we have highly detailed data and little useful prior information. Therefore, to 'let the data speak for themselves' we specify vague, or noninformative, prior distributions that essentially contain little or no information about the parameters (Gelman et al. 2003).

A uniform prior is the obvious choice for a completely flat prior density that assigns equal probability to all possible parameter values. This prior is well suited to probability parameters—as found in many applications in population ecology (e.g. survival rates, recapture probabilities, etc.)—because there are predefined bounds on the parameter space (i.e., they are contained in the interval [0,1]). However, when no bounds are imposed the uniform prior is an improper distribution, which can lead to an improper posterior and, in turn, the possible non-existence of a posterior mean (King et al. 2009). Another problem with specifying a flat prior arises under reparameterisations of the model, because a density that is flat or uniform in one parameterisation will not be in another (Gelman et al. 2003). For example, when considering logistic regression on probability parameters, placing a flat or noninformative prior on the logit-scale regression parameters induces a far from flat prior on the back-transformed probabilities (see King & Brooks 2008, with further clarification in King et al. 2009). A further difficulty with the use of vague priors, though not applicable to this thesis, is highlighted by Link & Barker (2006) in the context of multimodel inference and model selection: they note that Bayes factors (a

statistic used to compare competing models) are unstable in the presence of noninformative priors for model parameters, especially when there are varying numbers of parameters in the different models under consideration. Link and Barker's suggested approach to deal with this sensitivity, in the context of model selection for logistic regression, is to partition an estimated total prior variance of regression coefficients, thus fixing the total prior uncertainty in the linear predictor.

Some models require specifying a prior on the variance parameter of a normal distribution, two examples encountered in this thesis being the observation error for a state-space model and the variance of random effects models. A noninformative prior that has commonly been used for normal variance parameters is the inverse-gamma distribution, which in this case is a conjugate prior, that is, it is from the same distributional family as the posterior. Although not necessary in modern Bayesian analyses, conjugate priors can have advantages in terms of improving efficiency of computational algorithms (King et al. 2009). However, Gelman (2006) showed that the inverse-gamma distribution may not be suitable as a prior for variance parameters in hierarchical models (multilevel, or nested, models in which the prior parameters are themselves given prior distributions, called hyperpriors): he found that, when the variance is small, posterior inference is very sensitive to the choice of prior parameters. Instead, Gelman recommends the use of a noninformative uniform prior density, or a distribution from the half-t family, such as the half-Cauchy distribution, specified on the standard deviation parameter.

Regardless of the choice of prior distribution, its influence on the posterior should always be checked via a prior sensitivity analysis, even in the case of informative priors. See King et al. (2009), section 4.3, for details and examples; Millar (2004) describes a useful automated method for assessing sensitivity to informative priors. Given the priors specified on the parameters, we can write down the posterior distribution up to proportionality. Direct inference is typically not possible, but we can use MCMC to sample from the posterior.

1.3.3 Markov chain Monte Carlo

Recall that the derivation of marginal distributions or calculation of posterior summary statistics often involves complex, multi-dimensional integrals. However, instead of trying to integrate the joint posterior distribution analytically, we can employ simulation procedures to obtain samples from the posterior. One such procedure is Markov chain Monte Carlo (MCMC).

MCMC methods perform Monte Carlo integration using a Markov chain to generate observations from the posterior, π. Essentially, a Markov chain is constructed whose stationary distribution is the posterior distribution. If we run the chain for long enough until it has converged to the stationary distribution, subsequent simulated values can be treated as a sample from π and used to obtain empirical (Monte Carlo) estimates of posterior summary statistics of interest (see, e.g., Brooks 1998 for further details). Constructing a Markov chain requires an updating scheme in order to move from one state of the chain to the next, and there are a number of different approaches to achieve this. One is the Gibbs sampler (Casella & George 1992), which is often highly efficient but requires knowing the posterior conditional distribution of each parameter and being able to sample from this distribution directly. An alternative, more general updating scheme, and the one used exclusively in this work, is the Metropolis-Hastings algorithm (Chib & Greenberg 1995).

Metropolis-Hastings algorithm (single-update)

The Metropolis-Hastings algorithm is an extension of the Metropolis algorithm introduced by Metropolis et al. (1953), adapted and generalised by Hastings (1970) to focus on statistical problems. It is a form of generalised rejection sampler. The method begins with a density for generating candidate observations (the proposal distribution), which typically depends on the current state of the chain and, for single-update Metropolis-Hastings, is different for each parameter. Suppose that the Markov chain is currently at $\boldsymbol{\theta}^t = \{\theta_1^t, \ldots, \theta_m^t\}$, having been initialised with some starting parameter values $\boldsymbol{\theta}^0 = \{\theta_1^0, \ldots, \theta_m^0\}$ and updated through $\boldsymbol{\theta}^1, \ldots, \boldsymbol{\theta}^t$. Then at iteration $t+1$, a candidate value for θ_j^{t+1} $(1 \leqslant j \leqslant m)$, denoted ϕ_j, is generated from the proposal distribution $q_j(\phi_j|\theta_j^t)$.

The second step is to accept or reject the candidate value ϕ_j. Defining $\boldsymbol{\phi}_j = \{\theta_1^{t+1}, \ldots, \theta_{j-1}^{t+1}, \phi_j, \theta_{j+1}^t, \ldots, \theta_m^t\}$ and $\boldsymbol{\theta}_j^t = \{\theta_1^{t+1}, \ldots, \theta_{j-1}^{t+1}, \theta_j^t, \theta_{j+1}^t, \ldots, \theta_m^t\}$, we accept the candidate observation with probability $\alpha(\theta_j^t, \phi_j)$, given by

$$\alpha(\theta_j^t, \phi_j) = \min\left(1, \frac{\pi(\boldsymbol{\phi}_j|\boldsymbol{x})q_j(\theta_j^t|\phi_j)}{\pi(\boldsymbol{\theta}_j^t|\boldsymbol{x})q_j(\phi_j|\theta_j^t)}\right). \tag{1.4}$$

To actually implement this, we generate a $\mathrm{U}(0,1)$ random variable, U, and if $U < \alpha(\theta_j^t, \phi_j)$ we accept the proposed move and set $\theta_j^{t+1} = \phi_j$; otherwise we set $\theta_j^{t+1} = \theta_j^t$ (i.e., we reject the proposed move and the parameter remains at its current value).

We then move on and propose to update θ_{j+1}^{t+1}, and so on. Once all m parameters in $\boldsymbol{\theta}^t$ have been updated, the transition from $\boldsymbol{\theta}^t$ to $\boldsymbol{\theta}^{t+1}$ is complete and we move on to the next iteration, $t+2$.

Random walk updates

Where the proposal distribution for a parameter is centred around the current value, this is known as a random walk, and when the candidate generating function is symmetric (i.e., $q_j(\phi_j|\theta_j^t) = q_j(\theta_j^t|\phi_j)$, as for the uniform, normal or t-distribution), the acceptance probability reduces to

$$\alpha(\theta_j^t, \phi_j) = \min\left(1, \frac{\pi(\boldsymbol{\phi}_j|\boldsymbol{x})}{\pi(\boldsymbol{\theta}_j^t|\boldsymbol{x})}\right). \tag{1.5}$$

In the analyses contained herein, we use a Metropolis-Hastings random walk algorithm with uniform proposal density. In particular, suppose we are interested in updating a parameter θ^t, then we propose a new value ϕ such that $\phi \sim \mathrm{U}(\theta^t - \delta, \theta^t + \delta)$. Values for δ are tuned to achieve reasonable acceptance rates of 20–40% for proposed moves (Gelman et al. 1996).

Convergence/run length

Two practical considerations when determining how many MCMC iterations to run are (1) the time required for convergence, and (2) the post-convergence sample size required for suitably small Monte Carlo errors (King et al. 2009).

We are only interested in observations taken from the Markov chain once it has converged to the stationary distribution. Therefore, we discard observations within an initial transient phase, or burn-in period. There are a variety of methods for determining a suitable length for the burn-in, ranging from simply looking at MCMC trace plots (plots of iterations versus sampled values for each variable in the chain), to elaborate methods including eigenvalue estimation techniques and diagnostics based on analysis of variance (see Brooks 1998, King et al. 2009, and references therein). Within this thesis we use the Brooks-Gelman-Rubin (BGR) statistic, $\widehat{R}_{\text{interval}}$ (Brooks & Gelman 1998). The basic idea is to run multiple chains, initiated from overdispersed starting points, and assess convergence by comparing within- and between-chain variability over the second half of those chains. The width of the 80% credible interval for the parameter of interest is taken as the measure of variability, and $\widehat{R}_{\text{interval}}$ is

calculated as the ratio of pooled to average interval widths, i.e.,

$$\widehat{R}_{\text{interval}} = \frac{\text{width of 80\% credible interval of all chains combined}}{\text{average width of 80\% credible intervals of individual chains}}.$$

This tends to 1.0 as convergence is approached; for practical purposes convergence may be assumed when $\widehat{R}_{\text{interval}} < 1.05$ (Spiegelhalter et al. 2007), although generally it is preferable to use a more conservative burn-in if possible (King et al. 2009).

After the burn-in period, we need to take enough samples from the posterior to allow reliable inference to be made, but within the constraints of time and computational storage limits. Again, there are a number of formal techniques to determine how long the simulations need to be run (see Brooks 1998). In practice, it is common to run the chain for 2–10 times the burn-in length, and an adequate number of samples may generally be assumed if posterior summary statistics from multiple runs of the chain are identical to 2 or 3 significant figures, depending on the level of accuracy required.

1.3.4 Bayesian state-space model

We now consider the application of Bayesian methods to the fitting of state-space models. We are typically interested in obtaining estimates of the parameters within the process model (e.g. survival and productivity rates) and the observation error variance. The true underlying population sizes are essentially nuisance parameters which we wish to integrate out to form only the likelihood of the model parameters—although we are often interested in the population estimates as well—but this integration is impossible to do analytically. Classical analyses of state-space models typically employ numerical techniques such as the Kalman filter (Kalman 1960; see also Besbeas et al. 2002) to obtain estimates. However, use of the standard Kalman filter relies on assumptions of linearity and normality of the observation and process models, which in practice are often violated (King et al. 2009; but see Besbeas et al. 2008). It may be possible to use normal approximations to discrete distributions, for example for binomial or poisson models (e.g. Besbeas et al. 2002), but this approach will not be valid for small sample sizes (Brooks et al. 2004). Furthermore, while the Kalman filter can be extended to cope with non-normal or nonlinear models, it can be prohibitively complex to apply in these situations (Jamieson & Brooks 2004, King et al. 2009) and only provides approximate answers.

From the Bayesian perspective, we treat the true underlying population

sizes as auxiliary variables and form the joint posterior distribution over both the parameters and unknown population sizes. We can then use MCMC to sample from the posterior distribution, whereby we update the parameters and the auxiliary variables at each iteration of the MCMC algorithm and thus obtain marginal posterior distributions for both. It is then straightforward to obtain estimates of the true population sizes in the form of marginal posterior means or medians. It is equally simple to calculate error bands, in the form of posterior credible intervals, whereas this can be difficult or time consuming in the classical paradigm (Brooks et al. 2004). Further mathematical and implementational details of the Bayesian approach are provided for specific applications in later chapters (see, in particular, Sections 2.2.2 and 2.2.3), and see also King et al. (2009) for some additional, more general information.

1.4 Application: common guillemots in the UK

The UK is host to internationally important numbers of breeding seabirds—including around 12% of the world common guillemot *Uria aalge* population (Harris & Wanless 2004)—making them an important component of the nation's biodiversity. Furthermore, the position of seabirds at the top of the marine food chain makes them useful indicators of both the state of the marine environment and the effects of human activities upon it (Parsons et al. 2008). Thus, there is an incentive to collect and analyse data on seabird populations, both to assess their conservation status, and to monitor aspects of the health of the wider marine environment. In this thesis we focus on the integrated analysis of data collected on several UK populations of common guillemot. Our primary aim is the integration of multiple sources of data from a single colony, but we also consider how this may be beneficially combined with similar data from other populations.

1.4.1 Guillemot biology

The common guillemot (hereafter guillemot) is a medium-sized marine bird of the auk (Alcidae) family. The guillemot is one of the most abundant seabirds in temperate and colder parts of the northorn hemisphere, with very large populations in the Atlantic, Pacific and Arctic Oceans (Harris & Wanless 2004). It is primarily a pelagic species, but during the breeding season (April–September) birds return to land, forming large, dense colonies on coastal cliffs and rocky offshore islands. At this time they are highly visible and accessible, making

monitoring and data collection relatively straightforward and inexpensive compared to some terrestrial mammals, for example. Adult guillemots are highly territorial and site-faithful, returning to the same small area of cliff ledge year upon year (Harris et al. 1996b)—a characteristic that makes them particularly suitable for long-term, individual-based studies such as mark-recapture. Young guillemots also have a tendency to return to their natal areas during their pre-breeding years and many subsequently recruit nearby (Harris et al. 1996a), although a proportion of birds are known to recruit to other colonies (Halley & Harris 1993).

The guillemot is a typical 'K-selected' species (MacArthur & Wilson 1967), its life history being characterised by a long lifespan (expected 24 years: Robinson 2005), low reproductive rate (maximum clutch size 1 egg: Robinson 2005) and delayed maturity (median age of first breeding 5–7 years: Harris et al. 1994). Consequently, guillemots have low annual recruitment rates so populations tend to change slowly over time. In common with other species at the 'slow' end of the life-history continuum (Sæther & Bakke 2000), adult survival has a high contribution to the population growth rate.

1.4.2 Status and trends

The guillemot is Britain and Ireland's most abundant breeding seabird with one million pairs estimated in the Seabird 2000 census, the main concentrations of these being in the north and west (Harris & Wanless 2004). The total population increased substantially between 1969–70 and 1998–2002, although the rate of increase slowed from 4–5% per annum during the 1970s and '80s, to 2% during the 1990s (Harris & Wanless 2004). More recently, the population has levelled off or even started to decline (2% decline 2000–2008: JNCC 2009).

A greater cause for concern has been the recent decline in breeding performance of many UK seabird populations—the common guillemot included—which has made national headlines and featured prominently in high-profile publications (e.g. Eaton et al. 2005, 2007). Guillemot productivity in 2004 was by far the worst on record for many colonies in the North Sea and Northern Isles, with no chicks fledged at all from the large colony on Fair Isle (Mavor et al. 2005). In 2005 there was some improvement, although productivity was still markedly below the long-term mean and breeding failures were observed for the first time along the west coast of Scotland (Swann 2005, Mavor et al. 2006). The trend continued in 2006, with low levels of breeding success recorded throughout Britain: guillemots on Handa (northwest Scotland) experienced al-

most complete breeding failure, and record lows were observed at colonies as far apart as the Isle of May (southeast Scotland) and Skomer (Wales) (Mavor et al. 2008). Further decreases in mean UK guillemot productivity were recorded in 2007 and 2008 (JNCC 2009). Overall, annual productivity in guillemots declined by nearly 50% during the period 1989–2007, with most of that fall occurring since 2002 (Eaton et al. 2009).

The main reason for the poor breeding success appears to have been low availability and poor quality of the guillemot's main prey species, especially the lesser sandeel *Ammodytes marinus* (Mavor et al. 2005, Wanless et al. 2005); this, in turn, is thought to be linked through complex mechanisms to climate change (MCCIP 2009). Sea surface temperatures in UK coastal waters have been rising since the early 1980s by around 0.2–0.9°C per decade (Holliday et al. 2008), and warmer sea temperature has been correlated with poorer than average sandeel recruitment (Arnott & Ruxton 2002). This is presumed to be the mechanism linking high winter sea surface temperature to poor breeding success (and survival) in another seabird species, the black-legged kittiwake *Rissa tridactyla*, during the last two decades (Frederiksen et al. 2004b). Until recently the guillemot appears to have been largely buffered against these changes, possibly because it dives and thus may gain access to a wider variety of prey than surface feeders such as kittiwakes. The fact that guillemot breeding success is also now being affected thus points towards more severe food shortages in 2004 and subsequent years (Mavor et al. 2005).

Due to the low annual recruitment rate of most seabirds, even dramatic changes in productivity may take a number of years to manifest themselves as changes in population growth rates (Eaton et al. 2007). Changes in adult survival, on the other hand, have a more direct and immediate effect on breeding population size, and because population growth of long-lived species is most sensitive to variation in adult survival (Lebreton & Clobert 1991, Sæther & Bakke 2000) even small reductions can have large effects on population trends. A strong negative relationship has been identified between autumn sea surface temperature in the North Sea and adult survival of common guillemots from the colony of Hornøya, northern Norway, which are known to winter in the North Sea (Sandvik et al. 2005). Although no such relationship has yet been found among any UK guillemot populations, predictions from climate change scenarios of further increases in sea surface temperature (Lowe et al. 2009) must inevitably raise serious concerns about the future of common guillemots and other UK seabird populations.

1.4.3 Data collection

The Joint Nature Conservation Committee (JNCC)'s Seabird Monitoring Programme coordinates seabird monitoring on a UK-wide basis (Mavor et al. 2006). Under the Seabird Monitoring Programme, a variety of species have been routinely assessed for breeding numbers and breeding success at a representative sample of UK colonies since 1986. More intensive, individual-based monitoring schemes, providing information on survival rates, for example, have been conducted at a few geographically dispersed 'key sites': Isle of May (southeast Scotland), Fair Isle (Shetland), Canna (west Scotland), Colonsay (west Scotland), and Skomer (Wales). It is these detailed data that we are interested in here.

The Isle of May long-term study (IMLOTS; Centre for Ecology and Hydrology 2009) has provided a particularly rich dataset for common guillemots, including: annual counts, productivity estimates, mark-recapture and ring-recovery time series, data on chick diet and growth rates, laying dates, colony attendance patterns, etc. As a result this colony has been extensively studied (see, for example, references above and in later chapters), but most analyses have focused on a single aspect of guillemot biology and, until now, no attempts have been made to integrate the different data sources and model the complex dynamics of the population.

1.5 Thesis aims and outline

The theme of this thesis is the Bayesian analysis of integrated data, with particular application to seabird populations. The primary focus is the combined analysis, using an integrated population model, of several long-term datasets relating to the Isle of May guillemot colony. A general outline of the thesis is as follows.

In Chapter 2 we set the scene for the more advanced models to follow in later chapters by introducing the four key Isle of May guillemot datasets that describe the dynamics of the colony, namely, count data, two mark-recapture time series (from birds ringed as chicks and birds ringed as adults), and productivity data. Each dataset is presented separately, with corresponding preliminary model structures and Bayesian analyses.

The four sources of Isle of May guillemot data described in Chapter 2 contain information on common parameters. Therefore, to obtain full advantage from the data it is worthwhile to perform an integrated data analysis, in which

data from all sources are analysed simultaneously within a single, consistent framework. This approach pools the information on shared parameters to provide more robust parameter estimates that fully reflect all available information, and may permit the estimation of additional parameters that would be unidentifiable in a separate analysis. An integrated analysis of the Isle of May data is the focus of Chapter 3, in which the strength of the combined abundance and demographic data is utilised to gain a greater understanding of guillemot population dynamics.

The severe declines in demographic performance of many UK seabirds in recent years has heightened the need for models that can reliably predict population dynamics, including proper quantification of uncertainty and the ability to incorporate various modelling assumptions. Such models will form an essential part of the planning of effective conservation or management strategies. In Chapter 4, we use the integrated population model developed in Chapter 3 as a basis for predicting 10-year future population trajectories of the Isle of May guillemot colony under a range of assumptions about future demographic rates. The Bayesian approach provides probability distributions of future population sizes, which are easy to understand and communicate, provide clear indication of uncertainty, and can be queried for any number of relevant statistics.

Studies of wild populations often attempt to explain variation in survival using environmental covariates, but no suitable variables have previously been identified for the Isle of May guillemots; therefore, we do not try to incorporate covariates in the analyses of Chapters 2, 3 and 4. To at least gain some insight into the spatial scale(s) over which the drivers of variability in UK guillemot survival operate, in Chapter 5 we extend the Isle of May mark-recapture-recovery analysis to incorporate data from two west coast Scottish colonies. We look for spatial, temporal and age-related correlations in survival among the three colonies, and assess whether any pairwise correlations are associated with the degree of overlap in nonbreeding distribution. The consequences of spatiotemporal variation in survival for multi-population dynamics are discussed in the context of possible future climate change.

We finish with a general discussion in Chapter 6, in which we draw together the material presented in the thesis and suggest some potential directions for future research.

Chapter 2

Isle of May guillemot data and preliminary models

2.1 Overview

Located in the outer Firth of Forth, southeast Scotland, the Isle of May (56°11′N, 2°33′W) is one of the most important seabird breeding colonies on the British North Sea coast, with approximately 250,000 seabirds attending the island each year (Scottish Natural Heritage 2006). The Centre for Ecology & Hydrology has been carrying out research on the Isle of May's seabirds since 1973, monitoring many aspects of the biology of five key species, both to assess the status of their breeding populations, and to monitor the state of the marine environment. The Isle of May long-term study (IMLOTS; Centre for Ecology and Hydrology 2009) is currently the most data-rich and comprehensive study of its type in Europe.

In this thesis, we focus mainly on data collected on the Isle of May common guillemot *Uria aalge* population—although many of the analyses are also applicable to other seabird species—and particularly on several key datasets that provide information relevant to guillemot population dynamics. These data are: (1) abundance data in the form of annual colony counts (in latter years these have been made by Scottish Natural Heritage staff); (2) mark-recapture data from birds ringed as breeding adults; (3) mark-recapture and ring-recovery data from birds ringed as chicks; and (4) productivity data in the form of annual records of breeding success. In later chapters we consider combining these data to develop an integrated population model, and compare them with data from other UK colonies, but here we simply focus on introducing the individual Isle of May datasets, along with preliminary modelling approaches and corresponding Bayesian analyses.

In Section 2.2 we present an analysis of the count data. A state-space approach is used to model the underlying population dynamics generated by the counts alone, or additionally by point estimates of demographic rates derived independently from productivity and mark-recapture data. A combined analysis of the adult and chick mark-recapture data is described in Section 2.3, in which we attempt to explain the discrepancy in adult survival rates obtained from separate analyses of these two datasets. In Section 2.4 we present a Bayesian analysis of the productivity data, and we finish with some brief conclusions in Section 2.5.

2.2 Count data

2.2.1 Introduction

Abundance data are generally relatively easy to collect—particularly compared to detailed, individual-based demographic data—and are, therefore, often the only information available for a particular population of interest. However, abundance data provide relatively little information on the underlying demographic rates. Sometimes there may also be available estimates of demographic parameters, but no access to the raw data from which they were obtained. Here, we attempt to model the dynamics of the Isle of May guillemot colony without using the raw demographic data, that is, based only on the abundance data, or additionally on point estimates of the demographic parameters.

2.2.2 Data and model

We have abundance and demographic data from the Isle of May spanning 22 years, from 1983 to 2004, which we denote by $t = 1, \ldots, T$. The abundance data, hereafter referred to as count data, are annual estimates of the number of breeding pairs, derived from field counts of full-grown birds present in the colony during the first ten days of June. The field counts included one or two adults per breeding pair, plus a variable number of failed breeders (that continue to visit the colony), nonbreeders and prebreeders. Few guillemots occur outside the visible area and these were ignored. Each complete count took several days, so immediately before or after each partial count, which took approximately 3 hours, a count was made of guillemots present in smaller parts of the colony with a known number of breeding pairs (Harris 1989). This time-specific correction factor was used to correct the partial colony count to the

Table 2.1 Count data (N_t), productivity rates (ρ_t), and prebreeder ($\phi_{j,t}$) and adult ($\phi_{a,t}$) survival estimates for the Isle of May guillemot population from 1983 to 2004 ($t = 1, \ldots, T$). Corresponding estimates of combined female productivity–survival to adulthood are also provided ($\phi_{\rho,t} = \rho_t \phi_{j,t}/2$).

t	N_t	ρ_t	$\phi_{j,t}$	$\phi_{\rho,t}$	$\phi_{a,t}$
1	14750	0.771	0.313	0.121	0.957
2	13000	0.691	0.243	0.084	0.940
3	13000	0.825	0.366	0.151	0.936
4	13700	0.808	0.524	0.212	0.994
5	11680	0.795	0.167	0.066	0.931
6	11223	0.851	0.346	0.147	0.966
7	12736	0.849	0.215	0.091	0.965
8	12632	0.804	0.204	0.082	0.923
9	11440	0.832	0.497	0.207	0.955
10	11511	0.843	0.578	0.244	0.975
11	12418	0.769	0.437	0.168	0.947
12	13843	0.780	0.473	0.184	0.952
13	15326	0.802	0.323	0.130	0.920
14	14500	0.830	0.473	0.196	0.964
15	17152	0.783	0.455	0.178	0.944
16	17384	0.741	0.409	0.152	0.917
17	16933	0.668	0.350	0.117	0.956
18	17979	0.743	0.220	0.082	0.928
19	18442	0.638	–	–	0.936
20	20185	0.698	–	–	0.922
21	19162	0.702	–	–	0.942
22	19833	0.510	–	–	–
Mean	14947	0.761	0.366	0.145	0.942
SD	2938	0.083	0.123	0.052	0.027

Note: Data/estimates provided by M. Frederiksen; see text for further details.

number of pairs, and the corrected partial counts were then summed to give an annual estimate of the total breeding population. For simplicity, we focus on the number of breeding females, which we denote by N_t for $t = 1, \ldots, T$ (these are provided in Table 2.1).

The demographic data used in this analysis are time-specific estimates of breeding success and prebreeder and adult survival probabilities, denoted by ρ_t, $\phi_{j,t}$ and $\phi_{a,t}$, respectively (also provided in Table 2.1). These data were provided by M. Frederiksen as estimates with associated sample sizes (breeding success) or standard errors (survival rates). Breeding success, hereafter productivity, is defined as the mean number of chicks fledged per breeding pair; estimates for $t = 1, \ldots, T$ were derived from intensive monitoring of breeding guillemots in several study plots on the Isle of May (see Section 2.4 for further methodological details). Survival probabilities were estimated from mark-recapture data using

Program MARK (see Section 2.3 for a Bayesian analysis of these data using similar model structures). Prebreeder survival was derived from a dataset of chicks colour-ringed just prior to fledging, and is defined here as the probability of a bird fledged at time t surviving to time $t+4$ (i.e., the probability of surviving the first four years of life). From age 4 onwards, guillemots are assumed to have reached adulthood and survive with annual survival rate $\phi_{a,t}$, defined as the probability of an adult bird, alive at time t, surviving to time $t+1$; estimates of adult survival were derived from a separate dataset of birds ringed as breeders of unknown age. Estimates of $\phi_{a,t}$ are available for $t = 1, \ldots, T-1$, and estimates of $\phi_{j,t}$ for $t = 1, \ldots, T-4$ only.

The counts, N_t, are only estimates of the true population size and are therefore subject to error, both in the raw data collection process and in the subsequent estimation of the number of breeding pairs. This observation error is in addition to the noise in the underlying demographic process (de Valpine & Hastings 2002). To fit a model to the count data that simultaneously includes both types of noise, we consider a state-space approach (e.g. Newman 1998, Millar & Meyer 2000, de Valpine & Hastings 2002, Buckland et al. 2004, Jamieson & Brooks 2004, King et al. 2008b), which models observation error and process uncertainty separately so that the demographic model is fitted to the true underlying population sizes.

The observation model relates the observed annual counts to the true (but unknown) underlying population sizes. We assume that

$$N_t \sim \mathrm{N}(X_t, \sigma_N^2), \tag{2.1}$$

where X_t denotes the true underlying number of breeding females in year t and σ_N^2 is the observation error variance.

The process model describes changes in the true population size over time and represents the underlying biological system. For the adult population, we assume that the number of breeding females in year t is derived from the number surviving from year $t-1$, plus the number of new females recruiting into the breeding population. Although we assume guillemots reach adulthood at age 4, few ($\sim 5\%$) start breeding at this age on the Isle of May, and most start breeding at ages 5–7 years (Harris et al. 1994). For simplicity, we assume here that all birds recruit at age 5; thus, a simple model for the underlying number of breeding females is

$$X_t \sim \mathrm{Bin}(X_{t-1} + J_{t-5}, \phi_{a,t-1}), \tag{2.2}$$

where J_t denotes the number of female prebreeders that are fledged in year t and survive to age 4. A female guillemot lays a single egg per year (except that it may replace this if lost); therefore, each breeding pair can produce only a single chick per year. Assuming all adults breed every year, a similar model for the number of female prebreeders is

$$J_t \sim \text{Bin}(X_t, \rho_t \phi_{j,t}/2). \tag{2.3}$$

The term of 1/2 corresponds to the probability of a chick being female.

For notational convenience, we let $\phi_{\rho,t} = \rho_t \phi_{j,t}/2$ (the probability that a breeding attempt results in a female chick that survives to adulthood) and we define $\boldsymbol{\phi_\rho} = \{\phi_{\rho,t} : t = 1, \ldots, T-4\}$, with similar notation and appropriate time intervals for $\boldsymbol{\phi_a}$, $\boldsymbol{N}$, $\boldsymbol{J}$ and $\boldsymbol{X}$. The approximate likelihood for the observation model is then given by

$$L_{obs}(\boldsymbol{N} \mid \boldsymbol{X}, \sigma_N^2) = \prod_{t=6}^{T} \left[\frac{1}{\sqrt{2\pi\sigma_N^2}} \exp\left(-\frac{(N_t - X_t)^2}{2\sigma_N^2} \right) \right]. \tag{2.4}$$

Similarly, the approximate likelihood for the process model is

$$\begin{aligned} L_{sys}(\boldsymbol{J}, \boldsymbol{X} \mid \boldsymbol{\phi_\rho}, \boldsymbol{\phi_a}) = & \prod_{t=1}^{T-4} \binom{X_t}{J_t} (\phi_{\rho,t})^{J_t} (1 - \phi_{\rho,t})^{X_t - J_t} \\ & \times \prod_{t=6}^{T} \left[\binom{X_{t-1} + J_{t-5}}{X_t} (\phi_{a,t-1})^{X_t} (1 - \phi_{a,t-1})^{X_{t-1} + J_{t-5} - X_t} \right], \end{aligned} \tag{2.5}$$

and the joint likelihood for the count data is given by

$$L_N(\boldsymbol{N}, \boldsymbol{J}, \boldsymbol{X} \mid \boldsymbol{\phi_\rho}, \boldsymbol{\phi_a}, \sigma_N^2) = L_{obs}(\boldsymbol{N} \mid \boldsymbol{X}, \sigma_N^2)\ L_{sys}(\boldsymbol{J}, \boldsymbol{X} \mid \boldsymbol{\phi_\rho}, \boldsymbol{\phi_a}). \tag{2.6}$$

Note that t starts at 6 in both the observation likelihood (equation (2.4)) and adult breeder portion of the process likelihood (line 2 of equation (2.5)): these run in parallel, and because $X_1, \ldots, X_5$ depend on $J_{-4}, \ldots, J_0$ (i.e., birds hatched before the study began) they do not feature in either likelihood. Instead, we place priors on these initial population sizes (see Section 2.2.3). The portion of the process likelihood relating to prebreeders (line 1 of equation (2.5)) ends at $T - 4$ because estimates of $\phi_{\rho,t}$ are not available after this time.

We consider fitting three models to the count data, denoted M1, M2 and M3, which vary by their use of the available productivity and survival estimates.

These models are described in turn below.

M1 Constant ϕ_ρ and ϕ_a

In M1 we use only the count data, so productivity and survival are parameters to be estimated. Clearly, there are not enough data points to estimate time-specific rates for ρ_t, $\phi_{j,t}$ and $\phi_{a,t}$, so we assume them to take the constant values ρ, ϕ_j and ϕ_a. Furthermore, the parameters ρ and ϕ_j only appear in the process model as a product (see equation (2.3)) and are thus confounded; therefore, we estimate the combined productivity–survival parameter ϕ_ρ, as defined above.

M2 Time-specific $\phi_{\rho,t}$, constant ϕ_a

A model with constant productivity and survival is not very realistic because the only possible outcomes are exponential growth or exponential decline. In addition, there is a large amount of year-to-year variability in the Isle of May demographic data, particularly prebreeder survival (see Table 2.1). To incorporate this variability, in M2 we fix $\phi_{\rho,t}$ to the values provided in Table 2.1, but keep ϕ_a as a constant parameter to be estimated.

M3 Time-specific $\phi_{\rho,t}$ and $\phi_{a,t}$

In M3 we incorporate the time-specific estimates of both $\phi_{\rho,t}$ and $\phi_{a,t}$, so that the only thing the model has to estimate is the initial age structure of the population, to see if this completely explains the year-to-year variability in the counts.

2.2.3 Bayesian analysis

We undertake a Bayesian analysis of the data, in which the joint probability distribution for the count data is combined with prior distributions (where applicable) for the model parameters to obtain a posterior distribution for the parameters. A Bayesian approach avoids reliance on the assumptions of normality and linearity inherent to the classical approach (Millar & Meyer 2000, Jamieson & Brooks 2004) and provides a more flexible framework for obtaining parameter estimates than the Kalman filter (see, e.g., Besbeas et al. 2002). In addition, Bayesian methods provide a framework for using valuable prior information we may have about the model parameters (Hilborn & Mangel 1997).

Priors

In this analysis, we assume that we have no prior information; therefore, we specify vague priors containing essentially no information about the parameters. For the demographic parameters ϕ_ρ and ϕ_a, where estimated, we take Beta$(1,1)$ priors (equivalent to a U$(0,1)$ distribution) which restrict these probability parameters to lie within the limits of zero and one. For the observation error variance, we take the commonly used noninformative inverse-gamma prior $\sigma_N^2 \sim \Gamma^{-1}(10^{-3}, 10^{-3})$, which has a point mass at zero but is otherwise essentially uniform, particularly for high values such as we expect for σ_N^2.

Because of the way the process model is constructed, we also need to specify priors on the initial population levels $X_1, \ldots, X_5$, which depend on prebreeders fledged in years $t = -4, \ldots, 0$ (see equation (2.2)), about which we have no information. We make use of the observed counts $N_1, \ldots, N_5$ as prior information with the normal prior $X_t \sim \mathrm{N}(N_t, \sigma_N^2)$, where σ_N^2 is the estimated observation error variance. This choice of prior reflects our belief that the initial population levels should be related to the counts in the same way as those in the observation model (equation (2.1)).

Posterior distribution

The model depends on the demographic parameters ϕ_ρ and ϕ_a, and observation error variance σ_N^2—which we combine for notational convenience into the single parameter vector $\boldsymbol{\theta}$—and the underlying population levels $\boldsymbol{J}$ and $\boldsymbol{X}$. These are all values to be estimated using our observed data $\boldsymbol{N}$. Using Bayes' Theorem, the posterior distribution is given by

$$\pi(\boldsymbol{J}, \boldsymbol{X}, \boldsymbol{\theta} \mid \boldsymbol{N}) \propto L_N(\boldsymbol{N}, \boldsymbol{J}, \boldsymbol{X} \mid \boldsymbol{\theta})\, p(\boldsymbol{\theta}), \tag{2.7}$$

where $p(\boldsymbol{\theta})$ denotes the prior distribution for the parameters. We fit the model using Markov chain Monte Carlo (MCMC; Brooks 1998) with Metropolis-Hastings sampling to obtain a sample from π, which we use to obtain posterior summary statistics (e.g. means, standard deviations, 95% credible intervals) for the parameters and population sizes. For each model M1–M3, the MCMC algorithm was run for 10 million iterations, with the first 5 million discarded as burn-in and the remaining output thinned to every thousandth iteration to save storage space. Simulations were implemented in Fortran and took approximately 5 hours on a 1.8 GHz personal computer. We initially tried to use the specialist Bayesian analysis software WinBUGS (Spiegelhalter et al. 2007), and

then wrote our own code in [R] (R Development Core Team 2008), but in both cases found that computational efficiency was poor, requiring unfeasibly long running times to calculate the necessary number of iterations (e.g. $\sim$60 hours for 100,000 iterations in WinBUGS!). Thus, while Fortran programs generally take longer to write, the pay-off can be significant, particularly when many runs need to be performed, for example when checking convergence or prior sensitivity. Further advantages of writing bespoke code to implement MCMC algorithms are discussed by Brooks et al. (2004) and include the option to select and tune the MCMC proposals, and the ability to extend the code to incorporate reversible jump MCMC updates to allow for Bayesian model discrimination (though note that limited reversible jump MCMC may be achieved in WinBUGS by installing the Jump extension; see Gimenez et al. 2008).

Convergence issues

Three independent MCMC chains with overdispersed starting points were run for each model to check convergence. Standard convergence diagnostics and plots (the Brooks-Gelman-Rubin (BGR) statistic $\widehat{R}_{\text{interval}}$, with $\alpha = 0.2$; Brooks & Gelman 1998, Spiegelhalter et al. 2007) suggested rapid convergence for M2 and M3, so run lengths and burn-in periods were very conservative. However, M1 had failed to converge by the end of the burn-in period (e.g. $\widehat{R}_{\text{interval}}$ of 1.25 and 1.21 for ϕ_ρ and ϕ_a, respectively; convergence if $\widehat{R}_{\text{interval}} < 1.05$), and posterior inference varied drastically between runs. MCMC trace plots of the individual parameters indicated very slow mixing of the chain, despite reasonable acceptance rates, and they also highlighted a significant amount of codependence between ϕ_ρ and ϕ_a (see Section 2.2.4 for plots and summary statistics).

2.2.4 Results

Posterior means and 95% symmetric credible intervals (CIs) for the true underlying population sizes $\boldsymbol{J}$ and $\boldsymbol{X}$ for each of the three models are provided in Figure 2.1, and corresponding parameter estimates in Table 2.2. M1 provided a remarkably good fit to the data (Figure 2.1a), considering the constant productivity and survival rates, although this was largely facilitated by the relatively constant population growth indicated by the counts during the majority of the study period. Estimates of demographic rates ϕ_ρ and ϕ_a under M1 are provided in Table 2.2, separately for each of the three independent runs of the MCMC chain, denoted M1a, M1b and M1c. Run M1a was initiated using realistic parameter values and population sizes, based on means of the provided demo-

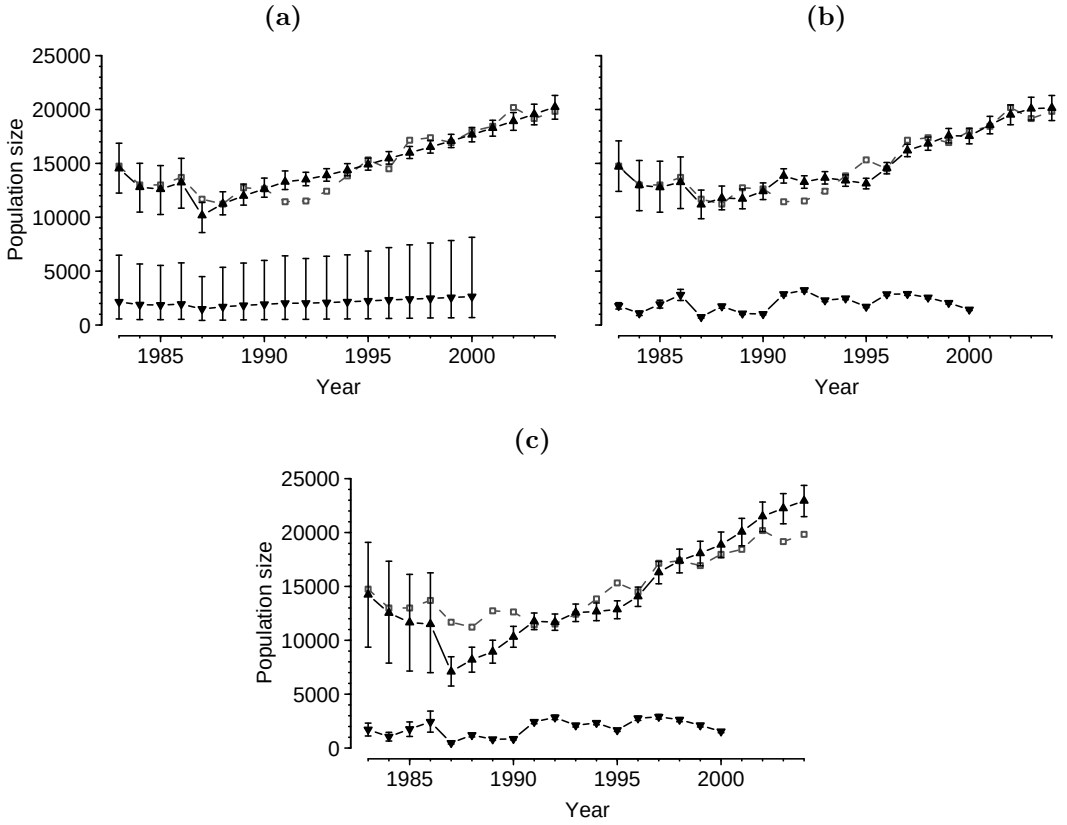

Figure 2.1 Posterior means and corresponding 95% symmetric CIs for the true underlying population levels of female prebreeders $\boldsymbol{J}$ (▼) and breeding females $\boldsymbol{X}$ (▲) over time under models M1 (run M1a) (a), M2 (b) and M3 (c). The Isle of May counts $\boldsymbol{N}$ (□) are plotted for comparison.

graphic estimates and the count data. Resulting parameter estimates (posterior means) were similar to the Isle of May time series means; however, posterior standard deviations were large, particularly for ϕ_ρ, and this is reflected in the huge CIs on the prebreeder population sizes (see Figure 2.1a). Runs M1b and M1c were initiated from overdispersed starting points (e.g. 0.99 and 0.01 for ϕ_ρ and ϕ_a, respectively, for M1b, and vice versa for M1c), and resulting posterior inference was significantly different, although in both cases the breeding adult population sizes were very similar to those estimated under M1a.

Table 2.2 Posterior means (SDs) for the parameters in M1 (a–c: three independent runs from different starting points), M2 and M3. Means (SDs) of the supplied time series of parameter estimates (Data) are included for comparison.

Parameter	Data	M1a	M1b	M1c	M2	M3
ϕ_ρ	0.15 (0.05)	0.15 (0.12)	0.41 (0.39)	0.29 (0.31)	–	–
ϕ_a	0.94 (0.03)	0.92 (0.07)	0.81 (0.19)	0.86 (0.15)	0.91 (0.004)	–
σ^2_N ($\times 10^6$)	–	1.35 (0.60)	1.65 (0.91)	1.55 (0.79)	1.47 (0.60)	5.98 (0.23)

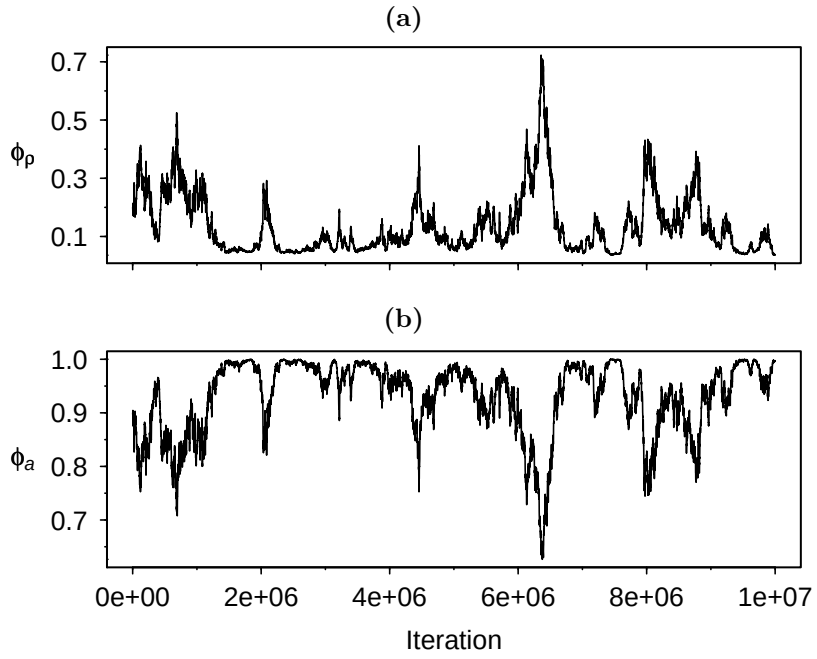

Figure 2.2 MCMC sample paths for ϕ_ρ (a) and ϕ_a (b), taken from run M1a and thinned to every 1000th iteration. Note the strong symmetry between the plots, indicating high codependence between these parameters.

MCMC trace plots for ϕ_ρ and ϕ_a are provided from run M1a in Figure 2.2 and clearly display very poor mixing of the chain and possible nonconvergence to the stationary distribution, even after the full 10 million iterations (a much longer burn-in would be needed before we could be certain about convergence). The plots also highlight very high codependence between the two survival parameters (when ϕ_ρ was high, ϕ_a was low, and vice versa; Spearman's rank correlation: $r_s = -0.995$).

The effect of incorporating the time-specific estimates of $\phi_{\rho,t}$ in M2 is clearly demonstrated in the pattern of variability in the prebreeder population sizes J_t and, with a 5-year time lag, in the adult population sizes X_{t+5} (Figure 2.1b). This model also provided a good fit to the count data, although the year-to-year fluctuations in the underlying adult population estimates do not precisely match those in the counts. To achieve this fit, constant adult survival was estimated to be lower than the Isle of May time series mean and with a very high degree of precision (see Table 2.2).

M3 also incorporated the time-specific estimates of $\phi_{a,t}$, to see if these helped to explain the variability in the counts. Together, the two time series of demographic estimates appear to have generated an expected population growth rate somewhat higher than that observed (Figure 2.1c). Note also the much larger observation error variance than either M1 or M2 (Table 2.2), which is probably

a consequence of the poor fit rather than a genuine reflection of the observation error.

2.2.5 Discussion

The analysis of count data alone provides very little information about the underlying demographic rates, as demonstrated by model M1. First, due to there being only a single data value per year, it was only possible to obtain constant estimates of the demographic rates. Second, productivity and prebreeder survival were confounded in our process model, so that it was only possible to estimate their product ϕ_ρ. Finally, there was too little information to even obtain reliable estimates of ϕ_ρ and adult survival ϕ_a: an increasing population, as indicated by the counts, could equally be the result of high productivity and prebreeder survival, or high adult survival, or moderate increases in both of the above rates. Nevertheless, it does not appear that these rates were completely confounded; in fact, the parameter trace plots (Figure 2.2) suggest that there was little overlap in their respective posteriors (assuming convergence), so there does appear to be some information in the count data to estimate the two parameters separately. However, there was still a problem of high codependence observed among the MCMC samples of ϕ_ρ and ϕ_a under M1, which in turn necessitated very narrow Metropolis-Hastings proposals, leading to slow mixing and possible lack of convergence after 10 million iterations of the MCMC chain. One possible solution to this last problem is to use block updates to update highly correlated parameters simultaneously (see, e.g., King et al. 2009, section 5.4.4).

Adding some rigidity to the model in M2 by fixing $\phi_{\rho,t}$ to the time-specific estimates significantly improved mixing and convergence, and constrained adult survival to a very narrow range of possibilities. However, to achieve the best fit to the count data, ϕ_a was estimated to be somewhat lower than the Isle of May time series mean (0.91 compared to 0.94, representing approximately a 50% increase in mortality). Furthermore, fixing both $\phi_{\rho,t}$ and $\phi_{a,t}$ to the time-specific estimates in M3 resulted in a very poor fit to the counts by producing an expected population growth rate considerably higher than the observed growth rate. These two results point towards an inconsistency between the count data and the estimates of survival derived from mark-recapture analyses; more specifically, they suggest that factors other than productivity and survival influence the dynamics of the Isle of May guillemot colony, for example, migration into or out of the system.

Halley & Harris (1993) showed that intercolony movement of prebreeding Isle of May guillemots does occur, and that birds may recruit to colonies other than their natal colony. Immigration would typically be inferred if survival rates from mark-recapture data predicted a population growth rate lower than that observed, or if survival estimated using count data was higher than the mark-recapture estimates. We found the opposite for the Isle of May data, suggesting substantial net emigration of prebreeders to recruit at other colonies. But emigration is essentially included in the survival estimates, because in the analysis of mark-recapture data death and permanent emigration are inseparable, both contributing to the 'apparent survival' rate. However, the process model did not account for the potential dispersal of prebreeders in the year immediately prior to recruitment: age 4 birds were assumed to recruit to the colony with the survival rate $\phi_{a,t}$ of established breeders, which rarely (if ever) change colony. Therefore, reconfiguring equation (2.2) to allow a proportion of new recruits to emigrate could be what is required to 'balance the books', so that the model fits the counts. We consider this approach in Chapter 3.

Another unrealistic feature of the count model was the use of point estimates for the time-specific productivity and survival rates, which, like the count data, are also subject to sampling error. Standard errors were provided with the estimates and could be used to sample productivity and survival rates at each iteration from beta distributions, for example. A preferable approach would be to fit the model simultaneously to the time series of counts and the raw productivity and mark-recapture data in a so-called 'integrated data analysis' (see, e.g., Besbeas et al. 2002, Brooks et al. 2004, King et al. 2008b). This approach is also described in Chapter 3. Along the same lines, the annual number of breeding pairs were not counted directly but were calculated from the total colony count using a time-specific correction factor (refer back to Section 2.2.2 for details). To better account for the way the data on population size were collected and analysed, it may be more realistic to fit the observation model to the raw colony counts, assuming observation error to come from a binomial sampling process (the n being the count and the p being the proportion of breeding pairs observed on the intensively monitored plots). Although we do not implement such an approach in the analyses contained herein, it may be worth considering in future studies.

2.3 Mark-recapture data

2.3.1 Introduction

Mark-recapture data from Isle of May guillemots ringed as chicks and from a separate set of birds ringed as breeding adults have previously been analysed independently to obtain estimates of, respectively, juvenile (Crespin et al. 2006a) and adult (Harris & Wanless 1995, Crespin et al. 2006b) survival rates. (Note that we refer to the data corresponding to birds ringed as chicks as 'chick data' and to birds ringed as adults as 'adult data'.) In addition, Harris et al. (2007b) provide an analysis of combined chick mark-recapture and ring-recovery data. In this section we focus on combining the adult and chick mark-recapture data and for the time being ignore the chick ring-recoveries, which are incorporated in the integrated model described in Chapter 3.

In combining the adult and chick mark-recapture data, a major assumption is that 'adult' (i.e., age 4 years and older) survival rate is a shared parameter between the two datasets. However, among the previously published estimates of adult survival there is a large discrepancy between estimates based on the adult data (0.90–0.99; Crespin et al. 2006b) and those based on the chick data (0.70; Crespin et al. 2006a). A proportion of birds emigrate prior to first breeding (Halley & Harris 1993) and those that remain tend to disperse through the breeding ledges of the colony and start losing their colour-rings. The combination of these factors result in the lower adult survival estimates from the chick data, which are in fact estimates of apparent survival. In addition, recaptures of birds aged 5-and-older that were ringed as chicks are sparse, so it is not possible to estimate year-specific survival rates for these birds. The adult data, on the other hand, contain many recaptures and are thus highly informative. Thus, by combining the two datasets, the adult data provide most of the information on adult survival rates, while the additional, alternative information provided by the chick data allows the estimation of a pre-recruitment dispersal rate.

2.3.2 Data and notation

The raw data for this analysis are the individual capture histories from which the survival point estimates used in the state-space model in Section 2.2 were derived. The capture histories consist of a series of ones and zeros, denoting for each capture occasion from year $t = 1, \ldots T$ whether an individual was seen alive (recaptured or resighted) or not seen, respectively. The first '1' indicates the year (or cohort) in which the bird was ringed, and the last '1' the year

the bird was last seen, though not necessarily the year in which it died. For example, the capture history

0 0 0 1 0 0 1 1 1 1 0 1 0 0 0 0 0 0 0 0 0 0 0 0

describes a bird (in this case a guillemot chick ringed on the Isle of May) ringed and released in the fourth year (1986) of a 23-year study, recaptured during 1989–1992, and again in 1994, after which it was not seen again. A total of 6396 guillemot capture histories are used in this analysis, consisting of 802 breeding adults captured and marked during 1982–2004, and 5594 chicks captured during 1983–2003, with resightings of both groups up to 2005. Thus, we have $T = 24$ capture/recapture occasions.

Modelling the recapture process requires two sets of parameters: survival rates and recapture probabilities. We let $R = \{0, 1, 2, 3, 4, 5^+, a\}$ denote the set of ages at which birds may be recorded, with a denoting the adult age-class. For $r \in R$ and $t = 1, \ldots, T-1$, we define

$$\phi_{r,t} = \Pr(\text{a bird of age } r, \text{ alive at time } t, \text{ survives until time } t+1);$$
$$p_{r,t+1} = \Pr(\text{a bird of age } r, \text{ alive at time } t+1, \text{ is resighted at that time}).$$

For notational convenience, we also define $\boldsymbol{\phi} = \{\phi_{r,t} : r \in R;\, t = 1, \ldots, T-1\}$ and $\boldsymbol{p} = \{p_{r,t} : r \in R;\, t = 2, \ldots, T\}$ to denote the set of all survival and resighting probabilities, respectively, and $\boldsymbol{\theta} = \{\boldsymbol{\phi}, \boldsymbol{p}\}$ to denote the full set of model parameters.

2.3.3 Analysis and results

We take a Bayesian approach to the analysis, using noninformative $\mathrm{U}(0, 1)$ priors on all probability parameters. MCMC, with updates by a Metropolis-Hastings random walk algorithm with uniform proposal density, is used to obtain a sample from the posterior distribution π, from which posterior summary statistics are extracted. The MCMC algorithms for the following models were all run for 100,000 iterations, with the first half of the chain discarded as burn-in. Standard convergence diagnostics and plots (BGR statistic; see Section 1.3.3) suggested that this burn-in period was very conservative, with rapid convergence indicated for all models. Simulations were implemented in Fortran and took from a few minutes to 10 hours (according to the model; see individual model descriptions, below) to run on a 1.8 GHz personal computer.

M1 Simple combined analysis

We begin with a straightforward combined analysis, where time-specific adult survival probabilities are assumed to be equal for the adult and chick data. This assumption is not made for adult resighting probabilities because resighting data for the two groups was collected by different methods. The model to describe the other chick survival parameters (i.e., for juvenile and immature birds) and the model for resighting parameters are based on biological reasoning and the amount of information in the data. One-year-old birds were never observed at the colony, so resighting probabilities for this age group are fixed to zero ($p_{1,t} = 0 \; \forall \; t$) and juvenile survival is therefore restricted to a composite estimate over the first two years of life, denoted by $\phi_{0\text{–}1,t}$. Survival of juvenile birds is allowed to vary annually, but for ages 2 and 3 it is constrained to be constant with time as there is not enough information in the data to permit time-specific estimates. Once birds reach age 4, they are assumed to survive with a time-dependent adult survival rate, in common with birds from the adult dataset ($\phi_{4,t} = \phi_{5+,t} = \phi_{a,t}$). Therefore, we have survival parameters $\phi_{0\text{–}1,t}$, ϕ_2, ϕ_3 and $\phi_{a,t}$. Resighting probability is assumed to be age-dependent up to 5 years because immature guillemots visit the colony with increasing frequency until they start breeding (Halley et al. 1995); it is also fully time-dependent for all age classes of birds ringed as chicks, and for birds ringed as adults. This gives the resighting parameters $p_{2,t}$, $p_{3,t}$, $p_{4,t}$, $p_{5+,t}$ and $p_{a,t}$, where $p_{5+,t} \neq p_{a,t}$.

Catchpole et al. (1998) derived an efficient form for the likelihood of joint mark-recapture and ring-recovery data that allows age- and time-dependence. Instead of using the individual capture histories, their approach requires summarising these raw data into four upper-triangular matrices, which form sufficient statistics for estimation of the parameters. Using a similar, but simplified approach for the mark-recapture data, we define the following three matrices:

$v_{r,t}$ = the number of birds of age r captured or resighted at time t and not seen again during the course of the study;

$w_{r,t}$ = the number of birds of age r at time t, resighted at time $t+1$;

$z_{r,t}$ = the number of age r birds at time t not resighted at time $t+1$ but seen alive later.

Two sets of these statistics are required: $\boldsymbol{x_j} = \{\boldsymbol{v_j}, \boldsymbol{w_j}, \boldsymbol{z_j}\}$ for the capture histories of birds ringed as chicks; and $\boldsymbol{x_a} = \{\boldsymbol{v_a}, \boldsymbol{w_a}, \boldsymbol{z_a}\}$ for those of birds ringed as breeding adults. The likelihood for the chick data is then expressed

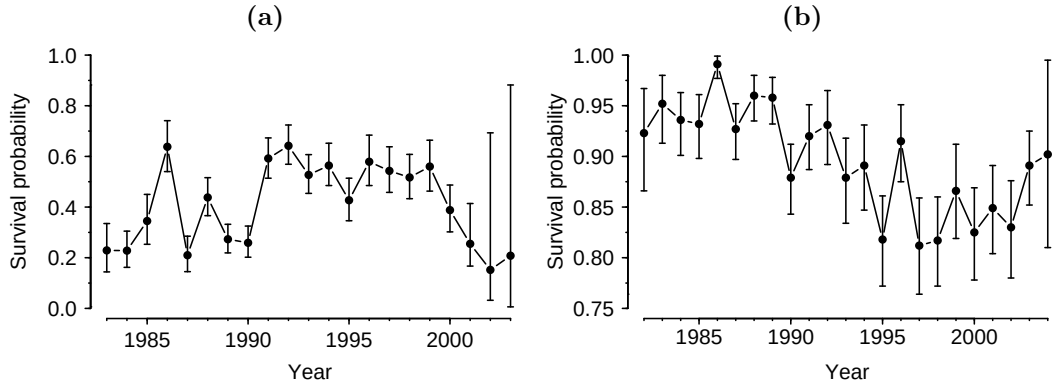

Figure 2.3 Posterior means and 95% symmetric CIs for survival rates under the combined adult-chick mark-recapture model: (a) juvenile survival (from fledging to age 2) of birds ringed as chicks, $\phi_{0\text{–}1,t}$; (b) combined adult survival of age 4^+ birds ringed as chicks and birds ringed as breeding adults, $\phi_{a,t}$. (Note the different y-scales.)

in the form

$$L_j(\boldsymbol{x_j} \mid \boldsymbol{\theta}) = \prod_{r \in R} \left[\prod_{t=1}^{T-1} (\phi_{r,t})^{w_{r,t}+z_{r,t}} (p_{r,t+1})^{w_{r,t}} (1-p_{r,t+1})^{z_{r,t}} \prod_{t=1}^{T} (\chi_{r,t})^{v_{r,t}} \right], \quad (2.8)$$

where $\chi_{r,t}$ denotes the probability that a guillemot of age r, alive at time $t = 1, \ldots, T$, is not observed after this time. For $t = 1, \ldots, T-1$, $\chi_{r,t}$ is given by the recursion

$$\chi_{r,t} = (1-\phi_{r,t}) + \phi_{r,t}(1-p_{r,t+1})\chi_{r+1,t+1}, \quad (2.9)$$

with $\chi_{r,T} = 1$. The likelihood for the adult data, $L_a(\boldsymbol{x_a} \mid \boldsymbol{\theta})$, is a similar expression with $r = a$, and the joint likelihood for the combined data is formed by multiplying the adult and chick expressions together.

The MCMC iterations for this model took $\sim$7 minutes of computing time (for 100,000 iterations), which is a reflection of the efficiency of the above method for calculating the likelihood.

Posterior means and associated 95% CIs for time-specific survival rates are provided in Figure 2.3. Survival from fledging to age 2 was highly variable between years, with posterior means during 1983–2001 ranging from 0.210 to 0.642 (Figure 2.3a). The large uncertainties in 2002/2003 reflect the fact that few chicks ringed in these years were resighted before the end of the study; furthermore, the 2003 estimate is confounded with age 2 resighting probability in 2005 (note the correspondingly large CI on the final $p_{2,T}$ in Figure 2.4a). Adult survival also varied significantly from year to year (0.812–0.991; Figure 2.3b), but over a much smaller range than juvenile survival (note that the magnitudes of the two survival rates are not directly comparable as juvenile survival covers

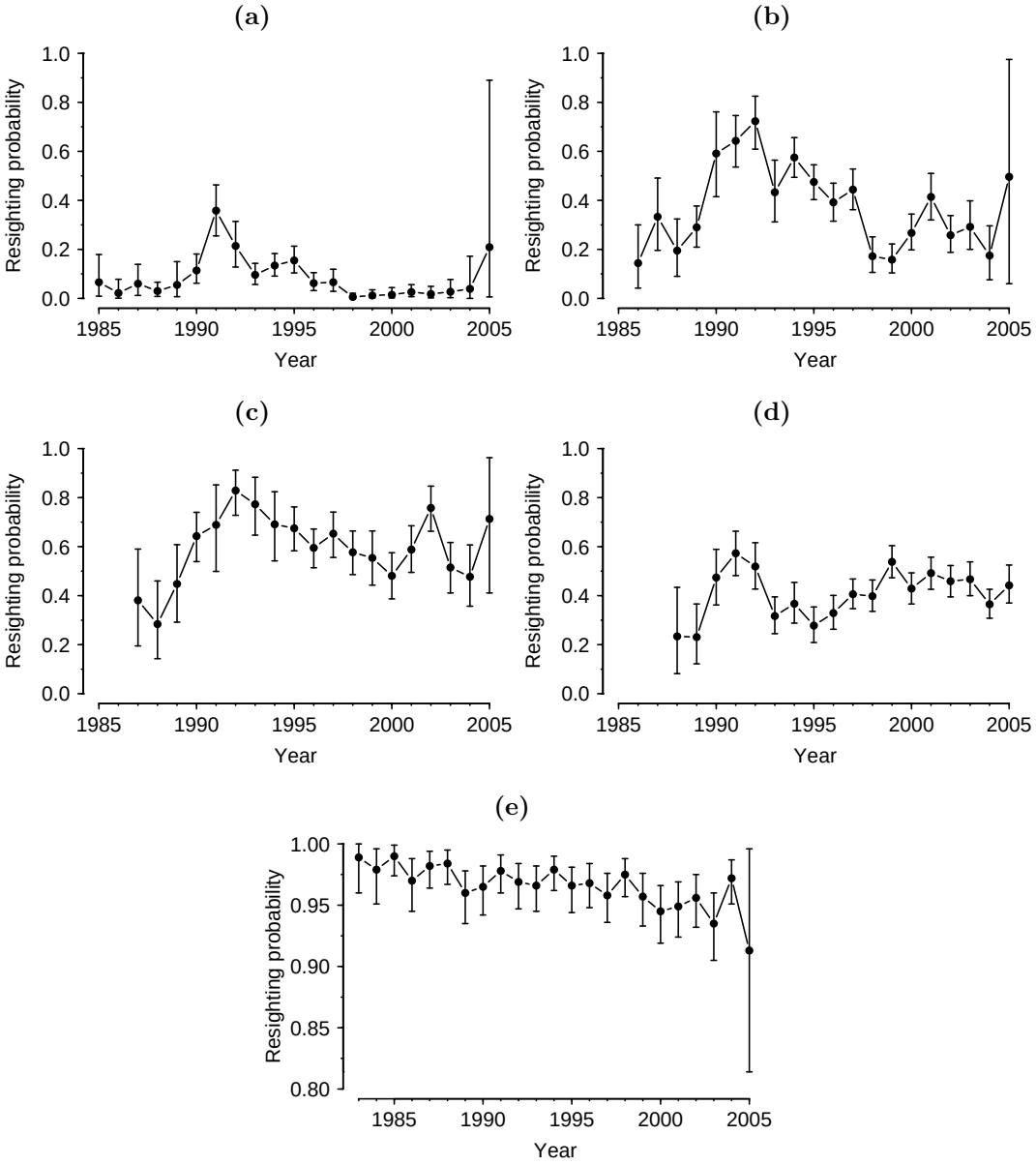

Figure 2.4 Posterior means and 95% symmetric CIs for resighting probabilities under the combined adult-chick mark-recapture model: (a)–(d) birds ringed as chicks, respectively $p_{2,t}$, $p_{3,t}$, $p_{4,t}$ and $p_{5+,t}$; (e) birds ringed as breeding adults $p_{a,t}$ (note the different y-scale for this plot).

a two-year period, whereas adult survival is only over a single year of life). The main detail to note is the steady decrease in adult survival after 1989 to a new, apparent lower level, and the associated increase in uncertainty of the estimates, the possible reasons for which will be discussed later. Constant survival estimates for immature birds were 0.915 (95% CI: $0.839, 0.979$) for ϕ_2, and 0.813 $(0.777, 0.849)$ for ϕ_3.

Resighting probabilities of birds ringed as chicks increased with age up to 4 years old (Figure 2.4a–c). Birds aged 5-and-older were resighted with lower

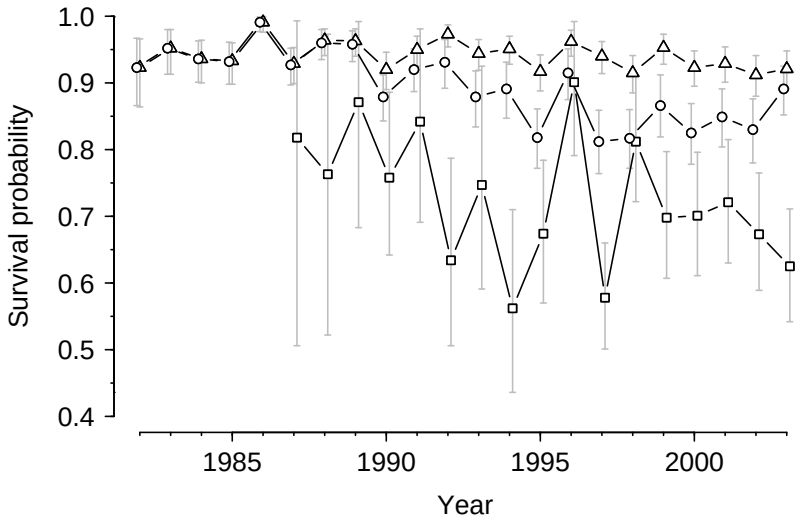

Figure 2.5 A comparison of adult survival estimates (posterior means and 95% CIs) obtained under combined adult-chick model M1 (○) with those from adult-only (△) and chick-only (□) analyses using identical model structures.

probability than age 4 birds (Figure 2.4d). This can be explained as these are birds of breeding age that would have dispersed throughout the densely packed breeding ledges of the colony making them harder to resight, and the wear and loss of colour-rings would also have started to occur. Resighting probabilities of birds ringed as breeding adults $p_{a,t}$ were very high throughout the study (Figure 2.4e), due to a combination of the intensity of observations on these birds and their site-faithfulness. The disparity between the estimates from birds ringed as adults and those ringed as chicks shows that it would be unrealistic to assume the same resighting probability for all breeding-age guillemots.

With the exception of ϕ_3 and $\phi_{a,t}$, all parameter estimates were essentially the same as those obtained from independent analyses of the adult and chick data (where applicable) using identical model structures. The posterior mean for third-year survival derived from the combined data (0.813) was 0.078 lower than the posterior mean from the chick data (0.891) with minimal overlap in the CIs. Combined adult survival estimates during 1982–1989 were very similar to those from the adult data only, but from 1990 onwards these estimates also diverged, with those from the combined analysis being consistently lower and with larger CIs; however, they were higher than the estimates of adult survival from the chick data (Figure 2.5). The combined estimates thus appear to reflect a compromise between the information about adult survival contained in the two datasets: in the early years there was little information (none before 1987) coming from the chick data as few marked birds had reached adulthood, so the estimates mostly reflect the information in the adult data; as time progresses,

however, more cohorts of birds ringed as chicks enter the adult age-class, giving the chick data greater weight (note the smaller CIs on the chick estimates in later years in Figure 2.5) and thus pulling the combined estimates away from what we assume to be the 'true' adult survival rates.

M2 Incorporating pre-recruitment emigration

The estimates of adult survival obtained from the chick data are clearly anomalously low when compared to what we believe to be the more realistic estimates from the adult data (see Figure 2.5). Because mark-recapture models are unable to distinguish permanent emigration from death (both result in zero future recaptures), emigration produces negatively biased survival estimates; indeed, Crespin et al. (2006a) attribute the discrepancy in adult survival on the Isle of May primarily to the permanent emigration of 'as many as 25%' of prebreeding guillemots to other colonies. Emigration is not an issue for the breeding adult mark-recapture data, as breeding guillemots rarely (if ever) change colonies. Therefore, if we assume that the difference between the two sets of adult survival estimates is due to permant pre-recruitment emigration, then accounting for this in the combined model should produce improved estimates of adult survival, plus an estimate of the rate of emigration.

On the Isle of May most guillemots start breeding at ages 5–7 years (Harris et al. 1994), but for simplicity we assume that all birds recruit at age 5 and, as already noted, that they survive with adult survival rate $\phi_{a,t}$ from age 4. Most chicks return to the Isle of May during their prebreeding years (Crespin et al. 2006a), so that we assume that all emigration takes place in the year immediately prior to first breeding, that is, at age 4. Using ψ to denote the emigration rate, survival for age 4 birds is now given by $\phi_{4,t} = (1-\psi)\phi_{a,t}$, while for birds aged 5-and-older we still have that $\phi_{5+,t} = \phi_{a,t}$.

Parameter estimates from this model were generally very similar to those from M1, notable exceptions being ϕ_3, which at 0.864 (95% CI: $0.821, 0.905$) was somewhat higher than the M1 estimate of 0.813, and adult survival $\phi_{a,t}$, which although still not as high as the estimates from the adult-only analysis, were a slight improvement over the model without emigration (Figure 2.6). The emigration parameter ψ was estimated to be 0.202 $(0.158, 0.244)$; this implies a permanent pre-recruitment emigration rate of about 20% from each cohort, which is not too dissimilar to the 25% estimated by Crespin et al. (2006a). Computation time for the MCMC iterations was essentially the same as for M1 ($\sim$ 7 minutes; only one additional parameter was updated at each iteration).

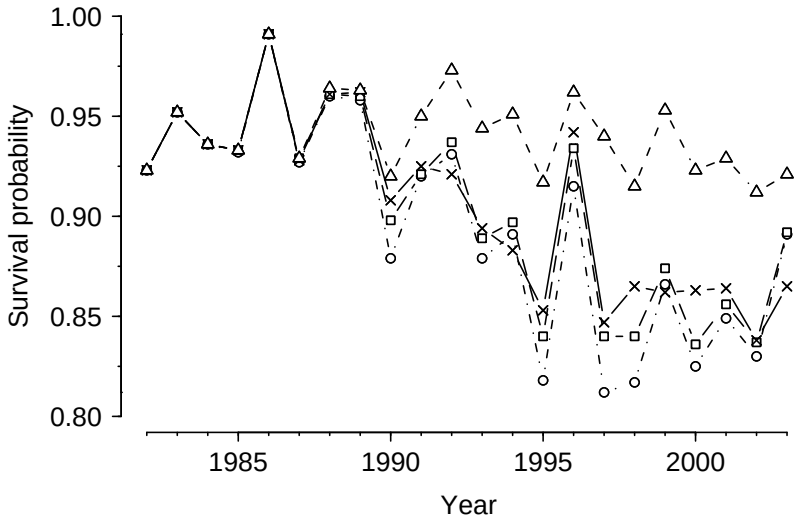

Figure 2.6 A comparison of adult survival estimates (posterior means) obtained under the following combined survival models: M1 (○; simple combined analysis); M2 (□; extended analysis incorporating pre-recruitment emigration); M3.1 and M3.2 (×; attempts to account for heterogeneity in age 5^+ resighting probabilities with, respectively, a mixture-distribution and random effects—results were essentially identical). The 'true' estimates given by the adult data are also plotted for comparison (△).

M3.1 Modelling heterogeneity in p_{5+}: two-component mixture-distribution

The fact that incorporating emigration in the combined model did not contribute significantly to improving estimates of adult survival suggests that we are still missing an important aspect of the system. We therefore hypothesise that, while part of the discrepancy between adult survival estimates from the independent chick and adult analyses may be explained by permanent emigration, unmodelled heterogeneity in age 5^+ resighting probabilities of birds ringed as chicks may also have an effect.

There are a number of factors that may affect the probability of resighting breeding-age guillemots that were ringed as chicks, making the assumption that all age 5^+ birds share the same resighting probability potentially unreasonable. According to our assumptions, guillemots recruit to the breeding population at 5 years of age. From then on, they are most likely to be resighted at the location of their breeding site, which generally remains the same from year to year (Harris et al. 1996b), so resighting probability is highly dependent on whether an individual recruits to a high- or low-visibility nest site: those recruiting to high-visibility sites are likely to be resighted with high frequency, whereas individuals recruiting to low-visibility sites will only be seen sporadically, if at all. A further potential source of heterogeneity is caused by wear and loss of colour-rings, which takes place once birds start breeding and spend much more

time ashore on the drier, more abrasive rock of the breeding ledges. Marked birds that have a missing or unreadable colour-ring can only be identified by means of their numbered metal ring, which are much more difficult to find during searches and are also harder to positively identify once discovered.

To model these two sources of heterogeneity we use a similar approach to Pledger et al. (2003), splitting p_{5+} into two separate parameters: the probability of resighting a bird given it is in a high-visibility location, denoted p^h_{5+}, and the probability of resighting a bird given it is in a low-visibility location, p^l_{5+}. The resulting posterior distribution for p_{5+} is a mixture of the two component distributions.

For this approach, we consider an individual-based approach to formulating the likelihood for the chick data. We let $\boldsymbol{x_j} = \{x_{i,t} : i = 1, \ldots, n;\ t = 1, \ldots, T\}$ denote the full set of $n = 5594$ chick capture histories, where each row i gives the capture history of a single individual and each column t represents a single capture occasion, containing a '1' if an individual was captured or resighted on that occasion and '0' otherwise. For each individual i, we denote the year of its first capture by t_{ci}, the year of its last capture by t_{ki} and its age at last capture by r_{ki}. At any time t, the age of an individual is given by $r = \min(t - t_{ci} + 1, G)$, where $G = 6$ is the total number of age classes. Then, for each individual we let

$$\delta^h_i = \begin{cases} 1, & t_{ki} = t_{ci}, \\ \displaystyle\prod_{t=t_{ci}}^{t_{ki}-1} \phi_{r,t}(p^h_{r,t+1})^{x_{i,t+1}}(1 - p^h_{r,t+1})^{1-x_{i,t+1}}, & t_{ci} < t_{ki} \leqslant T, \end{cases} \tag{2.10}$$

be the probability of observing that individual's capture history from first capture until its last recapture occasion, given that it is in a high-visibility location, with an analogous definition for δ^l_i by replacing $p^h_{r,t}$ with $p^l_{r,t}$. To complete the individual likelihood, we also need to define the probability that an individual is not observed after its last recapture occasion. In general, for an individual of age r, last seen at time t, this is given by the recursion

$$\chi^h_{r,t} = (1 - \phi_{r,t}) + \phi_{r,t}(1 - p^h_{r,t+1})\chi^h_{r+1,t+1}, \qquad t = 1, \ldots, T - 1, \tag{2.11}$$

with $\chi^h_{r,T} = 1$, given that the individual is in a high-visibility location, with an analogous definition for $\chi^l_{r,t}$. Then for $r \leqslant 4$ (i.e., prebreeders) we simply let $p_{r,t} = p^h_{r,t} = p^l_{r,t}$, while for breeders we specify that $p^h_{5+} > p^l_{5+}$, and so $p_{5+} = \pi^h p^h_{5+} + (1 - \pi^h)p^l_{5+}$, where π^h is the probability of being in a high-visibility

site. The full likelihood is calculated as the product of the probabilities of the individual capture histories and is given by

$$L_j(\boldsymbol{x_j} \mid \boldsymbol{\theta}) = \prod_i \left(\pi^h \delta_i^h \chi^h_{r_{ki},t_{ki}} + (1-\pi^h)\delta_i^l \chi^l_{r_{ki},t_{ki}}\right), \tag{2.12}$$

where $\boldsymbol{\theta} = \{\boldsymbol{\phi}, \boldsymbol{p}\}$ is a vector of model parameters, as defined in Section 2.3.2.

Computation time for this individual-based analysis was $\sim$5 hours, which is more than 40 times longer than for M1 or M2. This further highlights the considerable advantage of using Catchpole et al.'s (1998) approach based on the sufficient statistics, where possible, when implementing computationally intensive likelihood-based simulations such as MCMC.

Posterior means for the resighting probabilities p^h_{5+} and p^l_{5+} were 0.762 (95% CI: 0.708, 0.817) and 0.188 (0.145, 0.234), respectively, with the probability of being in a high-visibility site π^h being 0.386 (0.322, 0.451). This result clearly suggests that adult guillemots that were ringed as chicks are divided into (at least) two distinct groups with very different resighting probabilities, as we expected. However, while estimates of adult survival were improved further over the previous estimates from the emigration model, the difference was very small (Figure 2.6; also note the slightly different trend of survival estimates, which is most likely the result of p_{5+} no longer being time-specific, due to insufficient information in the data). In addition, the posterior estimate of the emigration rate ψ was drastically reduced in this model to 0.081 (0.012, 0.147). It is probable that this model is still not adequate to capture all the heterogeneity in p_{5+}, so with the following model we consider a random effects model.

M3.2 Modelling heterogeneity in p_{5+}: random effects

The most general option for modelling heterogeneity in p_{5+} is to model the parameter using random effects—essentially a form of continuous mixture model (Coull & Agresti 1999, Dorazio & Royle 2003)—which assumes that each guillemot has its own individual resighting probability derived from an underlying distribution. We denote the age 5^+ resighting probability of individual i by p^i_{5+}, which takes the form

$$\text{logit}(p^i_{5+}) = \mu + \epsilon_i, \tag{2.13}$$

where μ denotes the underlying resighting probability and ϵ_i denotes random effects, such that

$$\epsilon_i \sim \text{N}(0, \sigma^2_\epsilon). \tag{2.14}$$

The random effects variance σ_ϵ^2 is a parameter to be estimated. As with Model 3.1, this calls for a likelihood based on the individual capture histories. We define

$$\delta_i = \begin{cases} 1, & t_{ki} = t_{ci}, \\ \prod_{t=t_{ci}}^{t_{ki}-1} \phi_{r,t}(p^i_{r,t+1})^{x_{i,t+1}}(1-p^i_{r,t+1})^{1-x_{i,t+1}}, & t_{ci} < t_{ki} \leqslant T, \end{cases} \tag{2.15}$$

to be the probability of observing the capture history of individual i from first until last capture, and

$$\chi^i_{r,t} = (1-\phi_{r,t}) + \phi_{r,t}(1-p^i_{r,t+1})\chi^i_{r+1,t+1}, \qquad t \leqslant T-1, \tag{2.16}$$

with $r = r_{ki}$, $t = t_{ki}$, and $\chi^i_{r,T} = 1$, to be the probability that individual i is not observed after its last recapture occasion. For $r \leqslant 4$ we let $p^i_{r,t} = p_{r,t}\ \forall\ i$, and p^i_{5+} is given by equation (2.13). The full likelihood is simply given by

$$L_j(\boldsymbol{x_j} \mid \boldsymbol{\theta}) = \prod_i \delta_i \chi^i_{r_{ki},t_{ki}}, \tag{2.17}$$

where $\boldsymbol{\theta} = \{\boldsymbol{\phi}, \boldsymbol{p}, \mu, \epsilon_i, \sigma_\epsilon^2\}$ is a vector of survival rates, resighting probabilities and random effects parameters.

The underlying resighting probability μ and random effects variance σ_ϵ^2 for the model on p^i_{5+} require some attention regarding prior specification because, unlike all the other parameters specified in Section 2.3, they do not come under the umbrella of 'probability parameters' with the corresponding $\mathrm{U}(0,1)$ prior. Following King & Brooks (2008), the prior for μ is specified to have probability density function

$$f(\mu) = \frac{\exp(\mu)}{(1+\exp(\mu))^2}, \tag{2.18}$$

which exactly induces a $\mathrm{U}(0,1)$ prior on the resighting probability in the absence of random effects. Regarding σ_ϵ^2, we specify a prior of the form

$$\sigma_\epsilon^2 \sim \Gamma^{-1}(b_1, b_2), \tag{2.19}$$

for which we require the parameters b_1 and b_2 such that the corresponding prior distribution of ϵ_i approximately induces a $\mathrm{U}(0,1)$ prior on the resighting probability p^i_{5+}. Ignoring the μ term in the logistic regression, this is closely achieved by setting $b_1 = 3$ and $b_2 = 7$ (see Appendix A for a full discussion of the derivation of these parameters).

The estimate of the underlying resighting probability μ, on the logit scale, was -0.745 (95% CI: -0.960, -0.523), with a corresponding back-transformed estimate for p_{5+} of 0.322 $(0.277, 0.372)$. The random effects variance σ^2_ϵ, also on the logit scale, was 3.34 $(2.54, 4.27)$, which is rather large and reflects the great individual variation in resighting probabilities. Even so, this approach gave essentially identical estimates of adult survival to those from M3.1 (see Figure 2.6) and the emigration parameter ψ was reduced even further to 0.022 $(0.001, 0.073)$. Computation time was $\sim$10 hours, more than 80 times longer than M1 or M2, which demonstrates the considerable computational demand of implementing individual random effects in an MCMC simulation.

2.3.4 Discussion

The results from the models presented in this section suggest that modelling emigration and heterogeneity in p_{5+} are of limited benefit in achieving improved estimates of adult survival from the combined adult-chick mark-recapture model. Even allowing for individual variation in age 5^+ resighting probabilities, posterior means for $\phi_{a,t}$ remained well below those obtained from the breeding adult-only data. However, none of the above models account for the individuals that truly become invisible to future live detections, through dispersing to an 'invisible' location in the colony (where identification is impossible) and/or losing their colour-ring. Accounting for these individuals requires a way of knowing that they are still alive without the need for live resightings, and dead recoveries provide the answer: a bird may be recovered dead and identified via its numbered metal ring regardless of whether it is in an 'invisible' location, has lost its colour-ring, or even if it has emigrated and recruited to another colony.

Fortunately, information on recoveries is available for guillemots ringed as chicks on the Isle of May, and the combined analysis of mark-recapture and ring-recovery data for these birds provides a realistic estimate of adult survival (95%: Harris et al. 2007b), even without the additional information in the adult data. The inclusion of recoveries is considered in Chapter 3, as part of a fully integrated approach to analysing the Isle of May data.

2.4 Productivity data

2.4.1 Data and model

The productivity data analysed in this section are derived from daily monitoring of breeding guillemots in several study plots located in the main part of the Isle of May colony. Each year from 1983 to 2005 (denoted by $t = 1, \ldots, T$), 607–1014 pairs (representing on average 5.5% of the total colony) laid an egg in the study areas. The fates of these eggs were then followed through the breeding season, resulting in a known number of successfully 'fledged' chicks (fledging here being defined as a chick having left the colony, which usually occurs at around 3 weeks of age).

For $t = 1, \ldots, T$, we denote the number of observed breeding attempts in year t by $n_{e,t}$, and the number of successfully fledged chicks by $n_{f,t}$. Because a female guillemot only lays a single egg per year, each breeding attempt is an independent Bernoulli trial with probability ρ_t (the productivity rate at time t) and so we have that

$$n_{f,t} \mid \rho_t \sim \text{Bin}(n_{e,t}, \rho_t). \tag{2.20}$$

2.4.2 Analysis and results

We perform a Bayesian analysis of the data, and because the posterior distribution is of a simple form, we are able to derive it analytically in our case. Placing a Beta(α, β) prior on ρ_t, by Bayes' Theorem the posterior distribution for the productivity rate in year t is given by

$$\begin{aligned} \pi(\rho_t \mid n_{f,t}) &\propto f(n_{f,t} \mid \rho_t)\, p(\rho_t) \\ &\propto (\rho_t)^{n_{f,t}}(1-\rho_t)^{n_{e,t}-n_{f,t}}(\rho_t)^{\alpha-1}(1-\rho_t)^{\beta-1} \\ &= (\rho_t)^{n_{f,t}+\alpha-1}(1-\rho_t)^{n_{e,t}-n_{f,t}+\beta-1}. \end{aligned} \tag{2.21}$$

Then, by inspection, we have that

$$\rho_t \mid n_{f,t} \sim \text{Beta}(n_{f,t}+\alpha, n_{e,t}-n_{f,t}+\beta). \tag{2.22}$$

Therefore, the expected value (posterior mean) for ρ_t is given by

$$\mathbb{E}_\pi(\rho_t) = \frac{n_{f,t}+\alpha}{n_{e,t}+\alpha+\beta}, \tag{2.23}$$

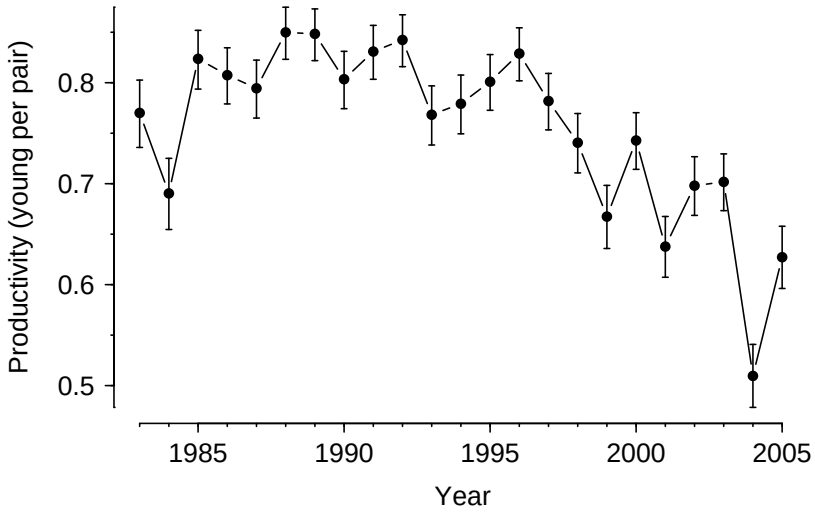

Figure 2.7 Posterior means and 95% symmetric CIs for productivity rates, ρ_t.

and the standard deviation by

$$\sigma_\pi(\rho_t) = \sqrt{\frac{(n_{f,t}+\alpha)(n_{e,t}-n_{f,t}+\beta)}{(n_{e,t}+\alpha+\beta)^2(n_{e,t}+\alpha+\beta+1)}}. \tag{2.24}$$

The symmetric $100(1-\alpha_c)\%$ credible interval (a, b) is defined such that

$$\int_0^a \pi(\rho_t \mid n_{f,t})d\rho_t = \frac{\alpha_c}{2} = \int_b^1 \pi(\rho_t \mid n_{f,t})d\rho_t,$$

i.e.,

$$\int_0^a (\rho_t)^{n_{f,t}+\alpha-1}(1-\rho_t)^{n_{e,t}-n_{f,t}+\beta-1}d\rho_t \\ = \frac{\alpha_c}{2} = \int_b^1 (\rho_t)^{n_{f,t}+\alpha-1}(1-\rho_t)^{n_{e,t}-n_{f,t}+\beta-1}d\rho_t. \tag{2.25}$$

The integration for the credible interval is not possible analytically; however, the necessary quantiles of the beta distribution may be obtained using computer routines such as the `qbeta` function in [R].

We have no prior information regarding the productivity rates, so we specify the prior parameters $\alpha = \beta = 1$, giving a prior equivalent to a $\mathrm{U}(0, 1)$ distribution. Resulting posterior means and corresponding symmetric 95% CIs are plotted in Figure 2.7. The CIs were quite small, due to the large sample sizes, and clearly there was a significant degree of year-to-year variation in productivity. This was particularly true during the later years of the study, when there appears to have been a significant decline in mean productivity and an increase

in interannual variability, both of which are likely to have a negative impact on the colony growth rate.

It is straightforward to incorporate the productivity data and model into an integrated analysis, and we do so in Chapter 3.

2.5 Conclusions

In this chapter, we have considered each of the Isle of May guillemot datasets separately. However, some of the parameters are common to more than one dataset, and treating the analyses separately can provide inconsistent results; in particular, we note the different survival rates generated by the count and mark-recapture data in Section 2.2, and the difference in adult survival estimated by separate analyses of the chick and adult mark-recapture datasets, as mentioned in Section 2.3. Furthermore, approaches that simply compare parameter estimates from separate analyses, to see whether they are compatible, are piecemeal and generally not statistically rigorous (Besbeas et al. 2002).

We want a robust analysis and, therefore, in the following chapter consider an integrated approach in order to 'borrow' information across the different data. For example, mark-recapture and ring-recovery data both contain information on survival rates, and may be analysed simultaneously to share this information and obtain more self-consistent survival estimates (Burnham 1993, Catchpole et al. 1998). We have also demonstrated that count data contains little information on demographic rates, but it too can be combined with MRR data to obtain more accurate demographic rates and, at the same time, improved population estimates (e.g. Besbeas et al. 2002, Brooks et al. 2004). In Chapter 3 we show, using the Isle of May guillemot data, how count, mark-recapture, ring-recovery and productivity datasets may be combined in an integrated population model, and how this enables the estimation of additional parameters that would be unidentifiable when using only a single data source.

Chapter 3

Integrated data analysis

3.1 Introduction

Long-term monitoring schemes for wildlife populations often involve the collection of several types of data relating to various aspects of the population (Besbeas & Freeman 2006). Abundance data are relatively easy to collect and are thus frequently encountered; they can provide estimates of total population size, or indices, from which population growth rates can be inferred. At the individual level common types of data include mark-recapture and ring-recovery time series (MRR data; respectively, records of live recaptures/resightings and dead recoveries of marked individuals), which contain information on survival probabilities, and records of breeding success (for example, nest record data) for estimating productivity rates. The forms of data collected are typically dependent on the underlying biological dynamics of interest and on practical constraints.

For a given population one may analyse each type of data in turn and, where two or more datasets contain information about common parameters, compare estimates to check for consistency. Survival and productivity estimates may also be incorporated into population models to see whether they explain observed year-to-year variations in population size—an approach which has been used to investigate causes of population decline in several species (e.g. Peach et al. 1999, Freeman & Crick 2003). However, these types of analysis do not use the data to their full potential (Besbeas et al. 2002).

Recent interest has focused on integrating all available data within a single, consistent framework (e.g. Catchpole et al. 1998, Besbeas et al. 2002, Brooks et al. 2004, Besbeas et al. 2008). Resulting parameter estimates and associated measures of precision then fully reflect all available information; this approach may also permit the estimation of parameters that are unidentifiable when using

only a single data source (Besbeas & Freeman 2006) and is useful for obtaining information from limited data (Schaub et al. 2007, Véran & Lebreton 2008).

Mark-recapture and ring-recovery data from the same individuals contain information on common survival parameters and are thus readily combined (Burnham 1993, Catchpole et al. 1998), allowing the estimation of 'fidelity' probabilities to account for permanent emigration from the study site and/or loss of marks (Frederiksen & Bregnballe 2000, Frederiksen et al. 2004a, Harris et al. 2007b). Abundance data provide information on population size but generally relatively little information on the underlying survival probabilities and productivity rates. Therefore, combining abundance data with MRR data in a single analysis permits improved estimates for survival and hence improved estimates for productivity and population size (Besbeas et al. 2002, Brooks et al. 2004). Previous studies have combined various different types of abundance and MRR data using both classical (e.g. Besbeas et al. 2002, Borysiewicz et al. 2008, Véran & Lebreton 2008) and Bayesian (Brooks et al. 2004, Goodman 2004, Schaub et al. 2007) approaches. If additional, independent productivity data are available these may also be incorporated (Gauthier et al. 2007), further refining estimates of demographic parameters and population size and providing greater flexibility to estimate additional parameters.

In this chapter we consider a combined analysis of abundance, mark-recapture, ring-recovery and productivity data from a long-term study of common guillemots *Uria aalge* on the Isle of May. Although the Isle of May guillemot colony has been extensively studied, previous analyses have focused on a single aspect of the population (for example, adult survival (Harris & Wanless 1995, Crespin et al. 2006b), juvenile survival and fidelity (Harris et al. 2007b), intercolony movement (Halley & Harris 1993), and philopatry (Harris et al. 1996a)) and have not considered the dynamics of the colony as a whole.

The dynamics of guillemot colonies are complex, due to variation in age of first breeding (Harris et al. 1994) and potentially high rates of emigration among prebreeders (Halley & Harris 1993). However, quantifying emigration rates for Isle of May prebreeders is difficult due to the scarcity of direct observational data: very few guillemots ringed on the Isle of May are subsequently resighted among the hundreds of thousands at other colonies. 'Fidelity' rates have been estimated using combined MRR data from birds ringed as chicks (Harris et al. 2007b), but it is not possible using these data alone to separate emigration from the confounding influences of colour-ring loss and the low visibility of breeders. Here we present an integrated analysis of the Isle of May guillemot data that provides a formal estimate of the rate of pre-recruitment emigration

and a separate parameter to account for ring loss and reduced visibility.

We describe the data and model in Section 3.2, and the corresponding Bayesian analysis that we implement in Section 3.3. In Section 3.4 we present our results and in Section 3.5 we provide a discussion, in which we compare parameter estimates with those from previous studies to check the performance of the integrated model.

3.2 Data and modelling

We have four separate sources of data relating to the Isle of May guillemots, collected as part of the Centre for Ecology and Hydrology's 'Isle of May long-term study': (1) abundance data in the form of annual colony counts, hereafter referred to as count data (in latter years these have been made by Scottish Natural Heritage staff); (2) mark-recapture data from birds ringed as breeding adults; (3) mark-recapture-recovery data from birds ringed as chicks; and (4) productivity data in the form of annual records of breeding success. Each dataset has a minimum of 23 years of observations from 1983 to 2005, which we denote by $t = 1, \ldots, T$.

We consider each of the data sources and their corresponding models and parameters in turn, before describing how they are combined in the integrated model. A summary of all the parameters in the analysis and their interconnections between models is provided in Table 3.1, at the end of the section, and may be used as a quick-reference guide.

3.2.1 Count data

The count data are annual estimates of the number of breeding pairs, derived from counts of the total number of full-grown birds present in the colony. These total counts include one or two adults per breeding pair plus a variable number of nonbreeders and prebreeders, so a count-specific correction factor (Harris 1989) was applied to obtain an estimate of the total number of breeding pairs (see Section 2.2.2 for further details of the count methodology). For simplicity we focus on the number of breeding females, which we denote by N_t for $t = 1, \ldots, T$.

Because the N_t are only estimates of the true population size we use a state-space approach to model the count data (e.g. Millar & Meyer 2000, Buckland et al. 2004, Jamieson & Brooks 2004, Brooks et al. 2008, King et al. 2008b), which models observation error (associated with the data collection process and subsequent estimation of the number of breeding pairs) and process uncertainty

(associated with the variability within the population itself) separately.

The observation model relates the observed annual counts to the true, but unknown, underlying population size. We assume that

$$N_t \sim \mathrm{N}(X_t, \sigma_N^2), \tag{3.1}$$

where X_t denotes the true underlying number of breeding females in year t and σ_N^2 is the observation error variance.

The process model describes changes in the true population size over time. For the adult population, we assume that the number of breeding females in year t is derived from the number surviving from year $t-1$, plus the number of new females recruiting into the breeding population. On the Isle of May most guillemots start breeding at ages 5–7 years (Harris et al. 1994), but for simplicity we assume that all birds recruit at age 5. We also assume that all birds have the same 'adult' survival rate from age 4. Although established breeding guillemots rarely (if ever) change colonies, a proportion of birds reared on the Isle of May recruit elsewhere (Halley & Harris 1993). Most surviving chicks return to the Isle of May during their prebreeding years (Crespin et al. 2006a, Harris et al. 2007b), so we assume that any emigration takes place in the year immediately prior to first breeding. The local apparent survival rate—the probability of surviving and returning to the colony the following year—for age 4 females will therefore be lower than for breeding females. The parallel process of birds born on other colonies recruiting into the Isle of May breeding population also occurs (Halley & Harris 1993); however, there is no data to estimate immigration directly, so for simplicity we assume there is none (but see discussion in Section 6.2). Therefore, we consider two components of the adult breeders: continuing female breeders Y_t, and new female recruits Z_t. We then assume that

$$Y_t \sim \mathrm{Bin}(X_{t-1}, \phi_{a,t-1}), \tag{3.2}$$

and

$$Z_t \sim \mathrm{Bin}(J_{t-5}, \psi\phi_{a,t-1}), \tag{3.3}$$

where J_t denotes the number of female prebreeders that are fledged in year t and survive to adulthood, $\phi_{a,t}$ denotes the adult survival rate in year t, and ψ is the fidelity rate of recruiting birds, which is assumed to be constant over time. Finally, the total number of female breeders in year t is $X_t = Y_t + Z_t$.

A female guillemot lays a single egg per year (except that it may replace

this if lost); therefore, each breeding pair can produce only a single chick per year. Assuming all adults breed every year, we model the number of female prebreeders by

$$J_t \sim \text{Bin}(X_t, \rho_t \phi_t^*/2), \tag{3.4}$$

where ρ_t denotes the productivity rate in year t (the mean number of chicks fledged per pair) and ϕ_t^* is the compound survival rate over the first four years of life for chicks fledged in year t. The term of $1/2$ corresponds to the probability of a chick being female.

For notational convenience we let $\phi_{\rho,t} = \rho_t \phi_t^*/2$ and we define $\boldsymbol{\phi_\rho} = \{\phi_{\rho,t} : t = 1, \ldots, T-4\}$, with similar notation and corresponding time intervals for $\boldsymbol{\phi_a}$, $\boldsymbol{N}$, $\boldsymbol{J}$, $\boldsymbol{X}$, $\boldsymbol{Y}$ and $\boldsymbol{Z}$. The approximate likelihood for the observation model is then given by

$$L_{obs}(\boldsymbol{N} \mid \boldsymbol{X}, \sigma_N^2) = \prod_{t=6}^{T} \left[\frac{1}{\sqrt{2\pi\sigma_N^2}} \exp\left(-\frac{(N_t - X_t)^2}{2\sigma_N^2} \right) \right]. \tag{3.5}$$

Similarly, the approximate likelihood for the process model is

$$\begin{aligned} L_{sys}(\boldsymbol{J}, \boldsymbol{Y}, \boldsymbol{Z} \mid \psi, \boldsymbol{\phi_\rho}, \boldsymbol{\phi_a}) = \prod_{t=1}^{T-4} \binom{X_t}{J_t} (\phi_{\rho,t})^{J_t} (1 - \phi_{\rho,t})^{X_t - J_t} \\ \times \prod_{t=6}^{T} \left[\binom{X_{t-1}}{Y_t} (\phi_{a,t-1})^{Y_t} (1 - \phi_{a,t-1})^{X_{t-1} - Y_t} \right. \\ \left. \times \binom{J_{t-5}}{Z_t} (\psi \phi_{a,t-1})^{Z_t} (1 - \psi \phi_{a,t-1})^{J_{t-5} - Z_t} \right], \end{aligned} \tag{3.6}$$

and the joint likelihood for the count data is given by

$$\begin{aligned} &L_N(\boldsymbol{N}, \boldsymbol{J}, \boldsymbol{Y}, \boldsymbol{Z} \mid \psi, \boldsymbol{\phi_\rho}, \boldsymbol{\phi_a}, \sigma_N^2) \\ &\quad = L_{obs}(\boldsymbol{N} \mid \boldsymbol{Y}, \boldsymbol{Z}, \sigma_N^2)\ L_{sys}(\boldsymbol{J}, \boldsymbol{Y}, \boldsymbol{Z} \mid \psi, \boldsymbol{\phi_\rho}, \boldsymbol{\phi_a}). \end{aligned} \tag{3.7}$$

Note that t starts at 6 in both the observation likelihood and adult breeder portion of the process likelihood (see Section 2.2.2 for explanation), so we need to place priors on the initial population sizes $X_1, \ldots, X_5$ (see Section 3.3.1).

3.2.2 Adult mark-recapture data

A total of 802 breeding adults of both sexes and unknown age were captured between 1982 and 2004 in five intensively monitored study plots on the Isle of May and marked with a numbered metal ring and an individually recognisable

combination of three colour-rings. The data take the form of encounter histories, which record annual resightings of individual birds (7294 in total) from 1983 to 2005. Resightings came mainly from the study plots because site-fidelity of breeding adults is high (Harris et al. 1996b), but wider searches were also regularly made. We ignore the recoveries of dead adult birds as there were too few (11) to justify the added complexity of the model.

We assume that all adults share common survival and resighting probabilities, regardless of sex or cohort, but allow both to vary annually. Using a to denote the adult age-class and taking into account that $t = 1$ corresponds to 1983, for $t = 0, \ldots, T-1$ we let

$$\begin{aligned} \phi_{a,t} &= \Pr(\text{an adult bird, alive at time } t, \text{ survives until time } t+1); \\ p_{a,t+1} &= \Pr(\text{an adult bird, alive at time } t+1, \text{ is resighted at that time}). \end{aligned}$$

We also define $\boldsymbol{\phi_a} = \{\phi_{a,t} : t = 0, \ldots, T-1\}$ and $\boldsymbol{p_a} = \{p_{a,t} : t = 1, \ldots, T\}$ to denote the set of all survival and recapture probabilities respectively, and $\boldsymbol{\theta_a} = \{\boldsymbol{\phi_a}, \boldsymbol{p_a}\}$ to denote the full set of model parameters for the adult data.

Catchpole et al. (1998) derived an efficient form for the likelihood of joint mark-recapture and ring-recovery data that allows age- and time-dependence (see also Catchpole et al. 2000, King & Brooks 2002). Using a similar approach, we define the following sufficient statistics for the adult mark-recapture data:

$$\begin{aligned} v_t &= \text{the number of adult birds captured or resighted at time } t \text{ and not seen} \\ &\quad \text{again during the course of the study;} \\ w_t &= \text{the number of adult birds resighted at time } t+1; \\ z_t &= \text{the number of adult birds not resighted at time } t+1 \text{ but seen alive later.} \end{aligned}$$

We let $\boldsymbol{x_a} = \{\boldsymbol{v_a}, \boldsymbol{w_a}, \boldsymbol{z_a}\}$ denote the full adult dataset. The likelihood is simply expressed by

$$L_a(\boldsymbol{x_a} \mid \boldsymbol{\theta_a}) = \prod_{t=0}^{T-1} (\phi_{a,t})^{w_t+z_t} (p_{a,t+1})^{w_t} (1-p_{a,t+1})^{z_t} \prod_{t=0}^{T} (\chi_{a,t})^{v_t}, \tag{3.8}$$

where $\chi_{a,t}$ denotes the probability that an adult guillemot, alive at time $t = 0, \ldots, T$, is not observed after this time, and for $t = 0, \ldots, T-1$ is given by the recursion

$$\chi_{a,t} = (1-\phi_{a,t}) + \phi_{a,t}(1-p_{a,t+1})\chi_{a,t+1}, \tag{3.9}$$

with $\chi_{a,T} = 1$.

3.2.3 Chick mark-recapture-recovery data

Chicks were ringed on the Isle of May in two areas (4127 chicks in area A, 1467 in area B; 5594 in total) during 1983–2003 with a numbered metal ring and a unique colour-ring readable at distances up to 75 m. Encounter histories record resightings of live birds on the Isle of May and recoveries of dead birds away from the island from 1984 to 2005. In all there were 3867 live resightings and 243 dead recoveries. Most resightings resulted from almost daily searches of the breeding ledges and tidal rocks in the general vicinities of the two ringing areas, because of the tendency of guillemots to return to their natal area during their prebreeding years and to subsequently recruit nearby (Harris et al. 1996a).

The likelihood for standard MRR data is a function of survival, recapture and recovery probabilities (Catchpole et al. 1998). In particular, letting $R = \{0, 1, 2, 3, 4, 5^+\}$ denote the set of ages at which birds may be recorded, for $r \in R$ and $t = 1, \ldots, T-1$ we define

$$\begin{aligned}
\phi_{r,t} &= \Pr(\text{a bird of age } r, \text{ alive at time } t, \text{ survives until time } t+1);\\
p_{r,t+1} &= \Pr(\text{a bird of age } r, \text{ alive at time } t+1, \text{ is resighted at that time});\\
\lambda_{r,t} &= \Pr(\text{a bird of age } r \text{ which dies in } (t, t+1) \text{ has its death reported}).
\end{aligned}$$

The model to describe the chick data is similar to that of Harris et al. (2007b): we assume that both survival and resighting probability are age-dependent for juvenile and immature birds. One-year-old birds were never observed at the colony, so resighting probabilities for this age group are fixed to zero. However, information provided by the dead recoveries allows the estimation of survival over the first year of life. First-year survival is allowed to vary annually, while from ages 1–3 survival rate varies with age but is contrained to be constant over time because there is not enough information in the data to permit time-specific estimates. Once birds reach age 4, they are assumed to survive with a time-dependent adult survival rate in common with birds from the adult dataset ($\phi_{4,t} = \phi_{5+,t} = \phi_{a,t}$). Therefore, we have survival parameters $\phi_{0,t}$, ϕ_1, ϕ_2, ϕ_3 and $\phi_{a,t}$ (with $\phi_{0,t}\phi_1\phi_2\phi_3 = \phi_t^*$). Resighting probabilities are assumed to be age-dependent up to 5 years because immature guillemots visit the colony with increasing frequency until they start breeding (Halley et al. 1995), and also time-dependent for 2- and 3-year-olds. Resighting probabilities for breeding-age birds (age 5^+) are not assumed to be the same as those for birds in the adult dataset due to the different methods used to obtain resighting data for the two groups. We also allow resighting probability to differ between

birds ringed in areas A and B. We therefore have resighting parameters $p_{2,t}(A)$, $p_{2,t}(B)$, $p_{3,t}(A)$, $p_{3,t}(B)$, $p_4(A)$, $p_4(B)$, $p_{5+}(A)$ and $p_{5+}(B)$. The probability of a bird being found dead and subsequently reported (recovery probability) is assumed to be the same over all age classes, but is constrained to change linearly (on the logit scale) over the period of the study. Systematic temporal declines in reporting rates in the UK have been found across a wide range of species, including seabirds (Robinson et al. 2004, Clark et al. 2005, Freeman et al. 2007), and this model allows for such a decline in Isle of May guillemot recoveries. Therefore, we simply have recovery parameters λ_t, given by

$$\text{logit}(\lambda_t) = \alpha_\lambda + \beta_\lambda \tau_t, \tag{3.10}$$

where τ_t are the normalised times $t = 1, \ldots, T-1$.

Combining the analysis of mark-recapture, ring-recovery and count data allows the estimation of fidelity rates. The count data enter here because they share some of the same parameters as the chick MRR model (see Section 3.2.1 and Table 3.1). We assume that the probability of a dead bird being recovered and reported is independent of permanent emigration, colour-ring loss, or any other factor acting to make birds permanently unavailable for future live detections (Burnham 1993, Frederiksen et al. 2004a, Harris et al. 2007b). Here we assume that overall 'fidelity'—the probability that a bird remains available for future live resightings—is the result of three independent processes: (1) true fidelity (i.e., the complement of permanent emigration), hereafter simply referred to as fidelity; (2) retention/continued readability of colour-rings (numbered metal rings are assumed to always remain intact and readable upon dead recovery); and (3) recruitment to, and continuation of breeding in, a visible location (a nest site at which it is possible to read a bird's ring; we assume that if a bird moves to an 'invisible' location it becomes unavailable for future live resightings but is still included in the counts). In reality, (2) and (3) are confounded, but fidelity may be estimated separately in the integrated model due to information contained in the count data. Therefore, for $r \in R$ and $t = 1, \ldots, T-1$, we define

$$\begin{aligned}\psi_{r,t} = \Pr(&\text{a bird of age } r, \text{ present in the colony at time } t,\\ &\text{does not permanently emigrate in } (t, t+1)),\end{aligned}$$

and

$$\begin{aligned}\tau_{r,t} = \Pr(&\text{a bird of age } r, \text{ potentially visible and identifiable}\\ &\text{at time } t, \text{ remains so at time } t+1),\end{aligned}$$

corresponding to processes (1) and (2)/(3) respectively.

In keeping with the model for the count data, we assume that fidelity is constant over time and only applies to age 4 birds, so that

$$\psi_{r,t} = \begin{cases} \psi, & r = 4,\ t = 1, \ldots, T-1, \\ 1, & \text{otherwise.} \end{cases}$$

Wear and loss of colour-rings is assumed to take place once birds start breeding, because they spend much more time ashore on the rough, dry rock of the breeding ledges. Thus, we let

$$\tau_{r,t} = \begin{cases} \tau, & r = 5^+,\ t = 1, \ldots, T-1, \\ 1, & \text{otherwise.} \end{cases}$$

We define the following vector notation for the parameters in the chick MRR model: $\boldsymbol{\phi_j} = \{\phi_{r,t} : r = 0, 1, 2, 3;\ t = 1, \ldots, T-1\}$, $\boldsymbol{\phi_a} = \{\phi_{r,t} : r = a;\ t = 1, \ldots, T-1\}$, $\boldsymbol{p_j} = \{p_{r,t} : r = 2, 3, 4, 5^+;\ t = 2, \ldots, T\}$ and $\boldsymbol{\lambda_j} = \{\lambda_t : t = 1, \ldots, T-1\}$. Finally, we let $\boldsymbol{\theta_j} = \{\boldsymbol{\phi_j}, \boldsymbol{\phi_a}, \boldsymbol{p_j}, \boldsymbol{\lambda_j}, \psi, \tau\}$ denote the full set of model parameters for the chick data. The likelihood takes the form of that derived by Catchpole et al. (1998), extended to incorporate fidelity and ring loss. The matrices $\boldsymbol{v_j}$, $\boldsymbol{w_j}$ and $\boldsymbol{z_j}$ take analogous definitions to those of $\boldsymbol{v_a}$, $\boldsymbol{w_a}$ and $\boldsymbol{z_a}$ given in Section 3.2.2, with appropriate modifications to allow for age-dependence. We also require $\boldsymbol{d_j}$, defined as follows:

$$d_{r,t,u} = \text{the number of birds of age } r \text{ at time } t, \text{ last seen alive at that time, and recovered dead in the interval } (u, u+1).$$

Letting $\boldsymbol{x_j} = \{\boldsymbol{v_j}, \boldsymbol{w_j}, \boldsymbol{z_j}, \boldsymbol{d_j}\}$ denote the full set of sufficient statistics for the chick dataset, the likelihood can be expressed in the form

$$L_j(\boldsymbol{x_j} \mid \boldsymbol{\theta_j}) = \prod_{r \in R} \Bigg[\prod_{t=1}^{T-1} (\psi_{r,t} \tau_{r,t} \phi_{r,t})^{w_{r,t}+z_{r,t}} (p_{r,t+1})^{w_{r,t}} (1 - p_{r,t+1})^{z_{r,t}} \times \prod_{t=1}^{T} (\chi_{r,t})^{v_{r,t}} \prod_{t=1}^{T-1} \prod_{u=t}^{T-1} (\xi_{r,t,u})^{d_{r,t,u}} \Bigg], \tag{3.11}$$

where $\chi_{r,t}$ denotes the probability that a bird of age r, alive at time $t = 1, \ldots, T$, is not observed after this time and $\xi_{r,t,u}$ denotes the probability that an individual aged r at time t and last seen alive at that time is recovered dead in $(u, u+1)$. We consider each of these probability terms in turn.

The χ-term needs to account for three possibilities: (1) the bird remains at a visible location in the colony and does not lose its colour-ring, but is simply not resighted; (2) the bird permanently emigrates from the colony, loses its colour-ring or moves to an 'invisible' location so that its future resighting probability becomes zero; (3) the bird dies but is not recovered. Obviously, any bird obeying (1) may switch to (2) or (3), and birds obeying (2) may either survive in their invisible state until the end of the study or die without being recovered. Therefore, for $t = 1, \ldots, T-1$, $\chi_{r,t}$ is given by the recursion

$$\begin{aligned}\chi_{r,t} = {} & \psi_{r,t}\tau_{r,t}\phi_{r,t}(1-p_{r,t+1})\chi_{r+1,t+1} \\ & + (1-\psi_{r,t}\tau_{r,t})\phi_{r,t}\nu_{r+1,t+1} + (1-\phi_{r,t})(1-\lambda_t),\end{aligned} \tag{3.12}$$

with $\chi_{r,T} = 1$, where the three individual terms correspond respectively to processes (1), (2) and (3) described above. Here $\nu_{r,t}$ is the probability that a bird which has emigrated from the colony or lost its colour-ring is not seen again (i.e., not recovered dead; recall that unique metal-rings always remain intact and readable on dead recovery, even if the colour-ring is lost), and is given by

$$\nu_{r,t} = (1-\phi_{r,t})(1-\lambda_t) + \phi_{r,t}\nu_{r+1,t+1}, \tag{3.13}$$

with $\nu_{r,T} = 1$, for all $r \in R$.

The ξ-term needs to account for two possibilities, which are the same as (1) and (2) in the χ-term above ((3) does not apply because we know the bird to be alive until the year of its recovery). We first define the probability that a bird of age r at time t, last seen alive at that time and recovered dead in $(u, u+1)$, is not seen from t to u, which for $t \leqslant u-1$ is given by the recursion

$$\omega_{r,t,u} = (1-\psi_{r,t}\tau_{r,t})\prod_{s=t}^{u-1}\phi_{r+(s-t),s} + \psi_{r,t}\tau_{r,t}\phi_{r,t}(1-p_{r,t+1})\omega_{r+1,t+1,u}, \tag{3.14}$$

with $\omega_{r,u,u} = 1$. Then $\xi_{r,t,u} = \omega_{r,t,u}(1-\phi_{r+(u-t),u})\lambda_u$. Note that this is essentially a rewriting of the γ-term in Burnham (1993).

3.2.4 Productivity data

The productivity data are derived from daily monitoring of breeding birds in several study plots located in the main part of the colony. Each year between 1983 and 2005, 607–1014 pairs, representing on average 5.5% of the total colony, laid an egg in the study areas. The fates of these eggs were then followed through

the breeding season resulting in a known number of successfully 'fledged' chicks. Fledging here is defined as a chick having left the colony, which usually occurs at around three weeks of age.

For $t = 1, \ldots, T$ we denote the number of observed breeding attempts in year t by $n_{e,t}$, and the number of breeding successes by $n_{f,t}$. Then we assume that

$$n_{f,t} \sim \text{Bin}(n_{e,t}, \rho_t), \tag{3.15}$$

where ρ_t denotes the productivity rate in year t. Letting $\boldsymbol{n_e} = \{n_{e,t} : t = 1, \ldots, T\}$, $\boldsymbol{n_f} = \{n_{f,t} : t = 1, \ldots, T\}$ and $\boldsymbol{n_\rho} = \{\boldsymbol{n_e}, \boldsymbol{n_f}\}$, we have a simple binomial likelihood to describe the data given by

$$L_\rho(\boldsymbol{n_\rho} \mid \boldsymbol{\rho}) = \prod_{t=1}^{T} \binom{n_{e,t}}{n_{f,t}} (\rho_t)^{n_{f,t}} (1-\rho_t)^{n_{e,t}-n_{f,t}}, \tag{3.16}$$

where $\boldsymbol{\rho} = \{\rho_t : t = 1, \ldots, T\}$ denotes the set of productivity parameters.

3.2.5 Integrated model

The model for the count data depends on the demographic parameters $\boldsymbol{\rho}$, $\boldsymbol{\phi_j}$ and $\boldsymbol{\phi_a}$, fidelity rate ψ, observation error σ_N^2, and the underlying population levels $\boldsymbol{J}$ and $\boldsymbol{X}$ $(= \boldsymbol{Y} + \boldsymbol{Z})$. Similarly to equation (3.7), the joint probability density for the observed data $\boldsymbol{N}$ in terms of these parameters is given by

$$\begin{aligned} &L_N(\boldsymbol{N}, \boldsymbol{J}, \boldsymbol{Y}, \boldsymbol{Z} \mid \boldsymbol{\rho}, \psi, \boldsymbol{\phi_j}, \boldsymbol{\phi_a}, \sigma_N^2) \\ &\quad = L_{obs}(\boldsymbol{N} \mid \boldsymbol{Y}, \boldsymbol{Z}, \sigma_N^2)\, L_{sys}(\boldsymbol{J}, \boldsymbol{Y}, \boldsymbol{Z} \mid \boldsymbol{\rho}, \psi, \boldsymbol{\phi_j}, \boldsymbol{\phi_a}). \end{aligned} \tag{3.17}$$

The mark-recapture-recovery model for birds marked as chicks depends on parameters $\boldsymbol{\phi_j}$, $\boldsymbol{\phi_a}$, ψ, τ, $\boldsymbol{p_j}$ and $\boldsymbol{\lambda_j}$, with corresponding density given by $L_j(\boldsymbol{x_j} \mid \boldsymbol{\phi_j}, \boldsymbol{\phi_a}, \psi, \tau, \boldsymbol{p_j}, \boldsymbol{\lambda_j})$. Similarly, for the breeding adult mark-recapture data we have density $L_a(\boldsymbol{x_a} \mid \boldsymbol{\phi_a}, \boldsymbol{p_a})$. Finally, we have the model for the productivity data, which depends only on $\boldsymbol{\rho}$ and has probability density $L_\rho(\boldsymbol{n_\rho} \mid \boldsymbol{\rho})$.

The full set of parameters and their connections with each of the four models are summarised in Table 3.1. Clearly there are several parameters that are common to more than one model: $\boldsymbol{\phi_j}$, ψ and $\boldsymbol{\rho}$ are each present in two models and $\boldsymbol{\phi_a}$ is present in three of the four models (count, adult MRR and chick MRR). By performing an integrated analysis, in which data from each of our four sources is analysed simultaneously, the information regarding these shared parameters may be pooled. With this in mind, and under the assumption of independence between all data sources, a joint probability distribution for

Table 3.1 List of all parameters in the integrated model and their interconnections with each of the four constituent models (presence in a model denoted by ✓). Several of the parameters are common to more than one model; information about these parameters is pooled in the integrated analysis.

	Model			
Parameter	**Count**	**Adult MRR**	**Chick MRR**	**Productivity**
$\boldsymbol{\phi_j}$	✓	–	✓	–
$\boldsymbol{p_j}$	–	–	✓	–
$\boldsymbol{\lambda_j}$ $(\alpha_\lambda, \beta_\lambda)$	–	–	✓	–
ψ	✓	–	✓	–
τ	–	–	✓	–
$\boldsymbol{\phi_a}$	✓	✓	✓	–
$\boldsymbol{p_a}$	–	✓	–	–
$\boldsymbol{\rho}$	✓	–	–	✓
σ^2_N	✓	–	–	–
$\boldsymbol{J}, \boldsymbol{Y}, \boldsymbol{Z}$	✓	–	–	–

the combined data is obtained by simply multiplying together the individual probability densities,

$$\begin{aligned} L_{int}(\boldsymbol{N}, \boldsymbol{J}, \boldsymbol{Y}, \boldsymbol{Z}, \boldsymbol{x_j}, \boldsymbol{x_a}, \boldsymbol{n_\rho} \mid \boldsymbol{\rho}, \boldsymbol{p_j}, \boldsymbol{p_a}, \boldsymbol{\lambda_j}, \boldsymbol{\phi_j}, \boldsymbol{\phi_a}, \psi, \tau, \sigma^2_N) \\ = L_N(\boldsymbol{N}, \boldsymbol{J}, \boldsymbol{Y}, \boldsymbol{Z} \mid \boldsymbol{\rho}, \psi, \boldsymbol{\phi_j}, \boldsymbol{\phi_a}, \sigma^2_N)\ L_j(\boldsymbol{x_j} \mid \boldsymbol{\phi_j}, \boldsymbol{\phi_a}, \psi, \tau, \boldsymbol{p_j}, \boldsymbol{\lambda_j}) \\ \times L_a(\boldsymbol{x_a} \mid \boldsymbol{\phi_a}, \boldsymbol{p_a})\ L_\rho(\boldsymbol{n_\rho} \mid \boldsymbol{\rho}). \end{aligned} \tag{3.18}$$

3.3 Bayesian analysis

Following the theme of the thesis, we approach this analysis from a Bayesian perspective, combining the joint probability distribution for the data with prior distributions for the model parameters to obtain a posterior distribution for the parameters. This has a number of advantages over the classical approach. In particular, in this analysis the true population sizes $\boldsymbol{J}$ and $\boldsymbol{X}$ are essentially nuisance parameters which we wish to integrate out to form only the likelihood of the model parameters. However, the integration is analytically intractable and Kalman filtering techniques can be prohibitively complex to apply (Jamieson & Brooks 2004). From the Bayesian perspective, we treat $\boldsymbol{J}$ and $\boldsymbol{X}$ as parameters (or auxiliary variables) and form the joint posterior distribution over all the parameters and auxiliary variables. Then, using Markov chain Monte Carlo (MCMC) to obtain a sample from the posterior distribution, we take the marginals of the distribution, essentially integrating out the auxiliary variables as part of the simulation process. This approach also allows us to obtain

posterior estimates of the true underlying population sizes.

3.3.1 Priors

We begin by constructing prior distributions for our model parameters that represent our beliefs about the parameter values before observing any data. Without any strong prior information we specify vague priors on all the parameters. Hence we take independent $\mathrm{U}(0,1)$ priors for the probability/rate parameters, which simply restrict the parameters to lie within meaningful limits, $\mathrm{N}(0,10)$ priors for the linear trend parameters α_λ and β_λ, and a $\mathrm{U}(0,10^4)$ prior for the observation error standard deviation σ_N, based on the recommendation of Gelman (2006). Finally, we need to specify priors on the initial population levels $X_1,\ldots,X_5$ because they are dependent on prebreeders fledged before the study began, about which we have no information. Here we make use of the observed counts $N_1,\ldots,N_5$ as prior information with the normal prior $X_t \sim \mathrm{N}(N_t,\sigma_N^2)$, taking the estimated observation error to be the prior variance. Note that here (and in the observation model), we use a normal approximation to a discrete distribution: this is simply for ease of analysis, and is justified due to the large values for the population sizes.

3.3.2 Posterior distribution

Using Bayes' Theorem, the posterior distribution is given by

$$\pi(\boldsymbol{J},\boldsymbol{Y},\boldsymbol{Z},\boldsymbol{\theta} \mid \boldsymbol{N},\boldsymbol{x_j},\boldsymbol{x_a},\boldsymbol{n_\rho}) \propto L_{int}(\boldsymbol{N},\boldsymbol{J},\boldsymbol{Y},\boldsymbol{Z},\boldsymbol{x_j},\boldsymbol{x_a},\boldsymbol{n_\rho} \mid \boldsymbol{\theta})\; p(\boldsymbol{\theta}), \quad (3.19)$$

where $\boldsymbol{\theta}$ denotes the vector of all parameters from all models and $p(\boldsymbol{\theta})$ the prior distribution for the parameters.

The posterior distribution is complex so we use MCMC to obtain a sample from π, which we can then use to obtain posterior summary statistics for parameters of interest. All parameters are updated using a Metropolis Hastings random walk algorithm with uniform proposal density (details provided in Section 1.3.3). The MCMC algorithm was run for 5 million iterations, with the first 1 million discarded as burn-in and the remaining output thinned to every hundredth iteration to save storage space. Simulations were implemented in Fortran and took approximately 67 hours on a 1.8 GHz personal computer.

3.3.3 Convergence and sensitivity

Three independent MCMC chains with over-dispersed starting points were run to check convergence. Initial values for these chains were chosen towards the upper or lower limit of what were considered plausible values for each parameter: 0.01 and 0.99 for the rate parameters; 1% and 99% quantiles of a normal distribution with mean N_1 and variance 1.5×10^6 for X_1 ($X_2, \ldots, X_T$, $\boldsymbol{J}$, $\boldsymbol{Y}$ and $\boldsymbol{Z}$ were simulated conditional on X_1, so that no impossible combinations of initial population sizes were generated); and 10^5 and 10^7 for the observation error variance. Essentially identical results were obtained from each run, MCMC trace plots showed all parameters to be mixing well, and standard convergence diagnostics and plots suggested sufficient convergence by at most 200,000 iterations for some of the population sizes and significantly sooner for most parameters. The convergence diagnostic used was the Brooks-Gelman-Rubin (BGR) statistic, $\widehat{R}_{\text{interval}}$ (Brooks & Gelman 1998)—a modification of the earlier Gelman-Rubin statistic (Gelman & Rubin 1992)—with $\alpha = 0.2$, as used in the WinBUGS software (Spiegelhalter et al. 2007). The maximum value of all the univariate $\widehat{R}_{\text{interval}}$ by the end of the burn-in period was 1.009 (for Y_6); Spiegelhalter et al. (2007) suggest that convergence may be assumed if $\widehat{R}_{\text{interval}} < 1.05$, so our burn-in period and run lengths appear to have been more than adequate.

To investigate the possible influence of prior choice on posterior inference, an extensive prior sensitivity study was performed, in which each prior distribution had its mean and/or variance modified by up to two orders of magnitude. The alternative priors tested are summarised alongside the original prior distributions in Table 3.2. Essentially identical results were obtained under all alternative prior specifications for the model parameters, suggesting that results are largely data-driven and robust to prior choice. Using a diffuse prior for the initial population sizes $X_1, \ldots, X_5$ resulted in much more diffuse posterior distributions on $X_1, \ldots, X_4$, with corresponding increases in uncertainty for

Table 3.2 Prior distributions specified in the standard model and alternative priors tested in the sensitivity analysis.

Parameter(s)	Original prior	Alternative priors
$\boldsymbol{\phi_j}, \boldsymbol{\phi_a}, \boldsymbol{p_j}, \boldsymbol{p_a}, \psi, \tau, \boldsymbol{\rho}$	$\mathrm{U}(0,1)$	$\mathrm{Beta}(\frac{1}{2},\frac{1}{2})$, $\mathrm{Beta}(1,2)$, $\mathrm{Beta}(2,1)$, $\mathrm{Beta}(2,2)$
$\alpha_\lambda, \beta_\lambda$	$\mathrm{N}(0,10)$	$\mathrm{N}(0,1000)$
σ_N	$\mathrm{U}(0,10^4)$	$\mathrm{U}(0,10^5)$
σ_N^2	–	$\Gamma^{-1}(10^{-3},10^{-3})$
$X_1, \ldots, X_5$	$\mathrm{N}(N_t, \sigma_N^2)$	$\mathrm{N}(N_t, 10^7)$

$J_1, \ldots, J_4$. The estimate for X_4 was also reduced, suggesting that the population count in 1986 may have been over-estimated; however, the 95% credible interval easily overlapped the count and posterior means and variances for $X_5, \ldots, X_T$ were essentially unchanged, so we conclude there is little prior sensitivity. We are thus assured that our choice of priors was suitable and did not unduly influence the outcome of the model.

In particular, we draw attention to the priors specified for the observation error variance σ_N^2. A commonly used noninformative prior for variance parameters is the inverse-gamma distribution with both parameters set to 10^{-3} (e.g. Brooks et al. 2004, Jamieson & Brooks 2004). However, Gelman (2006) suggested that for scale parameters in hierarchical models this prior can cause serious problems, particularly where σ is estimated to be near zero; therefore, we took a cautious approach and adopted Gelman's recommendation to use a noninformative uniform prior on the standard deviation. The results of our sensitivity analysis suggest that an inverse-gamma prior on σ_N^2 would have been equally suitable, presumably because σ_N is very large in comparison with typical hierarchical standard deviation parameters.

In addition to prior sensitivity, we also checked the robustness of the results to changes in some of the model assumptions. Increasing the age of recruitment from 5 to 6 or 7 years produced essentially identical results, as did allowing colour-ring loss to occur from age 3 onwards (estimates for ages 3 and 4 were close to zero with large credible intervals). Removing emigration, on the other hand, resulted in a very poor-fitting model, demonstrating the importance of accounting explicitly for this process.

3.4 Results

The count data are plotted in Figure 3.1, along with posterior means and associated 95% symmetric Bayesian credible intervals (CIs) for estimates of numbers of adult breeder and prebreeder females from the integrated model. There appears to have been an initial decline in the breeding population, followed by a steady increase from around 1991 to the end of the study period. The integrated estimates of the number of breeding females ($\boldsymbol{X}$) track the count data closely. Note the wider CIs for the initial population levels, especially X_1 to X_4, information for which come almost entirely from the normal priors placed on these parameters. However, some information is clearly filtering back into these estimates from later years. This is particularly noticeable for the final

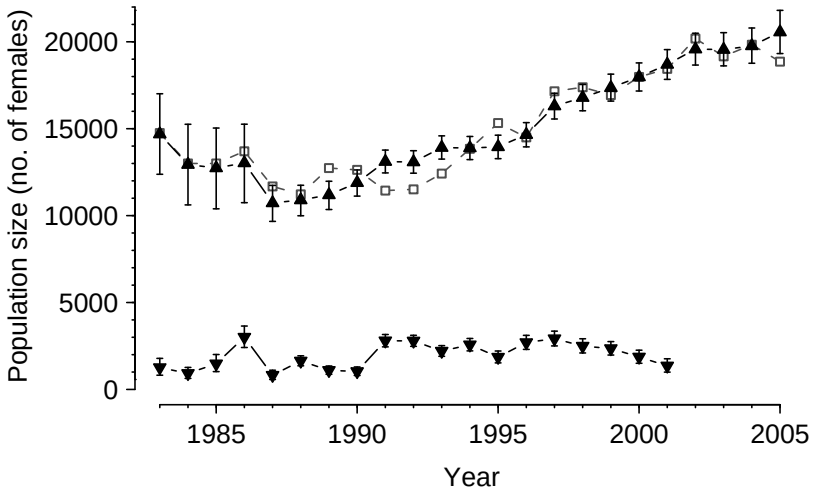

Figure 3.1 Posterior means and corresponding 95% symmetric CIs for the true underlying population levels of female prebreeders $\boldsymbol{J}$ (▼) and breeding females $\boldsymbol{X}$ (▲) over time under the integrated model. The Isle of May counts $\boldsymbol{N}$ (□) are plotted for comparison.

initial population level X_5, which has a considerably narrower CI that does not include the observed population count for that year.

We also note the small CIs on the underlying numbers of prebreeders ($\boldsymbol{J}$) estimated by the model, despite the lack of any data relating directly to population sizes of juvenile or immature birds. The large amount of year-to-year variability in the estimates of $\boldsymbol{J}$ (range of posterior means: 577–2995) is clearly illustrated in Figure 3.1 and appears to be driven mainly by variations in first-year survival and productivity (see Figures 3.2 and 3.3). The steady decline in numbers of prebreeders towards the end of the study period is despite a growing population of adult birds, and is a direct consequence of declines in first-year survival and productivity over the same period. It is not possible to obtain estimates of J_t from 2002 onwards, because full juvenile and immature survival information is unavailable for birds hatched in these years (as explained in Section 3.2.1); it would only be possible to estimate numbers of birds successfully fledged. However, as we can see in Figures 3.2 and 3.3, the last few years have some of the lowest juvenile survival and productivity estimates from the entire study. Numbers of prebreeders are therefore likely to have decreased even further over this period, which in turn has consequences for future adult population sizes (see Chapter 4).

Figure 3.2 gives posterior means and CIs for first-year and adult survival rates. Adult survival remained high throughout the study, with posterior mean estimates ranging from 0.904 to 0.991. First-year survival showed considerably greater interannual variation (range of posterior means: 0.130–0.879), and there

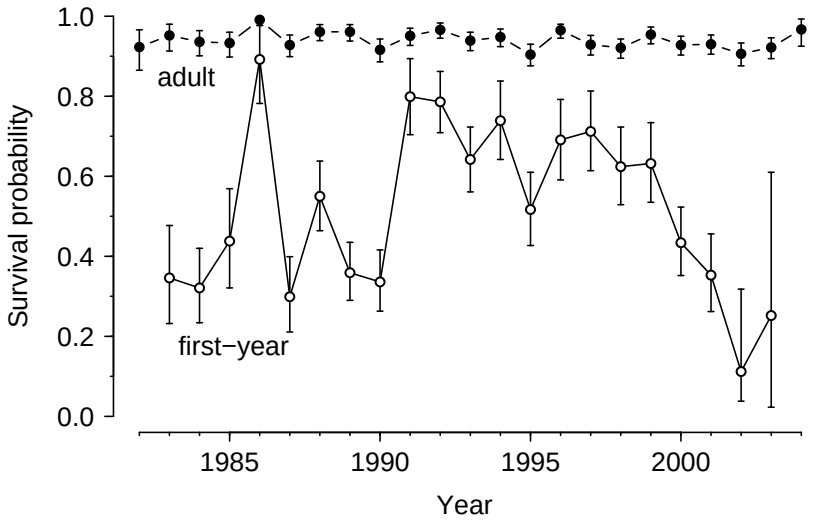

Figure 3.2 Posterior means and 95% symmetric CIs for adult and first-year survival under the integrated model.

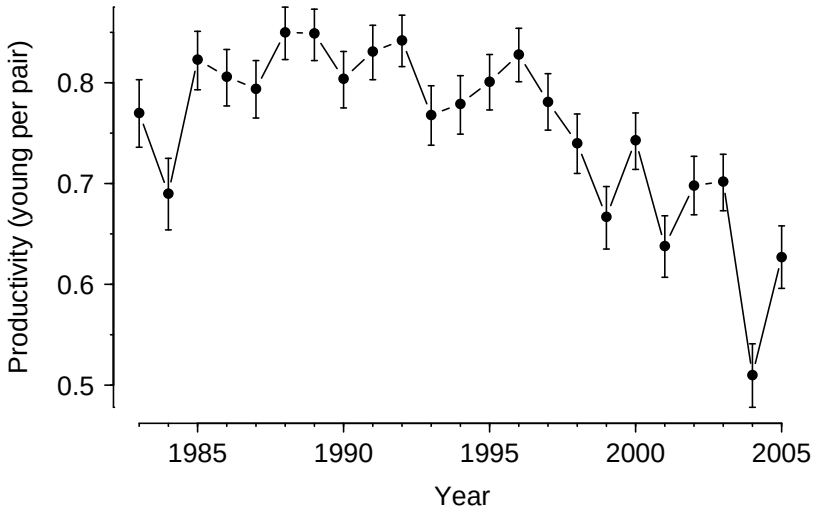

Figure 3.3 Posterior means and 95% symmetric CIs for productivity rates under the integrated model, defined as the mean number of chicks (males and females combined) fledged per breeding female.

appears to have been a steady decline in survival at the end of the study period. Constant survival estimates for immature birds (ages 1–3) are given in Table 3.3. Survival increased with age from age 0 (weighted mean survival over all years equal to 0.54) to age 2 years, by which time immature guillemots appear to have a survival rate approaching that of adult birds.

Figure 3.3 provides posterior means and CIs for productivity rates. Productivity was high and relatively stable during the first two-thirds of the study period, with all but one posterior mean estimate falling between 0.75 and 0.85;

Table 3.3 Posterior summary statistics for all time-invariant parameters: ages 1–3 survival; ages 4 and 5^+ resighting probabilities for birds ringed as chicks (areas A and B); regression parameters for recovery probabilities; fidelity rate and visibility parameter; and observation error variance.

Parameter	Mean	SD	95% symmetric CI
ϕ_1	0.76	(0.024)	$(0.72, 0.81)$
ϕ_2	0.93	(0.017)	$(0.89, 0.96)$
ϕ_3	0.91	(0.018)	$(0.87, 0.94)$
$p_4(A)$	0.62	(0.016)	$(0.58, 0.65)$
$p_{5+}(A)$	0.56	(0.013)	$(0.53, 0.58)$
$p_4(B)$	0.38	(0.024)	$(0.33, 0.43)$
$p_{5+}(B)$	0.34	(0.017)	$(0.31, 0.37)$
α_λ	-2.79	(0.067)	$(-2.92, -2.66)$
β_λ	-0.39	(0.073)	$(-0.54, -0.25)$
ψ	0.81	(0.022)	$(0.76, 0.85)$
τ	0.76	(0.010)	$(0.74, 0.78)$
σ^2_N	1.37×10^6	(6.01×10^5)	$(6.06 \times 10^5, 2.88 \times 10^6)$

however, a general and rather drastic decline is apparent from around 1998 onwards.

Resighting probabilities varied substantially over age, time and ringing area. Resighting probabilities of 2- and 3-year-old birds increased gradually between 1985 and 1990 and then declined in later years (see Figure 1 in Harris et al. 2007b). Harris et al. attribute these changes to increasing observer effort during the early years of the study and a real decline towards the end, when observers and methods remained constant. Age 3 resighting probabilities were somewhat higher than those for age 2 birds, and estimates were generally higher for birds ringed in area A compared to area B: ranges of posterior means for age 2 birds were (0.01–0.32) and (0.02–0.41) for areas A and B, respectively; corresponding ranges for age 3 birds were (0.16–0.80) and (0.02–0.63). Posterior means and CIs for constant resighting probabilities of chick-ringed birds aged 4 and 5 years-and-older are given in Table 3.3 and show a clear difference between birds ringed in areas A and B. Resighting probabilities of birds ringed as breeding adults were very high throughout the study (Figure 3.4; all posterior mean estimates except 2005 above 0.93) with little variation between years. The estimate for 2005 is unreliable (note the large CI) and is linked to the rather high estimate of adult survival in 2004. There does appear to have been a slight systematic decline in adult resighting probability through the course of the study, despite the fact that observer effort for these birds remained unchanged over the study period. Thus, it may be possible to model this parameter as a linear trend, which would also help to tie down final year survival estimates. The disparity

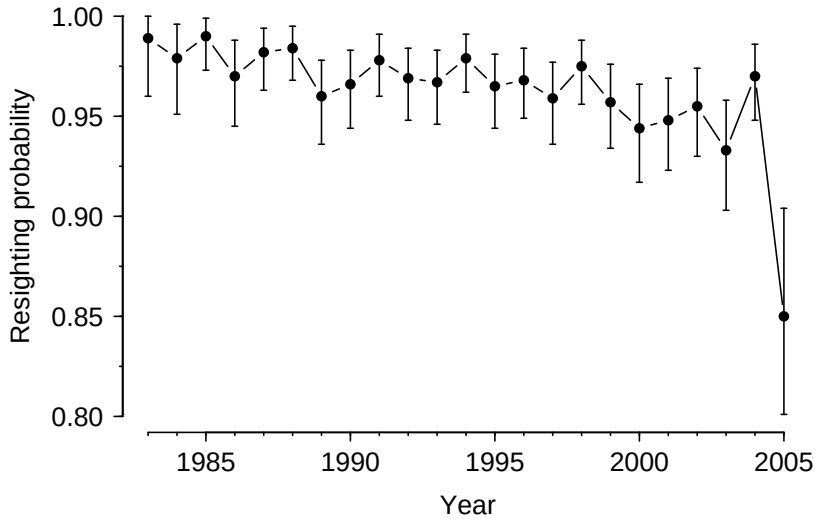

Figure 3.4 Posterior means and 95% symmetric CIs for resighting probabilities of birds ringed as breeding adults.

between the resighting probabilities of breeding birds ringed as adults ($p_{a,t}$) and those ringed as chicks (p_{5+}) clearly shows that it would be unrealistic to assume the same resighting probability for all ringed adults. As mentioned in Section 3.2.3, this is due to the different methods used to obtain resighting data for these two groups: birds ringed as breeding adults are resighted with high certainty within a confined area, whereas breeders that were ringed as chicks are widely dispersed and often difficult to see.

Posterior means and CIs for the intercept and slope parameters of the logit-linear trend on recovery probability (α_λ and β_λ, respectively) are given in Table 3.3. The negative estimate for β_λ and a 95% CI that does not include zero provide strong evidence for a temporal decline in recovery probability over the period of the study. Corresponding posterior estimates of λ_t range from 0.105 (95% CI: $0.082, 0.131$) at the beginning of the period to 0.032 ($0.024, 0.041$) at the end—a decrease of almost 70%.

Table 3.3 also provides posterior means and CIs for the fidelity rate ψ and visibility parameter τ. The estimate for fidelity implies a permanent pre-recruitment emigration rate of 19.5% from each cohort (95% CI: $15.0, 23.9$), and the estimate for τ suggests that among those birds ringed as chicks which do not emigrate, 24.2% ($22.2, 26.2$) per year lose their colour-rings or otherwise become unobservable once they have recruited.

3.5 Discussion

The focus of this chapter has been the combined analysis of count, mark-recapture, ring-recovery and productivity data from the long-running study of common guillemots on the Isle of May. We were able to develop a comprehensive process model for this population that incorporated delayed recruitment and accounted explicitly for the emigration of prebreeders, allowing us to estimate parameters that would have been unidentifiable with a single data series.

The integration of abundance and demographic data in models of wildlife population dynamics has been the subject of recent research by several authors. Previous studies have combined abundance data with ring-recoveries (Besbeas et al. 2002, Brooks et al. 2004, Besbeas & Freeman 2006), mark-recaptures (Goodman 2004, Schaub et al. 2007), mark-recapture and productivity data (Gauthier et al. 2007) and multi-site MRR data (Borysiewicz et al. 2008). However, as far as we are aware, this is the first study to integrate abundance data with all three of the major sources of demographic data.

Estimates of survival and productivity under the integrated model compared closely to those obtained from separate analyses of the MRR and productivity datasets using identical models. They were also consistent with previously published results based on these data (see, e.g., Harris et al. 2000, Crespin et al. 2006b, Harris et al. 2007b). Adult survival rates were similar to those from the separate analysis of the adult mark-recapture data, probably because the chick MRR data provides very little information on adult survival: although almost seven times as many birds were ringed as chicks, birds ringed as adults accounted for nearly three quarters of all adult resightings. Furthermore, there was no significant improvement in precision of the model parameters as a result of using the additional data. These findings suggest that most of the information on the survival and productivity parameters came from their respective datasets. Nevertheless, we are reassured that our model is reasonable, and the advantage of the combined parameter estimates is that they fully reflect all available information. We were also able to obtain improved estimates for the breeding adult population sizes due to 'borrowing' information from the other data sources, although an estimate of 1170 for the standard deviation of the count data ($\sqrt{\sigma_N^2}$; Table 3.3) suggests that the counts were reasonably precise.

The assumption of constant survival within the immature age classes is one aspect of the model that is perhaps unrealistic, and time-varying estimates may allow an improved fit to the count data. Although relatively few data are available to estimate survival of these ages, it may be more reasonable to assume

that they vary in parallel with those of first-years or adults in the same year (on the assumption that any annual variation in mortality would be likely to affect consecutive age-classes equally—especially as much is likely to be related to events away from the breeding grounds such as annual variation in weather, food supplies, oil spills, etc.). A model allowing parallel variation requires the same number of parameters as a constant survival model (one per age class for the immature age classes), and can be implemented by modelling survival for each age class as that of first-years or adults plus a difference parameter, preferably on the logit scale. Even more realistic, in a Bayesian framework, this difference parameter can even be modelled as a random effect using hierarchical models. We considered the former of these approaches in preliminary analyses using Program MARK, but there appeared to be less support in the data for such parallel survival models. Therefore, for the sake of simplicity and ease of interpretation, we favoured the constant survival model in the integrated analysis.

Previous studies all appear to suggest a marginally higher emigration rate for Isle of May prebreeders than our estimate of 19.5% (Harris et al. 1996a: 25–33%; Crespin et al. 2006a: 'perhaps as high as 25%'; Harris et al. 2007b: 'fidelity' estimates of 0.761 and 0.689 for birds aged 4 and 5^+ years respectively). However, their authors were unable to disentangle the effects of emigration, ring loss and reduced visibility of breeding birds. Because the count data also contained some indirect information on emigration, we were able to obtain separate, more robust estimates of emigration rate and the combined effects of colour-ring loss and low visibility. Our results suggest that over time the rate of ring loss from birds ringed as chicks, and their low visibility as adults, have an effect that is greater in magnitude than that of pre-recruitment emigration.

The contents of this chapter have been published as a paper in the *Journal of Agricultural, Biological and Environmental Statistics* (Reynolds et al. 2009).

Chapter 4

Predicting population change using an integrated model

4.1 Introduction

In the face of a changing climate and rapidly increasing human population, there is a growing need for reliable predictions of future trends in the size of wild animal populations, particularly for species of management or conservation concern. In particular, uncertainties in such predictions must be quantified and clearly presented. Forward projections and their associated estimates of uncertainty are already an important and popular piece of management advice in fisheries stock assessment, where they are used to inform quotas and predict the outcome of future management actions (Punt & Hilborn 1997, Maunder et al. 2006). Similarly, stochastic predictive models have been applied to other wild populations requiring active management: for example, to explore culling strategies for red deer *Cervus elaphus* (Trenkel et al. 2000) and great cormorants *Phalacrocorax carbo* (Smith et al. 2008), and for assessing the success of management policies for North American duck species (Jamieson & Brooks 2004). They also form the basis for population viability analyses to estimate species' extinction probabilities (Beissinger & McCullough 2002), and have been used to test assumptions about future environmental change in a number of species of conservation concern (e.g. black-legged kittiwake *Rissa tridactyla*: Frederiksen et al. 2004b; European shag *Phalacrocorax aristotelis*: Frederiksen et al. 2008; emporer penguin *Aptenodytes forsteri*: Jenouvrier et al. 2009a).

Predictions about future population size first require a model describing the population dynamics, and estimates of its component parameters. Two main types of predictive population model have been commonly applied: those based on historic time series of population fluctuations, with parameters such

as the specific population growth rate, the form of density regulation and the carrying capacity (e.g. Asbjørnsen et al. 2005, Sæther et al. 2007, 2009); and demographic models based on stochastic projection matrices (Caswell 2001), parameterised by estimates of fecundity and survival/growth rates (e.g. Nur et al. 1994, Stephens et al. 2002, Jenouvrier et al. 2009a). The type of predictive model used is usually determined by the available data for the species of interest. Where both abundance and demographic data are available, they may be combined in an 'integrated population model' (Brooks et al. 2004, Besbeas et al. 2005, 2008; see also Chapter 3). This approach has potential for obtaining more accurate and robust population predictions that fully reflect all available sources of information.

Environmental stochasticity influences fluctuations in the size of large populations (Sæther et al. 1998) and should always be considered when developing realistic predictive population models (Nur & Sydeman 1999, Maunder et al. 2006). Only with a stochastic framework is it possible to gain a sense of variability of outcome (Nur & Sydeman 1999), yet it is knowledge of this uncertainty that is often more interesting and useful than the average predicted trajectory. Quantifying environmental variability is usually by means of estimating the temporal process variance in population fluctuations or demographic rates, based on historical data. This is best implemented in a random effects framework (Gould & Nichols 1998, Loison et al. 2002): if both the estimated and predicted parameters are treated as random effects, there is no difference between the two so that, for example, future survival rates are no different from historical survival rates (Maunder et al. 2006). Investigations of small populations should also include the effects of genetic and demographic stochasticity (Nur & Sydeman 1999).

Reliable population projections also need to account for parameter uncertainty and errors in estimating population size, both of which affect the variability of the predictions (Sæther et al. 2009). The model parameters are not known with certainty and must be estimated from observable data, providing a range of possibilities for the 'true' parameter value. Projecting from parameter point estimates ignores this uncertainty—which in some cases represents the majority of the uncertainty in a model (Maunder et al. 2006)—and can lead to overly optimistic prediction intervals and considerable inaccuracies in estimating future quantities of interest (Sæther & Engen 2002). Likewise, treating estimates of population size as if they were the true values may result in biased population projections with far greater levels of uncertainty (Jamieson & Brooks 2004, Sæther et al. 2007). Consequently, it is also necessary to estimate

and model observation error, and the most common framework for this is a state-space model (e.g. de Valpine & Hastings 2002, Buckland et al. 2004).

The issues of model specification and model selection introduce yet further elements of uncertainty, and hence variability, into predictions about a particular ecological system (Harwood & Stokes 2003). Biological processes can often be described adequately by many rival models, and model uncertainty can form an important part of the predictive framework and management planning process. Model mis-specification, on the other hand, can contribute to errors in parameter estimation through the inferential process which will be amplified by the prediction process.

A Bayesian approach is the natural choice for analysing predictive population models, for a number of reasons. First, Bayesian analyses facilitate representing and accounting for uncertainties related to parameter values (and models, where more than one model is considered; Punt & Hilborn 1997, Jamieson & Brooks 2004). Each posterior sample is a plausible realisation of the parameters; therefore, each set of parameter values can be used sequentially as input parameters for stochastic projections (Taylor et al. 1996). Second, the Bayesian approach easily deals with the fitting of non-normal, nonlinear state-space models to estimate and model the true underlying population sizes (Newman 1998, Millar & Meyer 2000)—a process that can be complicated within the classical paradigm (Brooks et al. 2004, Jamieson & Brooks 2004, King et al. 2008b). Third, the difficulties involved in modelling random effects in a conventional likelihood-based framework are naturally dealt with within a Bayesian framework (Royle & Link 2002, Link & Barker 2004, King et al. 2009). Finally, Bayesian analyses yield probability distributions (posterior distributions) that are easy to understand and communicate to managers, stakeholders and policy makers, and can be queried for biologically important questions, for example: 'What is the probability that the population will decline by more than 25% over a 10-year period?' (Taylor et al. 1996, Wade 2000, Brooks et al. 2008).

In recent years, many UK seabird populations have experienced declines in demographic performance, including a number of high-profile breeding failures and severe mortality events (e.g. Eaton et al. 2005, 2007). However, while worrying long-term declines in population size have also been recorded for some species (e.g. the black-legged kittiwake: Heubeck 2004, JNCC 2009), others, particularly the offshore diving species (including the common guillemot *Uria aalge*), have increased in numbers or remained relatively stable over the same period (JNCC 2009). Most seabirds have low annual recruitment rates (small clutch sizes, deferred sexual maturity) and high adult survival (Croxall & Roth-

ery 1991), so populations tend to change slowly over time and even major declines in breeding success and/or juvenile survival can take a long time to show up as reductions in population size. Conversely, even if these rates return to 'normal' levels the breeding population may continue to decline for a number of years (Croxall & Rothery 1991), and its subsequent ability to recover is constrained by the naturally low reproductive output (Nur & Sydeman 1999). Given these characteristics and in light of the recent widespread breeding failures, an imminent decline in many UK seabird populations seems likely and their long-term futures are highly uncertain (Heath et al. 2009). There is thus an urgent need for predictions of the future consequences of current demographic trends, to investigate the expected magnitude and duration of any population declines and the likelihood of recovery under different scenarios.

Common guillemots are one of the species to be most affected by recent events, having suffered widespread declines in both breeding success (e.g. Mavor et al. 2005, 2008) and survival (e.g. Harris et al. 2007b) since the early 2000s (see also Chapter 3). In this study, we combine detailed abundance and demographic data from 25 years of intensive field research on common guillemots on the Isle of May, southeast Scotland, to predict 10-year population trajectories under a range of assumptions about future demographic rates. For example, we project productivity, juvenile survival and adult survival according to their long-term historical means and variabilities, and compare resulting population trajectories with those generated according to more recent trends in each, and all, of these parameters. An integrated population model, analysed in a Bayesian framework, simultaneously provides posterior distributions of historical and future parameter values and population sizes. By estimating the posterior probability of population decline from these distributions under each scenario, we investigate which parameter declines are of the greatest concern for the future of the population. Results are compared to a traditional sensitivity analysis and discussed in the context of environmental change.

4.2 Methods

4.2.1 Modelling framework

We use the integrated population model presented in Chapter 3 as a framework for predicting future population sizes of the Isle of May guillemot colony. To recapitulate, we have four sources of data and their corresponding models—counts, adult mark-recapture, chick mark-recapture-recovery, and productivity

(see Sections 3.2.1–3.2.4)—which we combine to form a joint probability distribution for the data (Section 3.2.5). This is analysed in a Bayesian framework using Markov chain Monte Carlo (MCMC) to obtain a posterior distribution for the model parameters (survival, recapture, recovery, fidelity, ring loss and productivity rates) and population sizes (numbers of female breeders $\boldsymbol{X}$ and prebreeders $\boldsymbol{J}$; Section 3.3).

In the present analysis we make use of two additional years of data, giving a total of 25 years (1983–2007, denoted $t = 1, \ldots, T$). As well as obtaining parameter and population estimates for these years, within the framework of the integrated model we also project the population forwards a further 10 years to 2017, thus providing posterior distributions of the predicted breeding adult and prebreeder population sizes. This approach ensures that all the major sources of uncertainty are accounted for in the population projections. Methodological details of the predictions are provided in the following sections.

4.2.2 Random effects modelling of demographic rates

To provide a framework for incorporating environmental stochasticity into the population projections, we modify the models for all time-dependent survival and productivity rates. First-year survival, adult survival and productivity were allowed to vary over time in Chapter 3 by specifying models containing fixed year-effects. Here, we alternatively account for year-to-year variation by assuming underlying random effects models for these parameters. Taking productivity, which for year t we denote by ρ_t, as an example, we assume that

$$\text{logit}(\rho_t) = \mu_\rho + \epsilon_{\rho,t}, \tag{4.1}$$

where

$$\epsilon_{\rho,t} \sim \text{N}(0, \sigma^2_\rho). \tag{4.2}$$

(Recall that, for guillemots, $0 \leqslant \rho_t \leqslant 1$, i.e., each female can produce a maximum of one chick per year.) Analogous models exist for first-year survival $\phi_{0,t}$ (with hyperparameters μ_0, $\epsilon_{0,t}$ and σ^2_0) and adult survival $\phi_{a,t}$ (hyperparameters μ_a, $\epsilon_{a,t}$ and σ^2_a). The $\mu_\cdot$ represent underlying survival and productivity rates, and the $\epsilon_{\cdot,t}$ denote random year effects, which are assumed to come from an underlying mean-zero normal distribution with variance $\sigma^2_\cdot$. It is the parameters of the underlying distributions (the $\mu_\cdot$ and $\sigma^2_\cdot$) that we are interested in, as we use the estimates of these parameters to simulate future survival and productivity rates (see below).

Priors

Prior distributions for the Bayesian analysis are specified on the random effects means and variances. We take a logistic prior for the $\mu_.$, which has the desirable property of inducing a $U(0,1)$ distribution on the corresponding survival/productivity rates in the absence of random year effects. For the variance parameters, we follow Gelman (2006) and use a noninformative uniform prior density on the standard deviation parameters $\sigma_.$. In some cases, where the uniform prior led to unrealistically high estimates of $\sigma_.$, we replace it with a half-Cauchy distribution with scale set to 2 (also after Gelman 2006). The half-Cauchy has a broad peak at zero and a gentle slope in the tail, and is thus considered a 'weakly informative' prior distribution. The value of the scale parameter is chosen to be a bit higher than the maximum we expect for $\sigma_.$, the aim being to restrict the sampler away from unrealistic values but otherwise let the data inform the posterior. Sensitivity to the chosen priors for the $\sigma_.$ was assessed by also specifying the traditional inverse-gamma prior with both parameters set to 10^{-3} on the $\sigma_.^2$. Prior distributions for the rest of the model parameters and the initial population levels are as described in Section 3.3.1.

4.2.3 Obtaining future population estimates

We describe two implementational approaches to obtaining posterior samples of future population sizes. In the first, we generate future survival and productivity rates and update the predicted population states within the MCMC algorithm (within-chain predictions). The second method initially obtains a posterior sample of the parameter values, excluding the future states; then, given the set of posterior values, we impute future parameter values for each individual posterior sample independently (independent post hoc predictions).

Within-chain predictions

At each iteration of the chain, we first update all historical parameter values and states for times $t = 1, \ldots, T$ or $T-1$ (dependent on the parameter) using a Metropolis-Hastings random walk algorithm with uniform proposal density, as described in Section 1.3.3. Using the same algorithm we then propose to update, for example, $\epsilon_{\rho,t}$ from $t = T+1, \ldots, T+P$, where $P = 10$ is the number of years to be predicted; however, because there are no data for this period, acceptance probabilities for proposed moves depend only on the process likelihood (equation (3.6)) and the normal 'prior' with variance σ_ρ^2 placed on the

$\epsilon_{\rho,t}$ (equation (4.2)). With the updated $\epsilon_{\rho,t}$ and current value of μ_ρ, we calculate future productivity rates ρ_t by the inverse-logit of equation (4.1). Similarly, we generate future first-year and adult survival rates from $t = T, \ldots, T + P$ by updating $\epsilon_{0,t}$ and $\epsilon_{a,t}$ for those years.

Given the future demographic rates, we update the corresponding future population sizes of female breeders Y_t and Z_t (respectively, continuing female breeders, equation (3.2), and new female recruits, equation (3.3); total breeders $X_t = Y_t + Z_t$) and female prebreeders J_t (equation (3.4)). There is only the process model involved in formulating future J and X values.

The above method is the more intuitive, and elegant, means of obtaining posterior samples of predicted population sizes. However, because the acceptance probability of any proposed update of future population sizes depends on the values of the future demographic parameters at the current iteration—and vice versa—the imputed predicted values are necessarily highly correlated. Correspondingly, proposal distributions need to be narrow and mixing of the MCMC chain is poor. Given the large degree of uncertainty in population sizes towards the end of the prediction period, this method proved impractical for obtaining suitable samples from the posterior: even after 10 million iterations (two weeks of computing time) the chain did not appear to have converged and the Monte Carlo error was unacceptably large.

Independent post hoc predictions

As an alternative to the above approach, we initially run the Bayesian integrated model to obtain a posterior sample of parameter values and population sizes for the historical period $t = 1, \ldots, T$ only. Then, for each posterior sample i from the MCMC chain ($i = 1, \ldots, S$, where S is the number of (thinned) post-burn-in samples) we first simulate new future productivity, first-year survival and adult survival rates by sampling from

$$\text{logit}(\rho_t^{(i)}) \sim \text{N}(\mu_\rho^{(i)}, \sigma_\rho^{2(i)}), \qquad t = T+1, \ldots, T+P, \tag{4.3a}$$

$$\text{logit}(\phi_{0,t}^{(i)}) \sim \text{N}(\mu_0^{(i)}, \sigma_0^{2(i)}), \qquad t = T, \ldots, T+P, \tag{4.3b}$$

and

$$\text{logit}(\phi_{a,t}^{(i)}) \sim \text{N}(\mu_a^{(i)}, \sigma_a^{2(i)}), \qquad t = T, \ldots, T+P. \tag{4.3c}$$

The normal distribution parameters in equations (4.3) are the underlying means and variances from the random effects models, with superscript '(i)' denoting the ith sample from the posterior distribution. Future values for time-constant

survival rates ϕ_1, ϕ_2 and ϕ_3, and fidelity rate ψ, simply take their values as at the ith iteration.

Given the demographic rates and the ith sample of the current population sizes X_T and J_{T-4}, we generate future breeding population trajectories for $t = T+1, \ldots, T+P$ and obtain the corresponding posterior distribution by sampling from

$$Y_t^{(i)} \sim \text{Bin}(X_{t-1}^{(i)}, \phi_{a,t-1}^{(i)}) \tag{4.4}$$

and

$$Z_t^{(i)} \sim \text{Bin}(J_{t-5}^{(i)}, \psi^{(i)}\phi_{a,t-1}^{(i)}), \tag{4.5}$$

with $X_t^{(i)} = Y_t^{(i)} + Z_t^{(i)}$ representing the total predicted population sizes of female breeders in year t. Similarly, for $t = T-3, \ldots, T+P$ we sample from

$$J_t^{(i)} \sim \text{Bin}(X_t^{(i)}, \rho_t^{(i)}\phi_t^{*(i)}/2) \tag{4.6}$$

to generate predicted population sizes of female prebreeders, where $\phi_t^{*(i)} = \phi_{0,t}^{(i)}\phi_1^{(i)}\phi_2^{(i)}\phi_3^{(i)}$.

The posterior distribution for the predicted states obtained using this approach will be the same as for the previous method. Both approaches take full account of all sources of uncertainty liable to affect the estimates of future population sizes: uncertainty in the demographic parameter estimates; uncertainty in the counts, and hence the values of the true underlying population sizes during the study period; and uncertainty caused by future environmental stochasticity (although in our approach this is limited to the range of historic interannual variation and does not account for potentially more extreme conditions in the future). However, the current approach significantly reduces the dependence of the predicted states, and hence increases the effective sample size (the number of effectively independent draws from the posterior distribution) of predicted values.

We ran the MCMC chain for 2 million iterations, discarding the first 1 million as burn-in, which convergence diagnostics indicated was ample for this model (see Section 3.3.3). To save storage space, and to reduce the autocorrelation among consecutive samples, we thinned the output to every one-hundredth iteration, thus providing 10,000 posterior samples. To boost the sample size of projected population sizes, we simulated 10 projections from each realisation of the posterior, resulting in 100,000 posterior samples for each predicted state. The MCMC simulation took approximately 40 hours, and the subsequent

projections took less than 1 minute!

4.2.4 Prediction scenarios

We apply several different scenarios for projecting future population trajectories, differentiated by variations in the models used to simulate future demographic parameters. We note in Section 3.4 that both first-year survival and productivity declined steadily towards the end of the study period (from around year 2000 to 2005; see Figures 3.2 and 3.3). Two further years of data suggest that this decline has continued; furthermore, adult survival also appears to have declined over the same period, with three of the four lowest survival estimates of the study occurring during this interval (2002, 2004 and 2005). For each of these three parameters, we therefore consider splitting the random effects model into two separate models: one for the period of (relatively) high and stable survival and productivity 1983–1999, and a second for the period of decreasing survival and productivity from year 2000 onwards. Thus, letting $t_K = 17$ (i.e., 1999), the model for productivity becomes

$$\text{logit}(\rho_t) = \mu_{\rho 1} + \epsilon_{\rho,t}, \qquad t = 1, \ldots, t_K, \tag{4.7a}$$

$$\text{logit}(\rho_t) = \mu_{\rho 2} + \epsilon_{\rho,t}, \qquad t = t_K + 1, \ldots, T, \tag{4.7b}$$

where

$$\epsilon_{\rho,t} \sim \text{N}(0, \sigma^2_{\rho 1}), \qquad t = 1, \ldots, t_K, \tag{4.8a}$$

$$\epsilon_{\rho,t} \sim \text{N}(0, \sigma^2_{\rho 2}), \qquad t = t_K + 1, \ldots, T, \tag{4.8b}$$

with similar definitions for first-year and adult survival. Assuming that recent conditions persist in the future, we can use the underlying means and variances from the latter period ($\mu_{\cdot 2}$ and $\sigma^2_{\cdot 2}$) to simulate future demographic rates according to equation (4.3), which we then feed in to equations (4.4) to (4.6) to project population sizes. By altering which demographic rates we predict according to the full time-series mean and variance, and which by the mean and variance for years 2000-onwards, we generate five prediction scenarios, summarised in Table 4.1.

We specify a prediction period of $P = 10$ years (taking the population to year 2017), which gives a reasonable time frame for the predictions to settle down and to observe potential future trends following the period of influence of recent survival and productivity rates (up to 2012). Given the posterior

Table 4.1 Description of the five scenarios used to simulate future demographic rates, and hence generate projections of population size.

Scenario	Definition
S1—'Business as usual'	Random effects means and variances derived from the entire study period are used to simulate future rates for all time-varying demographic parameters.
S2—'Productivity 2000'	Productivity rates simulated using random effects mean and variance from year 2000 onwards ($\mu_{\rho 2}$ and $\sigma^2_{\rho 2}$).
S3—'First-year survival 2000'	First-year survival simulated using random effects mean and variance from year 2000 onwards (μ_{02} and σ^2_{02}).
S4—'Adult survival 2000'	Adult survival simulated using random effects mean and variance from year 2000 onwards (μ_{a2} and σ^2_{a2}).
S5—'Worst case'	All three time-varying demographic rates simulated using random effects means and variances from 2000 onwards (combination of S2, S3 and S4).

distribution of current and future breeding population sizes generated by each scenario, we calculate the posterior probability of population decline below the current (2007) level, and probabilities of greater than 10% and greater than 25% declines, over the 10-year prediction period: these are, respectively, the proportions of posterior samples for which $X_{T+P} < X_T$, $X_{T+P} < 0.90X_T$ and $X_{T+P} < 0.75X_T$. Furthermore, we obtain the posterior distribution for the predicted proportional change in population size between 2007 and 2017, by calculating $(X^{(i)}_{T+P} - X^{(i)}_T)/X^{(i)}_T$ for each sample i.

4.2.5 Matrix population modelling

To explore the theoretical effect of changes in the different vital rates on population growth rate, we construct an age-classified matrix population model and conduct a perturbation analysis, to calculate sensitivities and elasticities (Caswell 2001). Sensitivity is defined as the absolute change in population growth rate given an absolute change in a vital rate. However, because the magnitude of vital rates may vary considerably it is usually more useful to work with elasticities, defined as the proportional change in population growth rate given a proportional change in a vital rate, that is, sensitivity rescaled to account for the magnitude of the vital rate.

In a stochastic environment such as ours, population growth is described by the time-varying matrix population model

$$\boldsymbol{n}(t+1) = \boldsymbol{A}_t \boldsymbol{n}(t), \tag{4.9}$$

where $\boldsymbol{n}(t)$ is a vector giving the numbers in each age class of the population at time t, and $\boldsymbol{A}_t$ is the projection matrix describing population growth of these age classes from time t to $t+1$ (Caswell 2001). Because guillemot breeding occurs annually over a relatively short period we consider a birth-pulse model, and we assume a prebreeding census. The population vector $\boldsymbol{n}(t)$ therefore contains five age-classes (1-year-old, 2-year-old, 3-year-old, 4-year-old and 5^+-year-old (adult) individuals) and the female-based projection matrix $\boldsymbol{A}_t$ is structured accordingly:

$$\boldsymbol{A}_t = \begin{bmatrix} 0 & 0 & 0 & 0 & \rho_t\phi_{0,t} \\ \phi_1 & 0 & 0 & 0 & 0 \\ 0 & \phi_2 & 0 & 0 & 0 \\ 0 & 0 & \phi_3 & 0 & 0 \\ 0 & 0 & 0 & \psi\phi_{a,t} & \phi_{a,t} \end{bmatrix}, \tag{4.10}$$

with the parameters taking analogous definitions to those previously defined.

Following Caswell (2001, 2005), we use numerical simulations to compute the stochastic growth rate λ_s and its sensitivity and elasticity to the entries of $\boldsymbol{A}_t$ and to lower-level parameters. We have a full sequence of $N = 24$ population projection matrices $\boldsymbol{A}_1, \ldots, \boldsymbol{A}_N$, parameterised by the corresponding survival, productivity and fidelity estimates (posterior means) for the period 1983–2006 derived from the output of S1, and we take this sequence as a sample of environmental variability. We additionally consider a reduced set of $N = 7$ projection matrices for years 2000–2006, corresponding to the later period in the prediction scenarios described above, which we parameterise with the appropriate posterior means from S5. Then, for a large number of time periods ($T = 50000$), we draw at each time an integer uniformly distributed between 1 and N and use the corresponding matrix to project the population.

Beginning with an arbitrary non-negative vector $\boldsymbol{w}(0)$, with $\|\boldsymbol{w}(0)\| = 1$ where $\|\cdot\|$ denotes the 1-norm, we generate and store a sequence of age distribution vectors

$$\boldsymbol{w}(t+1) = \frac{\boldsymbol{A}_t\boldsymbol{w}(t)}{\|\boldsymbol{A}_t\boldsymbol{w}(t)\|}, \qquad t = 0, \ldots, T-1, \tag{4.11}$$

and one-step growth rates

$$R_t = \frac{\|\boldsymbol{A}_t\boldsymbol{w}(t)\|}{\|\boldsymbol{w}(t)\|}, \qquad t = 0, \ldots, T-1. \tag{4.12}$$

Similarly, starting with an arbitrary non-negative terminal vector $\boldsymbol{v}(T)$ with $\|\boldsymbol{v}(T)\| = 1$, we use the same sequence of matrices to generate and store a

sequence of reproductive value vectors

$$\boldsymbol{v}^{\mathsf{T}}(t-1) = \frac{\boldsymbol{v}^{\mathsf{T}}(t)\boldsymbol{A}_{t-1}}{\|\boldsymbol{v}^{\mathsf{T}}(t)\boldsymbol{A}_{t-1}\|}, \qquad t = T, \ldots, 1. \tag{4.13}$$

The stochastic growth rate λ_s is taken as the average of the simulated R_t (Cohen et al. 1983), after discarding 5000 initial iterations to eliminate transient effects. Based on Tuljapurkar's (1990) derivation, the sensitivity of $\log \lambda_s$ to the elements a_{ij} of $\boldsymbol{A}_t$ is calculated by

$$\frac{\partial \log \lambda_s}{\partial a_{ij}} = \frac{1}{T} \sum_{t=0}^{T-1} \frac{v_i(t+1) w_j(t)}{R_t \boldsymbol{v}^{\mathsf{T}}(t+1) \boldsymbol{w}(t+1)}, \tag{4.14}$$

and the elasticities of λ_s to a_{ij} by

$$\frac{\partial \log \lambda_s}{\partial \log a_{ij}} = \frac{1}{T} \sum_{t=0}^{T-1} \frac{v_i(t+1) a_{ij}(t) w_j(t)}{R_t \boldsymbol{v}^{\mathsf{T}}(t+1) \boldsymbol{w}(t+1)}. \tag{4.15}$$

Several entries of $\boldsymbol{A}_t$ are defined in terms of lower-level parameters; for example, overall fecundity given by a_{15} is the product of annual productivity and first-year survival rates ($\rho_t \phi_{0,t}$), and apparent survival of 4-year-olds, a_{54}, is moderated by emigration ($\psi \phi_{a,t}$). Therefore, we require to calculate the sensitivity of $\log \lambda_s$ and the elasticity of λ_s to ρ, ϕ_0, ψ and ϕ_a. Denoting the lower-level parameter of interest by θ, Caswell (2005) derived the sensitivity of $\log \lambda_s$ to θ as

$$\frac{\partial \log \lambda_s}{\partial \theta} = \frac{1}{T} \sum_{t=0}^{T-1} \frac{\boldsymbol{v}^{\mathsf{T}}(t+1) \dfrac{\partial \boldsymbol{A}_t}{\partial \theta} \boldsymbol{w}(t)}{R_t \boldsymbol{v}^{\mathsf{T}}(t+1) \boldsymbol{w}(t+1)} \tag{4.16}$$

and the elasticity of λ_s to θ as

$$\frac{\partial \log \lambda_s}{\partial \log \theta} = \frac{1}{T} \sum_{t=0}^{T-1} \frac{\theta_t \boldsymbol{v}^{\mathsf{T}}(t+1) \dfrac{\partial \boldsymbol{A}_t}{\partial \theta} \boldsymbol{w}(t)}{R_t \boldsymbol{v}^{\mathsf{T}}(t+1) \boldsymbol{w}(t+1)}. \tag{4.17}$$

Simulations were implemented in program Octave (Eaton et al. 2008a) using code fragments provided by Caswell (2001, chapter 14), plus an additional algorithm for lower-level parameters described in Caswell (2005).

4.3 Results

4.3.1 Population projections

We projected the Isle of May guillemot population forward 10 years, using the second of the two methods described in Section 4.2.3 (independent post hoc predictions), under five different scenarios (S1 to S5; see Table 4.1). Table 4.2 provides posterior means and standard deviations for random effects means and variances estimated under each scenario, along with the corresponding simulated future demographic rates, averaged over all predicted years. Where split random effects models were used (S2 to S5), underlying means on the logit scale for years 2000-onwards ($\mu_{\cdot 2}$) were consistently lower than those for the earlier years ($\mu_{\cdot 1}$; 1983–1999), with no overlap in the corresponding 95% credible intervals (CIs; not shown) for productivity and adult survival models, and only slight overlap for the first-year survival model. Predicted rates on the real scale were correspondingly lower under scenarios with split random effects models than when based on the entire historical time series. With the exception of

Table 4.2 Posterior means (SDs) for random effects means $\mu_{\cdot\cdot}$ and variances $\sigma^2_{\cdot\cdot}$, and corresponding simulated real parameters ρ_t, $\phi_{0,t}$ and $\phi_{a,t}$ (averaged over all predicted years), under each prediction scenario.

	Prediction scenario				
Parameter	**S1**	**S2**	**S3**	**S4**	**S5**
$\mu_{\rho 1}$	1.01 (0.14)	1.34 (0.08)	1.01 (0.14)	1.00 (0.14)	1.35 (0.08)
$\sigma^2_{\rho 1}$	0.50 (0.16)	0.10 (0.05)	0.50 (0.16)	0.50 (0.16)	0.10 (0.05)
$\mu_{\rho 2}$	–	0.33 (0.34)	–	–	0.30 (0.30)
$\sigma^2_{\rho 2}$	–	0.85 (0.88)	–	–	0.81 (0.74)
ρ_t	0.71 (0.14)	0.57 (0.19)	0.71 (0.14)	0.71 (0.14)	0.57 (0.19)
μ_{01}	0.07 (0.21)	0.07 (0.22)	0.30 (0.22)	0.07 (0.20)	0.28 (0.25)
σ^2_{01}	0.87 (0.39)	0.86 (0.41)	0.86 (0.39)	0.86 (0.38)	0.87 (0.42)
μ_{02}	–	–	−0.74 (0.58)	–	−0.68 (0.52)
σ^2_{02}	–	–	1.83 (3.88)	–	1.36 (2.63)
$\phi_{0,t}$	0.52 (0.20)	0.51 (0.20)	0.36 (0.21)	0.51 (0.20)	0.37 (0.19)
μ_{a1}	2.72 (0.10)	2.73 (0.10)	2.73 (0.10)	2.88 (0.13)	2.89 (0.13)
σ^2_{a1}	0.19 (0.09)	0.20 (0.10)	0.21 (0.10)	0.22 (0.14)	0.23 (0.14)
μ_{a2}	–	–	–	2.34 (0.12)	2.34 (0.11)
σ^2_{a2}	–	–	–	0.06 (0.11)	0.06 (0.13)
$\phi_{a,t}$	0.93 (0.03)	0.93 (0.03)	0.93 (0.03)	0.91 (0.02)	0.91 (0.02)

Notes: Where estimates of $\mu_{\cdot 2}$ and $\sigma^2_{\cdot 2}$ are not provided, simulated rates for the corresponding demographic parameter are based on $\mu_{\cdot 1}$ and $\sigma^2_{\cdot 1}$, which are derived from the entire time-series of data. Estimates of $\mu_{\cdot 2}$ and $\sigma^2_{\cdot 2}$ indicate split random effects models (equations (4.7) and (4.8)), denoting the random effects mean and variance for years 2000-and-onwards, and simulated future demographic rates are based on these parameters.

adult survival, the recent period was also more variable than the earlier years ($\sigma^2_{\cdot 2} > \sigma^2_{\cdot 1}$), presumably due to this being a period of declining, rather than stable, dynamics. Regarding prior sensitivity for the variance parameters, in most cases the chosen priors (uniform: $\sigma_{\rho 1}$, $\sigma_{\rho 2}$, σ_{01}, σ_{a1}, σ_{a2}; half-Cauchy: σ_{02}) gave essentially identical results to the alternative inverse-gamma prior specified on the $\sigma^2_{\cdot\cdot}$. However, in the case of σ^2_{a2}, which was estimated to be very small, posterior inference appears to have been constrained by the inverse-gamma prior (see Gelman 2006), and therefore our choice of alternative priors appears to be more appropriate.

Posterior means and corresponding 95% CIs for historical and future estimates of population sizes $\boldsymbol{J}$ and $\boldsymbol{X}$ obtained under each scenario are provided in Figure 4.1. During 2008–2012, predicted breeding population sizes remained under the influence of recent (2003–2007) productivity and first-year survival rates, as the $J_{T-4}, \ldots, J_T$ matured and recruited into the breeding population. Following this transition period, the 'true' projected trend became apparent. Under S1, there was initially a period of stable or decreasing population sizes, followed by a steady increase similar in rate to the majority of the historical period (Figure 4.1a). S2, S3 and S4, characterised by low future productivity, first-year survival and adult survival, respectively, all exhibited similar projected population trajectories, with stable or slightly increasing breeding populations after the transition period (Figures 4.1b–d). When all three time-varying demographic parameters were projected at their post-2000 rates (S5), the predicted breeding population declined rapidly throughout the projection period, with a corresponding decline in the number of prebreeders (Figure 4.1e).

The count data, which are overlaid on each plot in Figure 4.1, indicate a sudden and dramatic decrease in breeding population size between 2005 and 2006, and subsequent counts—including the two most recent estimates for 2008 and 2009—suggest this decline has continued, albeit at a lower rate. The population model did not capture the initial decline in the counts, which was much faster than expected, and none of the prediction scenarios were able to replicate the more recent counts (none of the posterior 95% CIs for the 2006–2009 population estimates include the corresponding counts). However, 'worst case' scenario S5 appears to have approximated the 2005–2009 trajectory reasonably well, and continued at a similar rate of decline beyond this period.

All of the above descriptions of population trajectories are based on the posterior mean predicted population sizes; however, we note that the corresponding 95% CIs soon become very large so that there is a large amount of uncertainty. The posterior probabilities of population decline, provided in Table 4.3, sum-

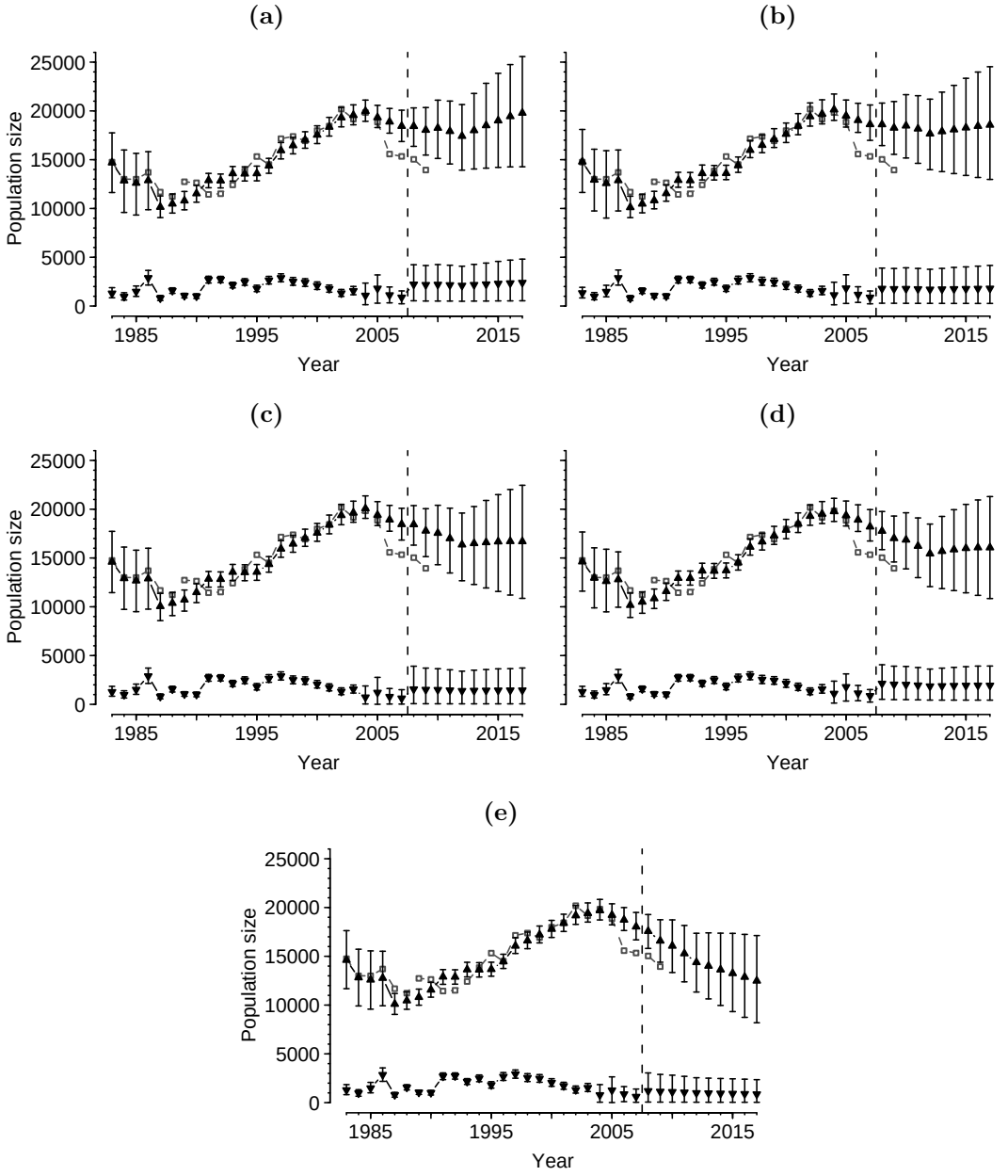

Figure 4.1 Posterior means and 95% symmetric CIs for historical and predicted population levels of female prebreeders $\boldsymbol{J}$ (▼) and breeding females $\boldsymbol{X}$ (▲), obtained under the five prediction scenarios: (a) S1—'business as usual'; (b) S2—future productivity simulated at post-2000 levels; (c) S3—future first-year survival simulated at post-2000 levels; (d) S4—future adult survival simulated at post-2000 levels; (e) S5—all three of the above demographic parameters simulated at post-2000 levels. The vertical dashed line indicates the beginning of the 10-year prediction period. The count data $\boldsymbol{N}$ are also plotted for 1983–2009 (□).

marise this uncertainty into a single statistic that is easy to compare between scenarios. S1 gave a probability of decrease of 0.305, which equates to a greater than even probability that the population will increase over the next 10 years. However, there remains a very small probability that the population will decline by more than 25% under these conditions. The probability of decrease

Table 4.3 Posterior probabilities of future population decline over a 10-year period (2007–2017) under each of the five scenarios, along with posterior means and 95% credible intervals for the predicted proportional change in population size over the same period (positive values indicate an increase, negative values a decrease).

	Pr(population decrease)			
Scenario	**Decrease**	**Decr. > 10%**	**Decr. > 25%**	**Proportional change**
S1	0.305	0.113	0.012	0.072 (−0.208, 0.357)
S2	0.520	0.251	0.042	0.004 (−0.284, 0.289)
S3	0.728	0.478	0.161	−0.095 (−0.399, 0.204)
S4	0.834	0.558	0.141	−0.119 (−0.380, 0.130)
S5	0.994	0.964	0.697	−0.309 (−0.534, −0.078)

became progressively larger moving from S2 to S4, which appears to mainly reflect differences in trajectory through the transition period, as all three populations appear to be stable or slightly increasing following this period (see Figures 4.1b–d). The 'worst case' scenario S5 gave a very high probability of population decline over a 10-year period of 0.994, and it is likely that this decline will be of a magnitude greater than 25%. This is confirmed by the proportional decline, also provided in Table 4.3, which suggests a mean predicted population decrease of approximately 31% after 10 years, corresponding to a growth rate of -3.6% year^{-1}. Furthermore, and unlike S1 to S4, the 95% CI for the proportional change under S5 does not include zero, so that there appears to be very strong evidence of a decline in population under these conditions.

4.3.2 Perturbation analysis

The estimated stochastic population growth rate λ_s based on the full set of $N = 24$ environments was 1.026, or $+2.6\%$ year^{-1}. This accords well with the post-transitional (after 2012) predicted growth rate under S1 (posterior mean 5-year proportional change of 0.135, giving an identical growth rate of $+2.6\%$ year^{-1}). Associated sensitivity and elasticity matrices corresponding to the projection matrix entries a_{ij} are shown in Figure 4.2, and sensitivities of $\log \lambda_s$ and elasticities of λ_s to lower-level parameters are provided in Table 4.4. The larger the elasticity of a parameter, the more sensitive the population growth rate to proportional changes in that parameter (this is not necessarily the case for sensitivities, as they are magnitude-dependent). Therefore, population growth rate appears to be most sensitive to proportional changes in adult survival and considerably less sensitive to changes in the other matrix elements and lower-level parameters, which all have the same elasticities. For example, a 10% decrease in adult survival would result in an approximately 7% decrease

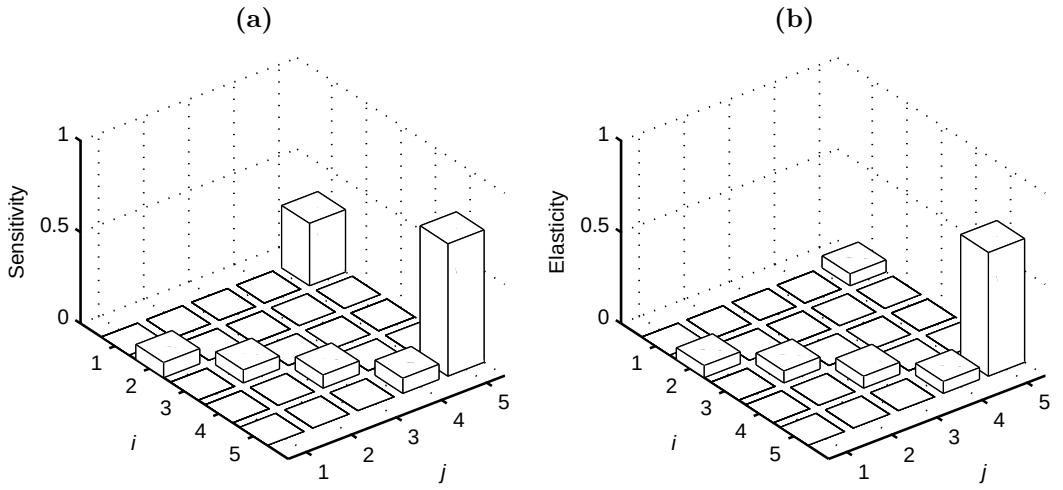

Figure 4.2 (a) Sensitivity ($\partial \log \lambda_s / \partial a_{ij}$) and (b) elasticity ($\partial \log \lambda_s / \partial \log a_{ij}$) of the stochastic growth rate λ_s to changes in the projection matrix entries a_{ij} (see equation (4.10); note that in (a) only the sensitivities to non-zero transitions are shown).

Table 4.4 Sensitivity and elasticity of the stochastic growth rate to changes in lower-level demographic parameters.

Parameter	Sensitivity	Elasticity
ρ_t	0.173	0.065
$\phi_{0,t}$	0.125	0.065
ψ	0.077	0.065
$\phi_{a,t}$	0.793	0.741

in population growth rate, while an equivalent decrease in, say, productivity would only result in a 0.7% decrease in population growth.

The reduced set of environments taken from the end of the study period (2000–2006) produced a stochastic growth rate λ_{s2} of 0.974, which corresponds to an annual growth rate of -2.5% year^{-1}. This is similar to the mean post-transitional growth rate under S5 of -2.9% year^{-1}. Patterns of sensitivity and elasticity were the same as for the full set of environments, although the elasticity of λ_{s2} to adult survival was slightly higher (0.797), and the elasticities of the other parameters were consequently lower (all 0.051).

4.4 Discussion

Effective conservation of wild animal populations requires accurate forecasts of population fluctuations, including reliable quantification of uncertainty. This

study shows how population projections may easily be incorporated into an integrated population model, using a Bayesian state-space framework with random effects models for the demographic parameters. Multiple sources of data simultaneously inform the projections, and all major sources of uncertainty are accounted for except model uncertainty, which if desired could also be incorporated via reversible jump MCMC (Green 1995, King & Brooks 2002, King et al. 2009). The resulting output takes the form of probability distributions (marginal posterior distributions) of future population sizes, which describe the uncertainty in an easy-to-understand format and from which any number of summary statistics and quantities of interest may be derived (Wade 2000). For example, our predictions of the Isle of May common guillemot population indicate that if recent poor demographic performance is continued in the future, there is a greater than 99% probability of population decrease after 10 years.

The stochastic matrix model produced similar population growth rate estimates to the corresponding integrated model scenarios, but was inferior in a number of respects. First, although environmental stochasticity was incorporated by using a sequence of projection matrices parameterised by estimates from the integrated model output, no sense of the variability of the outcome was provided. This would require carrying out additional Monte Carlo simulations. Second, projection matrices were parameterised using posterior means, but no consideration of the level of parameter uncertainty was incorporated. (Note that we could have used other posterior point estimates (e.g. the median) but this would have made little difference due to the largely symmetric posterior distributions of the parameters.) Simulating from the posterior would be an easy way to incorporate parameter uncertainty, but this clearly requires having already conducted a Bayesian analysis. Finally, we conducted a prospective perturbation analysis, which explores how much the population growth rate would change in response to specified changes in the vital rates. However, this says nothing about the observed variation in the vital rates—if a vital rate did not vary, it can have made no contribution to the observed variation in the growth rate—so to test this we would also need to conduct a retrospective analysis (see Caswell 2000). All of the above points were addressed by the Bayesian analysis.

To project the population using the integrated model, we first required predictions of future demographic rates. Predictions of productivity and first-year and adult survival were based on extrapolation of historical conditions into the future, by treating both the estimated and predicted parameters as random effects (Maunder et al. 2006). Posterior means of predicted rates generated according to the recent period of decline (2000 onwards) were all lower than those

based on the entire historical period (1983–2007; Table 4.2), as we expected. The respective variabilities of these predicted rates varied according to the parameter, from higher when based on the recent period (productivity), to about the same (first-year survival), to slightly higher when based on the historical period (adult survival). However, the random effects variance estimates for year 2000 onwards ($\sigma^2_{\cdot 2}$) were not very precise as they were only based on eight years of data, and even fewer reliable estimates in the case of the survival rates, particularly first-year survival where there was very little data to inform the last few years (Table 4.2; note the large posterior SDs relative to the means, especially for σ^2_{02}). This uncertainty in the variance estimates is also incorporated in the population predictions.

The recent population counts suggest that some factor, or combination of factors, is already having a major effect on the breeding population: after a long period of steady increase, the population declined by almost 6000 pairs between 2004 and the latest count in 2009, to the lowest level since 1994 (Figure 4.1). However, there was no information in the demographic data to support such a dramatic decrease: even assuming zero recruitment in 2006, an adult survival rate of 82.6% would have been required to generate the observed 2005–2006 population change, compared to the actual 2005 estimate of 90.7%, already well below the long-term average. Consequently, the observed decline was much faster than expected from the process model, highlighting that perhaps some other processes beyond demographic ones contributed to the decrease, although what these might have been is not clear. It is possible that the study plots and samples of marked chicks and adults are not representative of the whole population, but they do cover several locations and a range of breeding densities within the colony. Error in the counts may have been partly responsible; however, the 2006 count N_{24} was outside of the corresponding population estimate $X_{24} \pm 1.96\sqrt{\sigma^2_N}$ (i.e., outside that expected due to observation error) under all five scenarios, and the number of pairs that bred in the study plots followed a similar pattern (M. P. Harris pers. comm.), so even if the count was erroneously low that year, it is unlikely that observer error was the only cause of the discrepancy between it and the expected population size. Colony attendance patterns have changed in recent years, with guillemot parents spending a greater percentage of time away from the colony, apparently due to food shortages (Ashbrook et al. 2008), but the correction factor used to convert the actual counts of birds to the number of breeding pairs should have allowed for this. We can also discount the possibility of a sudden large increase in the proportion of nonbreeders entirely absent from the colony for the whole breeding season: this would generate a

significant decrease in adult resighting probability, which has in fact remained very high in recent years.

Putting the discrepancies aside, the true underlying population estimates also showed a clear switch between steady growth prior to 2004 and a rapid decline after (Figure 4.1). Adult survival was particularly low on the Isle of May in 2004 (as at a number of other UK colonies; see Chapter 5), and this probably triggered the decline. 2005 was another very poor year for adult survival, following which the post-2000 declines in productivity and first-year survival began to contribute to the population decrease, as reduced numbers of birds from those cohorts were available to recruit. The first five years of predictions (2008–2012) were also strongly influenced by recent observed fluctuations in productivity and first-year survival: the outcome of S1 suggests that, even if demographic parameters are assumed to return to 'normal' levels in the future, the population will continue to decline until 2012 (Figure 4.1a) due to demographic momentum (see, e.g., Koons et al. 2006). This clearly demonstrates the importance of monitoring seabird productivity and survival as well as population size, to provide an early warning system for impending changes in conservation status and a diagnosis of their cause (Eaton et al. 2008b). However, under S1 it is likely that the population would soon make a full recovery (the mean proportional population change for this scenario indicated a 7.2% increase in population size after 10 years, in spite of the initial decline), while a continuing decline beyond 2012 appears to be extremely improbable (even the lower 95% credible limits of predicted population sizes increased during this period).

S2, S3 and S4 all exhibited similar future dynamics (Figures 4.1b–d), although the recent trend in adult survival appears to give the greatest cause for concern (S4: 83.4% probability of population decrease), then first-year survival (S3: 72.8%) and recent productivity the least (S2: 52.0%). These differences appear to be largely determined by the predicted dynamics during 2008–2012, as the trajectories of all three scenarios after this transitional phase were very similar. The greater probability of decrease under S4 reflects the immediate influence of reduced adult survival on population growth from the beginning of the prediction period, compared to the 5-year time-lag following changes in productivity or first-year survival. What is noteworthy is that essentially identical dynamics were produced by a 29.5% decrease in mean predicted first-year survival and a 2.5% decrease in mean predicted adult survival—more than an order of magnitude difference—suggesting that population growth rate in guillemots is much more sensitive to variation in adult survival than either first-year survival or productivity. This finding is consistent with previous studies of long-lived

avian species (Lebreton & Clobert 1991, Rockwell et al. 1997, Sæther & Bakke 2000, Reid et al. 2004) and confirmed by the results of our perturbation analysis (Figure 4.2, Table 4.4). On the other hand, the similar realised contribution to population dynamics of the observed declines in first-year and adult survival also highlights that the demographic rates to which population growth is theoretically most sensitive are not necessarily those that contribute most to changes in growth rate over time (Gaillard et al. 1998, 2000, Sæther & Bakke 2000, Cooch et al. 2001, Coulson et al. 2005). This is due to the relative variabilities of the different traits: in general, those traits with the greatest potential contribution to the population growth rate tend to exhibit the least temporal variability (Gaillard et al. 2000, Sæther & Bakke 2000)—a phenomenon termed 'environmental canalization' (Gaillard & Yoccoz 2003). Therefore, while the elasticity of λ_s to adult survival of Isle of May guillemots was more than 10 times greater than to productivity or first-year survival, the coefficients of variation (CVs) of the latter two traits were 6 and 12 times greater, respectively, than that of adult survival ($CV_\rho = 19.1\%$, $CV_0 = 38.5\%$, $CV_a = 3.1\%$; CVs calculated from posterior means and process standard deviations of simulated ρ_t, $\phi_{0,t}$ and $\phi_{a,t}$ under S1, see Table 4.2).

The final scenario S5 predicted a rapid decrease in breeder and prebreeder population sizes throughout the 10-year prediction period (Figure 4.1e), with an expected decline over this period of 31% and only a 0.6% probability of population increase. Future simulations of productivity, first-year survival and adult survival for this scenario were based on data from the recent drop in demographic performance of Isle of May guillemots, which has also been a prominent feature at a number of other UK colonies, affecting the majority of seabird species (e.g. Mavor et al. 2005, 2008). These changes are presumed to be primarily due to a reduction in the abundance and quality of their main prey species, especially the lesser sandeel *Ammodytes marinus* (Mavor et al. 2005, 2008, Wanless et al. 2005, Heath et al. 2009), which in turn is thought to be linked to climate change (MCCIP 2009). Although the mechanisms involved in these connections are complex and not fully understood, in a recent review Heath et al. (2009) propose the following causative link: (1) warming sea temperature and changes in primary production patterns, leading to (2) changes in zooplankton communities and production, leading to (3) suppression of sandeel growth rate and recruitment, (4) changes in sandeel behaviour, (5) declining sandeel abundance, and hence (6) reduced food availability for seabirds and (7) reduced seabird breeding success, frequency of breeding, adult survival and/or increased age of first breeding. Indeed, reductions in both breeding success and adult sur-

vival of several seabird species, including the common guillemot, have already been correlated with increases in sea surface temperature and climate indices such as the North Atlantic Oscillation, with food availability implicated as the link (e.g. Frederiksen et al. 2004b, Harris et al. 2005, Sandvik et al. 2005, Votier et al. 2005). With climate change scenarios predicting that sea surface temperatures will increase around all UK coasts in the future (Lowe et al. 2009), S5 appears to be the most realistic of our five scenarios for Isle of May guillemots, at least in the short term. Similar implications may be assumed for future population dynamics at other UK colonies, some of which may have, as yet, shown no evidence of a population decrease, and also for similar species, such as the razorbill *Alca torda* and Atlantic puffin *Fratercula arctica*.

In fact, there are several reasons why 'worst case' scenario S5 may be conservative, and therefore not the worst possible case for the Isle of May guillemots. First, if demographic rates decrease further in the future in line with climate predictions, the population decrease will be greater. This could be modelled by adding trends to the random effects models and projecting these forwards with random variability, although it is unrealistic to assume that such trends would continue indefinitely. Second, productivity and survival were all strongly positively correlated during 1983–2006 (post hoc Spearman's rank correlations: $r_s(\rho_t, \phi_{0,t}) = 0.54$, $p = 0.007$; $r_s(\rho_t, \phi_{a,t}) = 0.65$, $p < 0.001$; $r_s(\phi_{0,t}, \phi_{a,t}) = 0.61$, $p = 0.001$). The stochastic matrix model approach accounted for this by permuting entire matrices rather than each parameter separately, and the good agreement between the two approaches in terms of projected growth indicates that ignoring this correlation does not induce significant bias in the population growth rate. It could, however, lead to underestimating the variability of the predictions (see Coulson et al. 2005), with potential consequence of underestimating the probability of large (e.g. $> 50\%$) declines. Nur et al. (1994) incorporated covariation among survival rates in their predictive model by simulating adult survival and then assuming that immature survival rates were directly proportional, and a similar approach might be suitable here. Finally, due to a lack of information in the data, immature (ages 1–3) survival rates in this study were estimated as constant parameters and assumed to maintain these values (with parameter uncertainty) during the projections; however, it is likely that they have also declined since 2000. Given that random effects provide a compromise between constant and fully time-dependent models (Royle & Link 2002), there may be some merit in modelling immature survival with random effects to estimate pre- and post-2000 means and process variances, similarly to productivity, first-year survival and adult survival.

As a final point, we note that although we have a very rich dataset and a model that provides a good fit, credible intervals on the population sizes still 'explode' as soon as we start to predict, creating even more uncertainty over the future of the population. As an example, S2 predicted an approximately even probability of a decrease in population size after 10 years, but the uncertainty in the estimates mean that the actual population change over this period could feasibly be anywhere from a 28% decrease to a 29% increase. There would thus be little benefit in projecting further than 10 years, as the uncertainty in the estimates would become too large to be of any scientific value. Even more uncertainty is introduced by the different scenarios, such that in total we have realistic estimates of population change ranging from -53% to $+36\%$, depending on the model assumptions. Furthermore, the projections are based on the assumption that current conditions hold for the duration of the prediction period (Coulson et al. 2001). Environmental conditions were actually relatively stable throughout much of the historical period, but the rapid changes in UK coastal waters of late suggest it is unlikely that conditions will remain constant in the future, even for the next 10 years. Nevertheless, realistic predictive models can still serve a useful purpose (Nur & Sydeman 1999), including: investigating the future population consequences of known changes (for example the possible effects during the next 5 years of recent breeding failures); evaluating the significance of declines in different life stages in influencing population growth; and exploring the implications of various model assumptions to see where restoration efforts might be best rewarded.

Chapter 5

Multi-population modelling of survival rates

5.1 Introduction

Year-to-year variation in demographic parameters is often pronounced, presumably related to features of the environment, and a large number of ecological studies have focussed on detecting and explaining such variation (see Grosbois et al. 2008 for an overview of survival studies and, e.g., Gaston & Smith 2001, Rodriguez & Bustamante 2003, Dickey et al. 2008, Jüssi et al. 2008 for reproductive parameters). Relatively fewer studies have addressed the issue of geographical variation among populations of the same species, and fewer still variation over both time and space (but see, e.g., Grosbois et al. 2009). This disparity is primarily due to the difficulty—in terms of time, cost and logistics—of obtaining sufficiently detailed long-term data at the multi-population scale to permit rigorous comparisons (Koenig 1999, Frederiksen et al. 2005). However, life-history traits can vary as much among populations as between species (Dhondt 2001); indeed, spatial variation in demographic rates may well be higher than the corresponding temporal variation (Paradis et al. 2000) and can have a profound influence on population dynamics of species inhabiting heterogeneous landscapes (Ozgul et al. 2006). Therefore, findings from smaller-scale studies may fail to represent larger-scale dynamics across a species' range, particularly for species inhabiting large geographical areas (Baker & Thompson 2007). Conversely, spatial comparisons of geographically widespread populations could improve our understanding of population dynamics and the evolution of life histories (Frederiksen et al. 2005), and may aid in establishing which environmental factors contribute to variations in demographic parameters and when and where they exert their influence (e.g. Schaub et al. 2005, Grosbois

et al. 2006, Jenouvrier et al. 2009b).

Many studies of time series of population abundance have considered the mechanisms behind multi-population dynamics (reviewed in Liebhold et al. 2004). These mechanisms are difficult to infer via the sole analysis of population time series (Bjørnstad et al. 1999, Liebhold et al. 2004), but may be interpreted more easily through the analysis of demographic parameters at multi-population spatial scales (Grosbois et al. 2009). The recent literature has seen an increase in the number of studies investigating spatiotemporal variation in demographic rates, and in particular survival, presumably related to increasing availability of long-term datasets with the necessary level of spatial and temporal detail, and the evolution of statistical tools to analyse them. Findings from the majority of these studies seem to suggest that temporal variations in survival are often correlated among different populations: these findings extend to a number of species and across a variety of spatial scales, from a few kilometres (yellow-bellied marmot *Marmota flaviventris*: Ozgul et al. 2006) to several thousand kilometres incorporating a substantial part of a species' distribution range (Atlantic puffin *Fratercula arctica*: Harris et al. 2005, Grosbois et al. 2009; white stork *Ciconia ciconia*: Schaub et al. 2005; Hawaiian monk seal *Monachus schauinslandi*: Baker & Thompson 2007; Cory's shearwater *Calonectris diomedea*: Jenouvrier et al. 2009b). Baker & Thompson (2007) note that such spatial synchrony in survival rates among subpopulations 'presumably results from individuals at different sites experiencing similar conditions', which can occur because 'either environmental conditions span more than one site or animals from different sites move sufficiently that their ranges overlap'.

Environmental conditions that may act as synchronising agents include large-scale climatic phenomena such as the North Atlantic Oscillation (NAO) and Southern Oscillation (SO), which influence weather and oceanographic conditions over vast geographic areas (see, e.g., Hurrell et al. 2003, Stenseth et al. 2003) and have been linked with spatiotemporal correlations in survival (Jenouvrier et al. 2009b) and multi-population dynamics (Post & Forchhammer 2002, Sæther et al. 2006). Other large-scale or spatially correlated environmental covariates found to explain synchronous survival include snow cover (Grøtan et al. 2005), sea surface temperature (Grosbois et al. 2009), and vegetation indices (Schaub et al. 2005). However, a correlated environment does not necessarily result in synchrony, as demonstrated by findings of asynchronous survival and reproductive success in an insular metapopulation of house sparrows *Passer domesticus* (Ringsby et al. 1999, 2002). The second of Baker & Thompson's (2007) criteria, movement resulting in overlapping ranges, is particularly true

of populations of migratory or dispersive species. Although widely separated during the breeding season, such species often overlap in nonbreeding distribution (e.g. Newton 1995, Schaub et al. 2005, Jenouvrier et al. 2009b) where they may be exposed to a common environment and when highest mortality tends to occur (Newton 1998). A third factor to consider is how the synchronising effects of environmental conditions and movement on survival might vary according to age: in long-lived species, survival rates of young animals are generally lower and more variable than those of adults (e.g. Gaillard et al. 1998, Doherty et al. 2004, Ozgul et al. 2006) and may respond differently to changes in the environment.

In some cases, despite extensive searching, no covariates can be found that explain variation in survival. This is the case for Isle of May common guillemots *Uria aalge* (Harris et al. 2007b). The available evidence suggests that the main mortality of guillemots occurs during the nonbreeding season (Harris et al. 2007b), so it seems likely that some aspect of winter environment is responsible for interannual variation in survival. To test this, we compare juvenile and adult survival of guillemots from three widely separated Scottish colonies that have varying overlap in winter distribution among age classes. The three colonies considered are: the Isle of May, situated in the North Sea off the southeast coast of Scotland; Canna, in the Sea of the Hebrides off the west coast of Scotland; and Colonsay, in the outer Firth of Lorn, also off the west coast. These are all substantial colonies, between them containing somewhere in the region of 5% of the total British and Irish breeding population; their locations provide a comparison between east and west coast populations which, at least during the breeding season, are effectively geographically isolated; and they have all been the subject of long-running, individual-based field studies, providing mark-recapture and ring-recovery data.

Due to their isolation, it is to be expected that birds from the east and west coasts will experience different conditions during breeding, and so have different productivities. However, during nonbreeding guillemots disperse over large areas of ocean and there is much mixing between birds from different populations, potentially exposing them to the same environmental conditions; furthermore, juvenile and immature birds disperse further from the colonies than adults (Harris & Swann 2002), so it is less clear what might be expected as regards differences in annual survival. Previous analyses have concentrated on the Isle of May, which has the more detailed data and for which there are recent published estimates of time-specific juvenile (Crespin et al. 2006a, Harris et al. 2007b) and adult (Crespin et al. 2006b) survival. Field studies at Canna

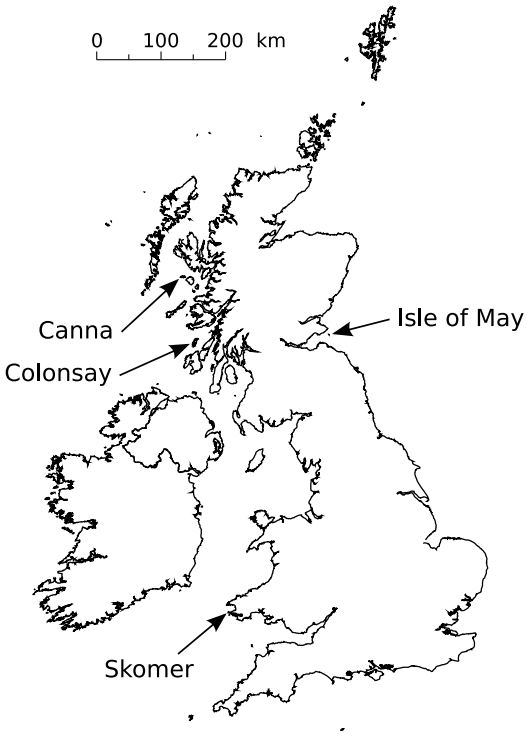

Figure 5.1 Map of the British Isles showing locations of the four common guillemot colonies mentioned in this chapter: Isle of May, southeast Scotland; Canna and Colonsay, west Scotland; Skomer, southwest Wales.

and Colonsay have been less intensive, so the data are sparser and only time-constant estimates of adult survival have previously been published for these colonies (Harris et al. 2000), although this study did not incorporate information on dead recoveries in the survival analysis. Using mark-recapture and ring-recovery data, we look for spatial, temporal and age-related correlations in survival among the three colonies and, for Isle of May and Canna birds, use information on ring recovery locations to test whether any pairwise correlations in survival are associated with evidence that their nonbreeding distributions significantly overlap.

5.2 Data and analysis

5.2.1 Mark-recapture-recovery data and modelling

As mentioned in the Introduction, mark-recapture-recovery (MRR) data are available for three Scottish common guillemot colonies (see Figure 5.1). Data from Canna and the Isle of May both cover the same period (1983–2006) and comprise capture histories of guillemots marked as chicks and as breeding adults,

whereas the Colonsay data cover a much shorter period (1990–2006) and only comprise birds ringed as adults. Therefore, we restrict the formal comparative analysis to the Isle of May and Canna, and compare Colonsay adult survival separately on an ad hoc basis.

Unlike previous chapters in this thesis, where Bayesian analyses are conducted using bespoke Fortran code, analyses of survival data in this chapter are all conducted in Program MARK (White & Burnham 1999) using a combination of Bayesian MCMC and classical maximum likelihood techniques. The use of MARK is possible due to the fact that we are dealing with relatively simple MRR data, rather than the analysis of multiple, integrated data types with complex models for which no prewritten software exists; it is also desirable because of its flexibility, given that we would like to use Bayesian methods (to continue the theme of earlier analyses and for estimation of correlation parameters) but have a large number of models to fit and compare. We accommodate these requirements in MARK by considering a two-step process: (1) model selection (separately for each colony) using maximum likelihood estimation and AIC, which has a more rigorous framework than the corresponding process using MCMC and DIC, accommodates goodness-of-fit testing, and is much faster than MCMC estimation; (2) combining the Isle of May and Canna datasets and fitting them using MCMC (with the chosen model structures from step 1) to obtain posterior distributions for the parameters, including pairwise process correlations among first-year and adult survival rates. Step 1 is described in this section, and step 2 in Section 5.2.2.

The analysis of MRR data depends upon four sets of parameters—survival, recapture, recovery and fidelity probabilities—which are estimated in MARK using Burnham's model for both live encounters and dead recoveries (Burnham 1993). Initially we analyse each colony separately, using maximum likelihood estimation for goodness-of-fit (GOF) testing and subsequent model selection on the Isle of May and Canna combined adult and chick datasets, and the Colonsay adult data. For each dataset, we first identify a candidate model set representing biological knowledge and statistical considerations (Lebreton et al. 1992). To confirm that the most general, or 'starting', model in the candidate set (i.e., the most parameterised model that has few or no estimability problems) adequately fits the data, we conduct a goodness-of-fit test using the bootstrap GOF procedure in MARK. This procedure yields an estimate of a variance inflation factor, denoted $\widehat{c}$ and defined as the ratio of the model χ^2 (model deviance) divided by the degrees of freedom (Burnham et al. 1987). The variance inflation factor quantifies the amount of extrabinomial variation,

or overdispersion, and is a measure of the lack of fit between the general model and a saturated model. If the model fits the data perfectly then $\widehat{c} = 1$, and a value of $\widehat{c} > 1$ indicates some degree of overdispersion, although $\widehat{c} \leqslant 3$ is generally considered to be acceptable (Lebreton et al. 1992). Provided the fit of the general model is adequate, we then select the most appropriate model using Akaike's Information Criterion, adjusted for effective sample size and any lack of fit using the estimate of $\widehat{c}$ obtained from the GOF test (QAIC_c; Burnham & Anderson 2002).

Notation in this chapter is as follows: survival probabilities are denoted by $\phi_{r,t}^{loc}$, recapture probabilities by $p_{r,t}^{loc}$, recovery by $\lambda_{r,t}^{loc}$ and fidelity by $\psi_{r,t}^{loc}$. Three-letter superscripts denote colony location, i.e., $loc \in \{iom, can, col\}$; $r \in \{0, 1, 2, 3, 4, 5, a\}$ denotes age class from first-year to adult; $t = 1, \ldots, T$ denotes time. The data and models are described separately for each of the three colonies.

Isle of May

The Isle of May is located in the outer Firth of Forth, southeast Scotland (56°11′N, 2°33′W). The island is 1.8 km long and 0.5 km wide, and has its major seabird breeding colonies on the high cliffs of the west coast. The guillemot population was estimated at 15,578 breeding pairs in 2006. The island was permanently occupied by a team of researchers throughout the 1983–2006 breeding seasons, during which guillemots were caught and marked annually and the colony was intensively monitored on a daily basis. The practical methods for both initial capture and subsequent recaptures differed greatly between birds marked as adults and those marked as chicks, and they are described separately below.

Breeding adults were initially captured by noose or crook, or by mist-netting during the winter, and marked with a numbered metal ring and an individually recognisable combination of three colour-rings. Otherwise birds were not handled and subsequent identifications were by resighting using binoculars or a telescope. Resightings came mainly from the intensively monitored study plots where the birds were ringed, because site-fidelity of breeding adults is high (Harris et al. 1996b), but wider searches were also regularly made. Individuals were frequently seen several times within a single year, or capture occasion, but we take no account of the number of observations and simply denote a resighting by a single record per individual, per year (the same applies to Isle of May chick resightings, below). In total 730 adults were ringed during the study period,

resulting in 6292 live resightings, hereafter referred to as recaptures for consistency with the other studies. Recoveries of dead adult birds are ignored as there were too few (11) to justify their inclusion in the model.

Chicks were caught by hand in two easily accessible breeding areas, referred to as areas A and B, and marked with a numbered metal ring and a unique colour-ring readable at distances up to 75 m with a telescope. Most resightings (hereafter referred to as recaptures) resulted from almost daily searches of the breeding ledges and tidal rocks within a few hundred metres of the two ringing areas, because of the tendency of guillemots to return to their natal area during their prebreeding years and to subsequently recruit nearby (Harris et al. 1996a), although opportunistic observations were made throughout the island. Recoveries of dead birds away from the island were also recorded. A total of 6145 chicks were ringed during the study, with 4678 of these in area A and 1467 in area B. These gave, respectively, 3264 and 861 live recaptures, and 169 and 85 dead recoveries.

We base the starting model for the combined adult-chick dataset on that used in Chapter 3, which in turn is based on the reference model of Harris et al. (2007b): survival is assumed to be time-dependent for first-years and adults (adult survival includes age 4^+ birds ringed as chicks) and constant for ages 1–3; recapture probabilities for birds ringed as chicks are age- and time-dependent up to 5 years (except for one-year-olds, which are fixed to 0) and are allowed to differ between areas A and B, with separate time-specific estimates for birds ringed as adults; recovery probabilities are allowed to vary over time but are assumed to be the same for all age classes (recovery probability of birds ringed as adults is fixed to 0); and fidelity is assumed to be constant over time for age 4 and age 5^+ birds ringed as chicks, and fixed to 1 for all other age classes (including birds ringed as adults). The bootstrapped estimate of $\widehat{c}$ for this model (observed $\widehat{c}$/expected $\widehat{c}$) was 1.23, indicating only slight overdispersion and satisfactory model fit. Replacing any of the time-dependent parameters in the starting model with constant ones resulted in significantly worse-fitting models ($\Delta\text{QAIC}_c > +20$). However, a more parsimonious model ($\Delta\text{QAIC}_c = -7.45$) was achieved by constraining recovery probabilities to change linearly (on the logit scale), which allows for a potential systematic temporal decline in reporting rates over the period of the study (Clark et al. 2005).

Canna

Canna is located in the Inner Hebrides of Scotland, approximately 14 km southwest of Skye (57°03′N, 6°35′W). It is a small island around 7 km long by 1.5 km wide and its northern coastline is dominated by steep, basalt cliffs where the major seabird breeding colonies are located. The island's guillemot colony numbered in the order of 2000–3000 breeding pairs in 2006 (R. Swann pers. comm.).

Breeding areas were (mostly) visited once per summer 1983–2006, when chicks, immatures and adults were caught by hand or crook and marked with a numbered metal ring. Recaptures of previously ringed birds were by the same method. Recoveries of dead birds were also recorded. Capture histories of birds initially ringed as chicks were kept separate from those ringed as immatures or adults, and the latter group formed the breeding adult dataset based on the following criteria: known breeders were recorded from their first capture, while for all other birds the initial capture was discarded and they were regarded as breeders from their first recapture. The analysis also excluded birds marked with older 'G-series' rings (mostly prior to 1983) because these were more prone to wear and loss than the replacement type. The final dataset contains a total of 44,799 chick and 4298 adult capture histories, with respectively 6078 and 5357 live recaptures, and 939 and 97 dead recoveries.

We specify a starting model for the Canna data that has time-dependence in survival for all age classes from first-year ($\phi^{can}_{0,t}$) to adult (combined estimate for birds ringed as chicks and adults: $\phi^{can}_{4+,t} = \phi^{can}_{a,t}$). As with the Isle of May guillemots, one-year-olds were never observed at the colony, so recapture probabilities for these birds are fixed to 0. For ages 2, 3 and 4 years, recapture probabilities are specified to be constant due to data limitations, but we allow them to vary over time for age 5^+ birds ringed as chicks and for birds ringed as adults, which we treat separately. Recovery probabilities are assumed to be the same for all ages and for birds ringed as both chicks and adults, and are allowed to vary over time. Time-constant fidelity is estimated separately for birds of all age classes 0–5^+ years that were ringed as chicks. To accommodate birds moving site following the disturbance associated with catching (Harris et al. 2000) we also estimate fidelity of birds ringed as adults, with separate estimates for the year following initial capture and all subsequent years, denoted ψ^{can}_{a1} and ψ^{can}_{a2+}, respectively. The estimate of $\widehat{c}$ for this model was 1.14, which gives no concerns regarding model fit.

Fidelities of age 0 and age 1 birds were inestimable in the general model, so fixing them both to 1 resulted in an improved model ($\Delta\text{QAIC}_c = -4.03$).

Survival estimates of 2- and 3-year-olds were very similar to each other, and combining them into a single age-class ($\phi^{can}_{2-3,t}$) improved the model considerably further ($\Delta\text{QAIC}_c = -25.05$). Recovery probability clearly varied over time ($\Delta\text{QAIC}_c = +72.39$ when setting recovery to constant), but as with the Isle of May model, a linear constraint (on the logit scale) appeared to adequately explain this variation and resulted in the most parsimonious model ($\Delta\text{QAIC}_c = -23.37$).

Colonsay

Colonsay, also in the Inner Hebrides, lies around 100 km south of Canna between the islands of Mull and Islay (56°05′N, 6°10′W). It is approximately 13 km long by 5 km wide, with major cliffs on the north and west coasts which contained 26,469 individual guillemots in 2000 (Jardine et al. 2002), equating to approximately 17,700 breeding pairs (using a correction factor of 0.67: Harris 1989).

Two visits (only one in 1990) were made each summer 1990–2006 to catch breeding adults using a noose or crook and mark them with a numbered metal ring. Previously marked birds were recorded as recaptures. Recoveries of dead birds were also recorded. In total 895 individuals were marked, resulting in 1630 live recaptures and 11 dead recoveries. Because of the small size of the dataset, initial captures were not discarded.

For the starting model, we assume time-dependence in survival and recapture probabilities, and also in fidelity probability in the year following initial capture, denoted ψ^{col}_{a1}. Fidelity in subsequent years is specified to be time-constant, and there were too few recoveries (less than one per year, on average) to permit time-specific estimates of recovery probability, so we assume this to be constant too. The estimate of $\widehat{c}$ for this model was 1.07, suggesting a satisfactory fit.

Fidelity in years two-or-more after initial capture was estimated at 1 in the starting model, so we first fixed this to 1 ($\Delta\text{QAIC}_c = -2.08$). Precisions on survival estimates were poor, and a further reduction in QAIC_c of 13.36 points was achieved by setting survival to be constant. However, although there was too little information in the data to permit full annual variation, survival in 2004 appeared to be somewhat lower than the other years and allowing a separate estimate for this year improved the fit of the model ($\Delta\text{QAIC}_c = -3.50$). There was no improvement upon adding a logit-linear trend to the recovery probability ($\Delta\text{QAIC}_c = +0.30$; confidence interval of slope parameter includes zero), but

because it had very similar support to the constant recovery model, and for consistency with the other colonies, we keep the trend in the final model.

5.2.2 MCMC modelling of process correlations

We implement the MCMC estimation procedure in MARK to model the Colonsay data and a combined Isle of May–Canna dataset, using the model structures selected in Section 5.2.1, in order to obtain posterior parameter distributions for survival, recapture, recovery and fidelity probabilities. We also estimate pairwise process correlations in survival probability between and among first-year and adult guillemots on the Isle of May and Canna. For each MCMC run we specify 4000 'tuning' samples, a burn-in period of 1000 samples, and 10,000 subsequent samples to be stored from the posterior distribution. Multiple chains (three for each model) are run to assess convergence using the Gelman (1996) diagnostic statistic $\widehat{R}$, as calculated by MARK.

Priors in MARK are specified on the β parameters (logistic regression parameters, one for each column of the design matrix) because the MCMC update procedure is performed on these. Priors for parameters not in hyperdistributions (i.e., all parameters except those pairs having their process correlation estimated) are normally distributed with mean 0 and variance 1.75^2. This is the default prior in MARK, specified such that the back-transformed distribution on the 'real' parameter is approximately uniform with 95% of its probability between about 0.03 and 0.97. Pairs of survival parameters for which we estimate process correlations have hyperdistributions specified on their β parameters, i.e.,

$$\text{logit}(\phi_t) = \beta_t, \tag{5.1}$$

where

$$\beta_t \sim \text{N}(\mu, \sigma_\beta^2). \tag{5.2}$$

The hyperdistribution means, μ, take normally distributed priors with mean 0 and standard deviation 100, giving a very flat and noninformative prior; an inverse-gamma distribution with parameters $\alpha = 3$, $\beta = 7$ (see Appendix A) is specified on the hyperdistribution variances σ_β^2. The correlation between two sets of time-specific survival parameters, for example $\phi_{1,t}$ and $\phi_{2,t}$, is calculated by

$$\text{corr}(\phi_1, \phi_2) = \frac{\text{cov}(\phi_1, \phi_2)}{\sigma_{\phi_1}\sigma_{\phi_2}}, \tag{5.3}$$

and denoted by ρ_{ϕ_1,ϕ_2}. In MARK, estimating the correlation between sets of

parameters is achieved by specifying the upper off-diagonal elements of the variance-covariance matrix: for a model with three capture occasions, the appropriate upper-diagonal portion of the variance-covariance matrix looks like the following

$$\begin{bmatrix} \sigma_{\phi_1} & 0 & 0 & \rho_{\phi_1,\phi_2} & 0 & 0 \\ & \sigma_{\phi_1} & 0 & 0 & \rho_{\phi_1,\phi_2} & 0 \\ & & \sigma_{\phi_1} & 0 & 0 & \rho_{\phi_1,\phi_2} \\ & & & \sigma_{\phi_2} & 0 & 0 \\ & & & & \sigma_{\phi_2} & 0 \\ & & & & & \sigma_{\phi_2} \end{bmatrix}. \tag{5.4}$$

On the diagonal of the matrix are the σ values, the first three corresponding to the hyperdistribution on $\phi_{1,t}$ and the remaining three corresponding to the hyperdistribution on $\phi_{2,t}$. The three ρ_{ϕ_1,ϕ_2} entries correspond to the correlations of $\phi_{1,1}$ with $\phi_{2,1}$, $\phi_{1,2}$ with $\phi_{2,2}$, and $\phi_{1,3}$ with $\phi_{2,3}$. Priors for ρ parameters are taken to be uniform with bounds of -1 and 1.

5.2.3 Ring-recovery location data and analysis

Direct assessment of the nonbreeding season distribution of guillemots is not possible, due to the difficulties involved in simply finding birds, let alone identifying individuals. However, locations of recoveries of dead guillemots form a useful proxy for the location of live birds at that time, and the age class and natal colony of recovered birds is also known. In this section, we describe three methods for assessing overlap in recovery distributions: a simple visual comparison of recovery locations and densities, and two statistical tests (two-dimensional Kolmogorov-Smirnov and χ^2).

Recovery location plots

Recoveries of guillemots ringed on Canna and the Isle of May, and reported during the period October–March, inclusive, were separated by age into first-year (age 0) and adult birds (age 4-or-more years old, ringed as either chick or adult). Recoveries of immature age classes were discarded, as were those reported during the breeding period (defined as April–September). Locations of recoveries were then plotted separately according to age and natal colony (i.e., Canna age 0, Canna age 4^+, Isle of May age 0, and Isle of May age 4^+) along with 95, 75 and 50% kernel density contours, following the methodology

of Votier et al. (2008). The resulting plots were compared visually for overlap in recovery distributions. ArcView GIS 3.2 with the Animal Movement extension, version 2.04 beta (Hooge et al. 1999), was used to produce the distribution maps.

Two-dimensional Kolmogorov-Smirnov test

The distribution of recovery locations was divided into pairs according to age (0 or 4^+) and/or colony (Canna or Isle of May; six pairings in total) and then compared statistically using a two-sample two-dimensional Kolmogorov-Smirnov test. This test—first proposed by Peacock (1983) and later improved by Fasano & Franceschini (1987)—is a generalisation of the one-dimensional K-S test: the two-dimensional K-S statistic essentially defines the maximum cumulative difference between two two-dimensional distributions (Press et al. 1994), as described below.

In a two-dimensional distribution, each data point is characterised by a pair of values (x, y). To calculate cumulative differences in two dimensions, Fasano & Franceschini (1987) made use of the total number of points in each of the four quadrants around a given point (x_i, y_i), namely the fraction of data points in the regions $(x < x_i, y < y_i)$, $(x < x_i, y > y_i)$, $(x > x_i, y < y_i)$, $(x > x_i, y > y_i)$. The two-dimensional K-S statistic, D_{KS}, is taken to be the maximum difference between the fractions of data points of each sample in any two matching quadrants, ranging over all data points; in other words, the K-S test finds that data point containing the maximum difference between the fraction of sample 1 and the fraction of sample 2 in one of its quadrants. Because the value of D_{KS} is likely to depend on which of the two samples is ranged over, an effective D_{KS} is defined as the average of the two values obtained by ranging over each sample separately. The significance level can be calculated by the approximate formula

$$\Pr(D_{KS} > \text{observed}) = Q_{KS}\left(\frac{\sqrt{N}D_{KS}}{1 + \sqrt{1 - r^2}\,(0.25 - 0.75/\sqrt{N})}\right), \tag{5.5}$$

where the function Q_{KS} is given by

$$Q_{KS}(\lambda) = 2\sum_{j=1}^{\infty}(-1)^{j-1}\exp(-2j^2\lambda^2), \tag{5.6}$$

r is the average of the coefficients of correlation of the two samples, and $N = N_1N_2/(N_1 + N_2)$. Fortran code for the above implementation of the two-

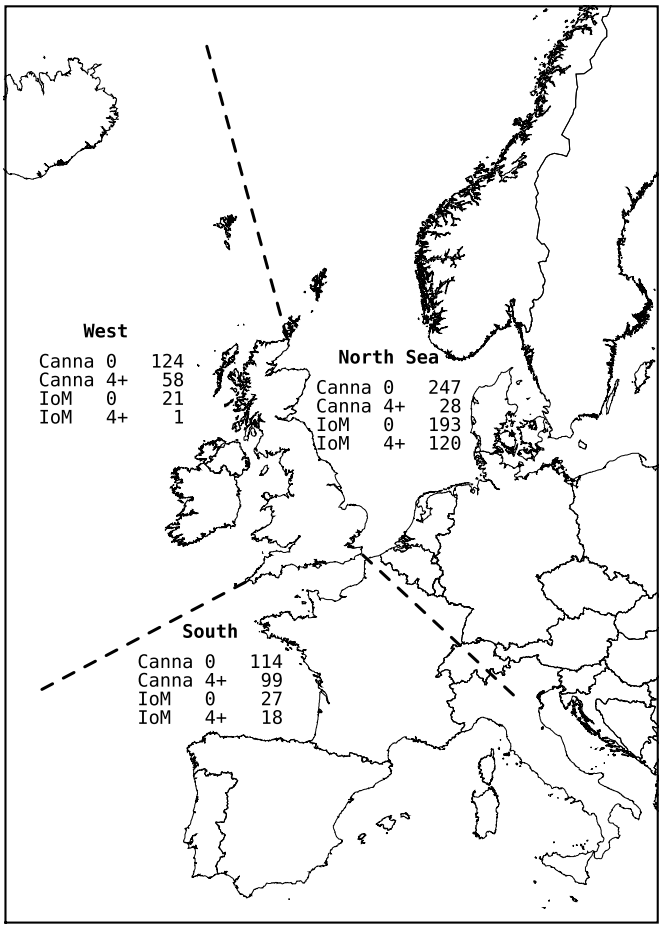

Figure 5.2 Map showing geographical regions defined for the χ^2 tests on guillemot recovery frequencies. Mini-tables provide frequencies of dead recoveries for each region by natal colony and age class.

dimensional K-S test is provided by Press et al. (1994). In addition to calculating the significance level for each pairing using the approximate equation (5.5), we also checked p-values by conducting a Monte Carlo test on each age/colony pairing, using 999 randomised datasets.

Chi-squared test

For a less sensitive (and more subjective) statistical test, we also divided the recovery location data according to three geographical regions—'North Sea', for all recoveries on North Sea shores (including the Skagerrak and Kattegat), Orkney, Shetland and the Norwegian coast; 'South', incorporating the English Channel and Bay of Biscay; and 'West', for recoveries on the west coast of the UK, Irish coast, and including the north Scottish coast, Faeroe Islands and Iceland (see Figure 5.2)—and carried out pairwise χ^2 tests on the frequencies of recoveries in each region, for each of the six combinations of colony and age.

5.3 Results

5.3.1 Mark-recapture-recovery analysis

All summary statistics provided below are posterior means and, where applicable, 95% symmetric credible intervals (CIs) derived from MCMC simulations conducted in Program MARK. Convergence was assessed by the Gelman (1996) $\widehat{R}$ diagnostic provided by MARK, and was satisfactory in all cases (all $\widehat{R}$ less than 1.05), suggesting that 10,000 simulations were sufficient for these analyses.

Isle of May

The selected model for Isle of May guillemots had year-to-year variation in first-year and adult (age 4^+) survival, with constant survival for intermediate age groups; year-to-year variation in recapture probability independently for birds ringed as adults, and 2-, 3-, 4-, and 5^+-year-olds ringed as chicks in areas A and B; a linear trend on recovery probability (same for all age classes); and separate fidelity estimates for age 4 and age 5^+ birds ringed as chicks.

Parameter estimates were very similar to those provided in Section 3.4. One noteworthy difference is the estimate of ψ_4, which at 0.855 (95% CI: 0.809, 0.901) is somewhat higher than the 0.805 estimated by the integrated model. This is possibly due to the additional year of survival data, or perhaps the lack of influence from the count data. Survival probabilities of first-years and adults are provided for ease of reference in Figure 5.3; note the additional year of data compared to the integrated analysis of Chapter 3 and how this drastically alters the 2004 adult survival estimate, now significantly lower than all other years (cf. Figure 3.2).

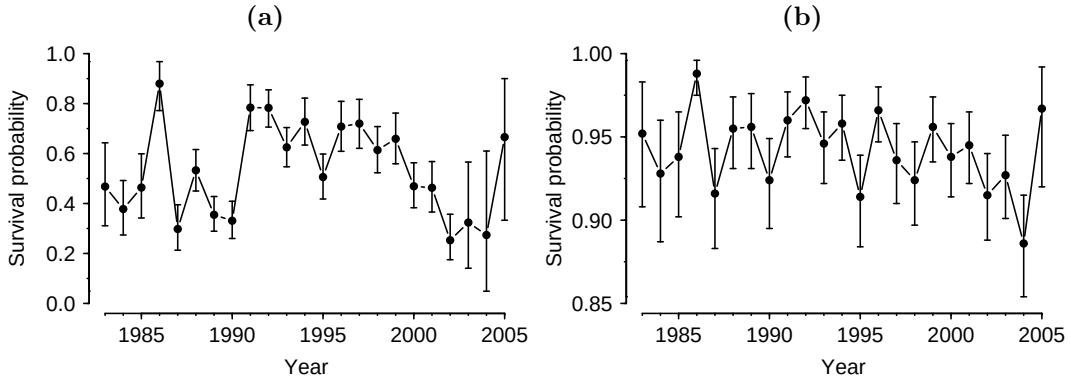

Figure 5.3 Posterior means and 95% symmetric CIs for survival probabilities of Isle of May guillemots: (a) first-years; (b) adults.

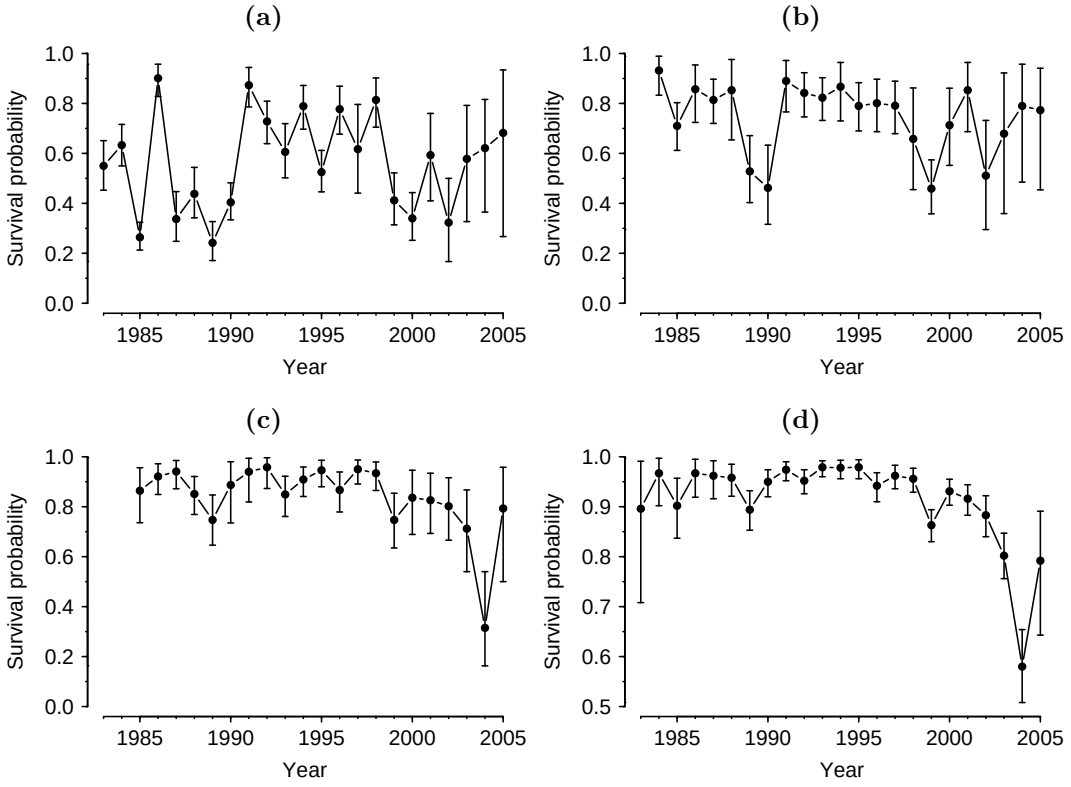

Figure 5.4 Posterior means and 95% symmetric CIs for survival probabilities of Canna guillemots: (a) first-years (age 0); (b) age 1; (c) ages 2–3; (d) adults (note the different y-scale for this plot).

Canna

The selected model for Canna guillemots had year-to-year variation in survival for ages 0, 1, 2–3 combined, and adult; age variation in recapture probability for 2-, 3- and 4-year-olds, with additional time variation for age 5^+ birds ringed as chicks, and birds ringed as adults; a linear trend on recovery probability; and age variation in fidelity for 2-, 3-, 4- and 5^+-year-olds ringed as chicks, and also for birds ringed as adults, separately for the year following initial capture and all subsequent years.

Survival estimates and associated 95% CIs for all age classes are provided in Figure 5.4. First-year (age 0) survival varied strongly from year to year over a similar range to that of Isle of May first-years, with a range of posterior means 0.242–0.901 (Figure 5.4a; Isle of May range 0.253–0.880). There appear to have been sustained periods of lower survival during years 1987–1990 and 1999–2002, separated by a period of above-average survival, but there does not appear to have been the same steady decline in survival at the end of the study period as noted for Isle of May first-years (Section 3.4; Harris et al. 2007b). There was enough information in the Canna dataset to allow time-specific survival

Table 5.1 Posterior summary statistics for time-constant parameters of Canna guillemots.

Parameter	Mean	SD	95% symmetric CI
p_2	0.0009	(0.0002)	(0.0005, 0.0013)
p_3	0.004	(0.001)	(0.003, 0.006)
p_4	0.016	(0.002)	(0.012, 0.020)
α_λ	−2.99	(0.079)	(−3.14, −2.84)
β_λ	−1.25	(0.133)	(−1.51, −0.98)
ψ_2	0.797	(0.090)	(0.648, 0.973)
ψ_3	0.870	(0.083)	(0.692, 0.987)
ψ_4	0.766	(0.073)	(0.632, 0.926)
ψ_{5+}	0.996	(0.003)	(0.989, 0.999)
ψ_{a1}	0.866	(0.014)	(0.840, 0.894)
ψ_{a2+}	0.977	(0.005)	(0.968, 0.985)

estimates for two immature age classes (age 1 and ages 2–3 combined), which was not possible for Isle of May guillemots despite higher return rates; this may be attributed to the extremely large number of birds ringed on Canna, where ringing totals were approximately seven times those of the Isle of May. Survival of age 1 birds followed a broadly similar pattern over time to first-year survival, although it was higher and less variable (0.459–0.932; Figure 5.4b). Age 2–3 and adult survival both remained high throughout much of the study period and followed a similar pattern to each other, but different to that of age 0 and age 1 birds (Figures 5.4c, d). In both of these age classes there appears to have been a decrease in survival from around year 2000, culminating in extremely low survival in 2004 followed by partial recovery in 2005 (although this estimate is unreliable due to confounding with the 2006 recapture estimate).

Recapture probabilities for birds aged 2, 3 and 4 years are provided in Table 5.1, and time-specific estimates for adult birds in Figure 5.5. Recapture probability increased with age and, for adult birds, varied considerably over time. It was also clearly higher for adults ringed as breeders than those ringed as chicks (age 5^+ birds), particularly during earlier years of the study, although the temporal trends were essentially the same. The estimates in 2006 are confounded with adult survival in 2005, hence the large credible intervals. Mean age 5^+ and adult recapture probabilities were markedly lower than equivalent Isle of May recapture rates (actually resighting probabilities): weighted means were 0.111 and 0.172 for Canna age 5^+ and adults, respectively, with corresponding Isle of May weighted means of 0.441 for age 5^+ (averaged over areas A and B) and 0.969 for adult birds, presumably reflecting the different recapture methods and the much greater field effort put into the Isle of May study.

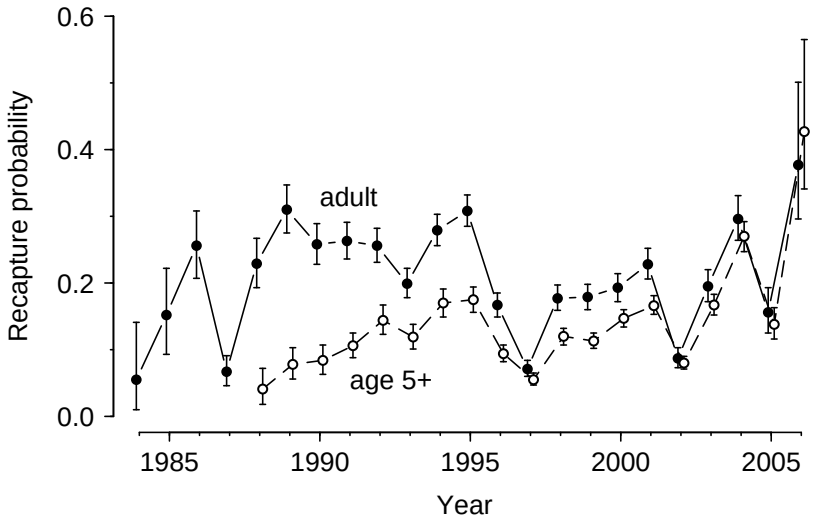

Figure 5.5 Posterior means and 95% symmetric CIs for recapture probabilities of 'adult' Canna guillemots, i.e., aged 5^+ birds ringed as chicks and birds ringed as adults.

Posterior means for the intercept and slope parameters of the logit-linear trend on recovery probability, denoted α_λ^{can} and β_λ^{can} respectively, are given in Table 5.1. The negative estimate for β_λ^{can} and a 95% CI that does not include zero provide strong evidence for a temporal decline in recovery probability over the period of the study, which appears to be a common trend for many avian populations (Baillie & Green 1987, Clark et al. 2005). Corresponding posterior estimates of λ_t^{can} are approximately half the magnitude of recovery rates of Isle of May guillemots, and range from 0.046 (95% CI: $0.040, 0.052$) to 0.014 ($0.012, 0.016$).

Fidelity probabilities for all age classes are also provided in Table 5.1. Fidelity probabilities of 2-, 3- and 4-year-olds were quite similar to each other and were estimated with low precision (note the large CIs) so it is not possible to draw any meaningful conclusions about how fidelity changed over these age classes. Age 5^+ fidelity of birds ringed as chicks was very high (essentially 1), as was fidelity of birds ringed as adults, from the second year after initial capture onwards. However, fidelity of adult birds in the year immediately following initial capture was rather lower, suggesting some degree (approximately 13%) of transience among newly ringed adults.

Colonsay

The selected model for Colonsay guillemots (birds ringed as adults only) had constant survival probability, with a separate estimate for 2004; year-to-year variation in recapture probability; a linear trend on recovery probability; and

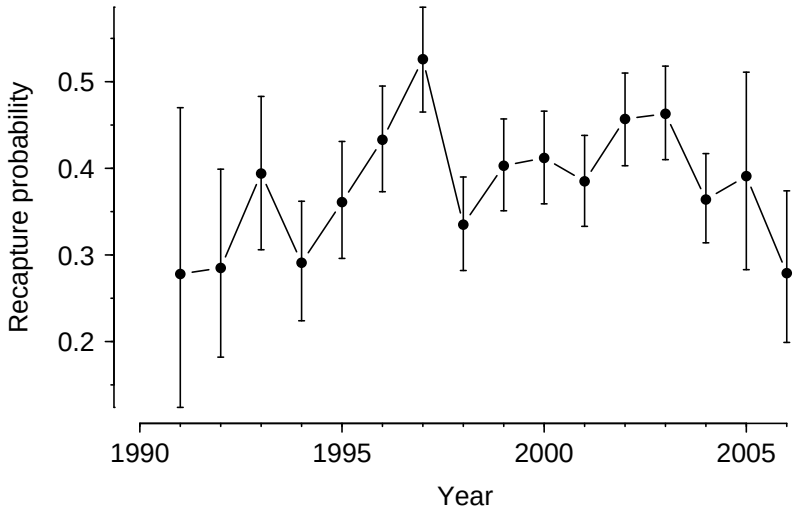

Figure 5.6 Posterior means and 95% symmetric CIs for recapture probabilities of Colonsay guillemots ringed as adults.

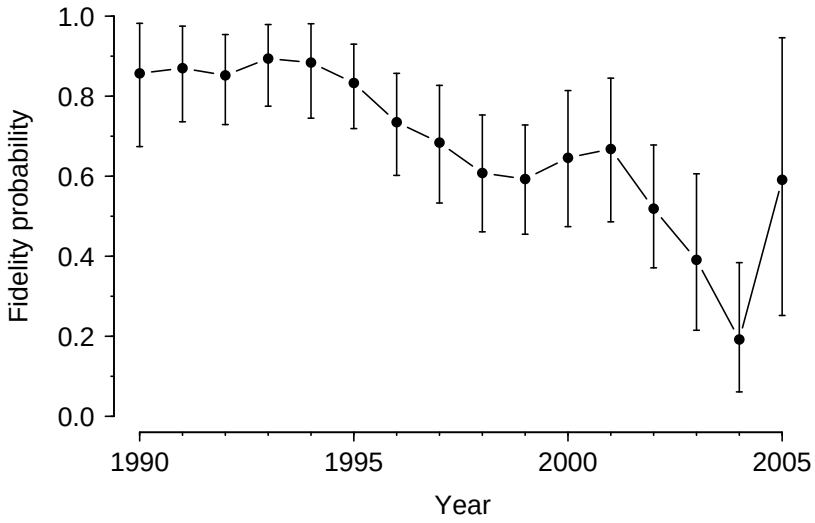

Figure 5.7 Posterior means and 95% symmetric CIs for fidelity probabilities of Colonsay guillemots in the year following initial capture (fidelity in subsequent years was fixed to 1).

year-to-year variation in fidelity probability in the year following initial capture only.

Constant survival probability was 0.955 (95% CI: 0.944, 0.965), with the 2004 estimate being considerably lower at 0.654 (0.494, 0.850). Recapture probabilities and corresponding 95% CIs are provided in Figure 5.6. As on Canna, recapture probability varied strongly over time, but although recaptures were by the same method as Canna, the Colonsay estimates were, on average, considerably higher (weighted mean of 0.397).

The intercept α_λ^{col}, and slope β_λ^{col}, of the logit-linear trend on recovery were

-2.42 $(-3.86, -1.13)$ and -0.106 $(-0.22, 0.02)$, respectively. The negative estimate for β_{λ}^{col} is indicative of a temporal decline in recovery probability, although the relationship is weak and the 95% CI includes zero; however, strong evidence provided by the Isle of May and Canna data for similar temporal declines suggest that this is not a spurious finding, but rather is due to the small size of the Colonsay dataset.

Fidelity in the year after marking was less than 1 and appears to have decreased dramatically over time (Figure 5.7; 0.857 in 1990 to 0.192 in 2004). This indicates a significant degree of transience among newly ringed adults: fewer than 20% of birds ringed in 2004 were expected to subsequently return to the study plot.

Survival comparison between colonies and age classes

Time-specific survival probabilities of Isle of May and Canna first-years and adults are compared pairwise in Figure 5.8, and posterior summary statistics of pairwise process correlations are provided in Table 5.2. First-year and adult survival of Isle of May guillemots were strongly correlated, and this is clearly apparent in the comparison plot (Figure 5.8a). Canna first-years and adults, on the other hand, had rather different patterns of survival over time (Figure 5.8b) and this is reflected by a low estimated correlation with a 95% CI that includes zero. Comparing survival between colonies, Isle of May first-year survival was very strongly correlated with Canna first-year survival (Figure 5.8c). Adult survival did not appear to be correlated between the two colonies (Figure 5.8d; 95% CI of correlation parameter includes zero) but survival in 2004 was the lowest estimate of the study in both cases, and by quite some margin for Canna; furthermore, 2004 adult survival of Colonsay guillemots was also significantly lower than the other years (ΔQAIC_c of -3.50 for this model, compared to a

Table 5.2 Posterior summary statistics for pairwise process correlations between Isle of May and Canna first-year and adult survival parameters.

Correlation	Mean	SD	95% symmetric CI
$\phi_{0,t}^{iom}$, $\phi_{a,t}^{iom}$	0.794	(0.134)	$(0.435, 0.951)$
$\phi_{0,t}^{can}$, $\phi_{a,t}^{can}$	0.273	(0.265)	$(-0.284, 0.715)$
$\phi_{0,t}^{iom}$, $\phi_{0,t}^{can}$	0.845	(0.096)	$(0.605, 0.956)$
$\phi_{a,t}^{iom}$, $\phi_{a,t}^{can}$	0.225	(0.353)	$(-0.489, 0.778)$
$\phi_{0,t}^{iom}$, $\phi_{a,t}^{can}$	0.678	(0.194)	$(0.178, 0.913)$
$\phi_{0,t}^{can}$, $\phi_{a,t}^{iom}$	0.569	(0.247)	$(-0.104, 0.881)$

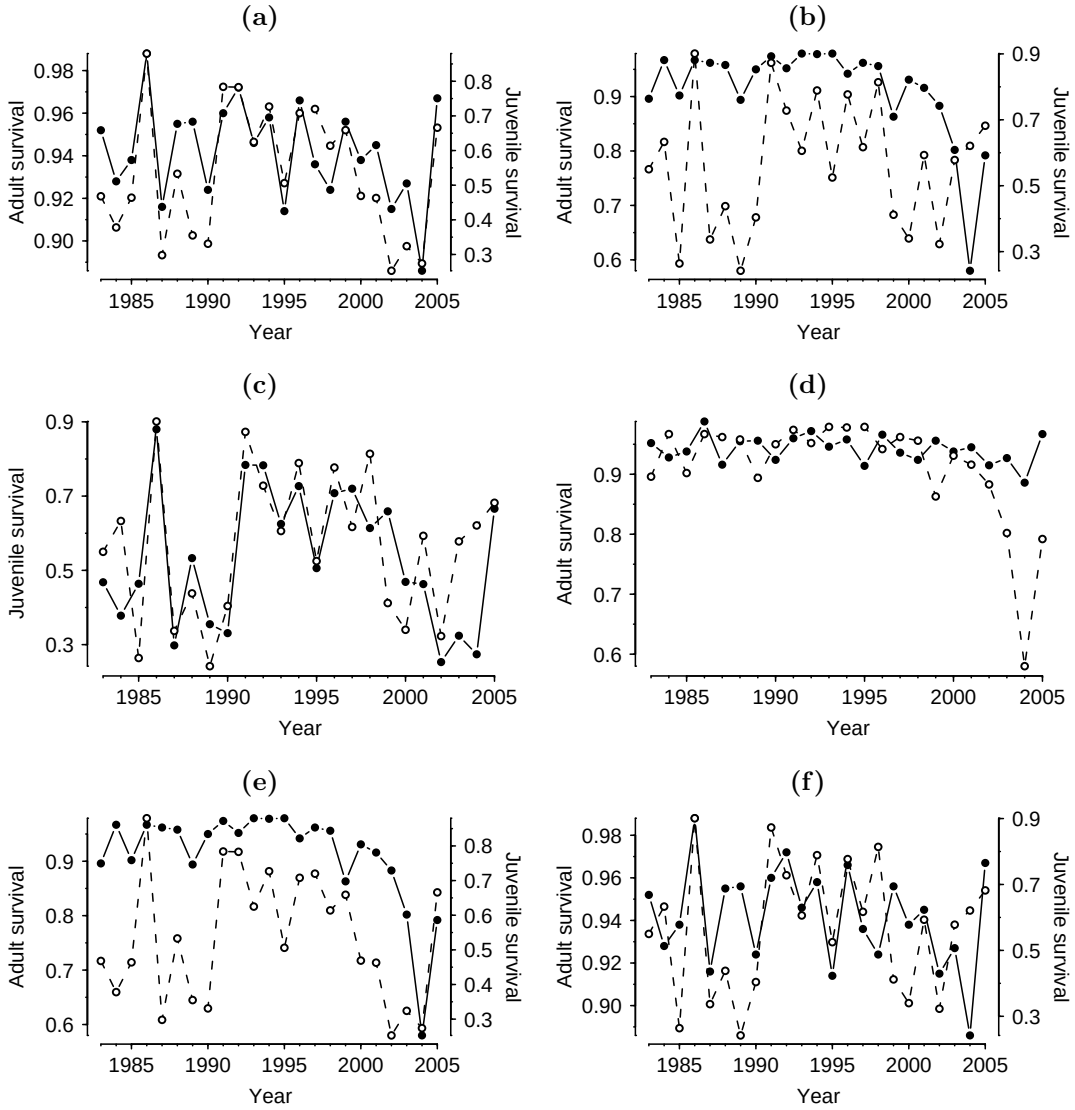

Figure 5.8 Pairwise survival comparison plots for first-year and adult guillemots ringed on Canna and the Isle of May. (a) Isle of May first-years and Isle of May adults; (b) Canna first-years and Canna adults; (c) Isle of May and Canna first-years; (d) Isle of May and Canna adults; (e) Isle of May first-years and Canna adults; (f) Canna first-years and Isle of May adults. Filled circles show adult survival ((a), (b), (e), (f)) or survival of Isle of May birds ((c), (d)), and open circles show first-year survival or Canna survival in these respective plots. Survival estimates are posterior means.

model with constant survival over all years). Isle of May first-year survival did not appear to be particularly strongly correlated with Canna adult survival (Figure 5.8e; although the posterior mean of the correlation is reasonably high, the 95% CI is very wide indicating a high degree of uncertainty in the estimate). Canna first-year survival followed a similar trend to Isle of May adult survival in some years, but was quite different in others (Figure 5.8f), and this is reflected in the process correlation estimate which, although reasonably high, has a 95% CI that includes zero. Regardless of the degree of temporal correlation,

Table 5.3 Mean survival probabilities of Isle of May, Canna and Colonsay guillemots.

	Survival probability (by age)				
Colony	**0**	**1**	**2**	**3**	**4^+ (adult)**
Isle of May	0.542†	0.782	0.922	0.900	0.952†
Canna	0.556†	0.779†	0.898†	0.898†	0.950†
Colonsay	–	–	–	–	0.955‡

† Weighted mean of time-specific estimates.
‡ Constant estimate does not include 2004 survival (estimated separately at 0.654).

when averaged over time survival rates were remarkably similar among all three colonies for all age classes (where applicable; Table 5.3).

5.3.2 Ring-recovery locations

Locations of ring-recoveries of Canna age 0, Canna age 4^+, Isle of May age 0 and Isle of May age 4^+ guillemots are plotted in Figure 5.9. The core areas of the recovery distributions are defined as being contained by the 50% kernel density contours. Apart from a small area in the northern Bay of Biscay, there is no overlap in the core recovery areas of the two Canna age classes (Figures 5.9a, b): age 0 birds were also recovered in high concentrations throughout the North Sea, including the Skagerrak and Kattegat, along the Norwegian coast and around the Faeroe Islands, but age 4^+ core areas are restricted almost entirely to northern Biscay, with some recoveries in the English Channel and up the west coast of the UK. Within the Isle of May age classes there is a high degree of correlation in core areas, with major concentrations of recoveries along the southern and western shores of the North Sea; however, 75 and 95% contours show Isle of May age 4^+ recoveries to be almost exclusively within these zones, whereas age 0 recoveries also extend into Biscay, the Faeroes, and in particular the Skagerrak and Kattegat (Figures 5.9c, d). Hence, there is a very high degree of correspondence between Canna and Isle of May age 0 distributions: although the core areas differ in some respects, the 90% regions are extremely similar, with the only real difference being that the Canna distribution extends further. Conversely, Canna and Isle of May age 4^+ recoveries show almost no overlap. Neither is there much correspondence between Canna age 4^+ and Isle of May age 0 distributions, and although Canna age 0 and Isle of May age 4^+ recoveries share a core area on the east coast of the UK, there is little other correspondence in these distributions.

Two-sample p-values from pairwise two-dimensional Kolmogorov-Smirnov

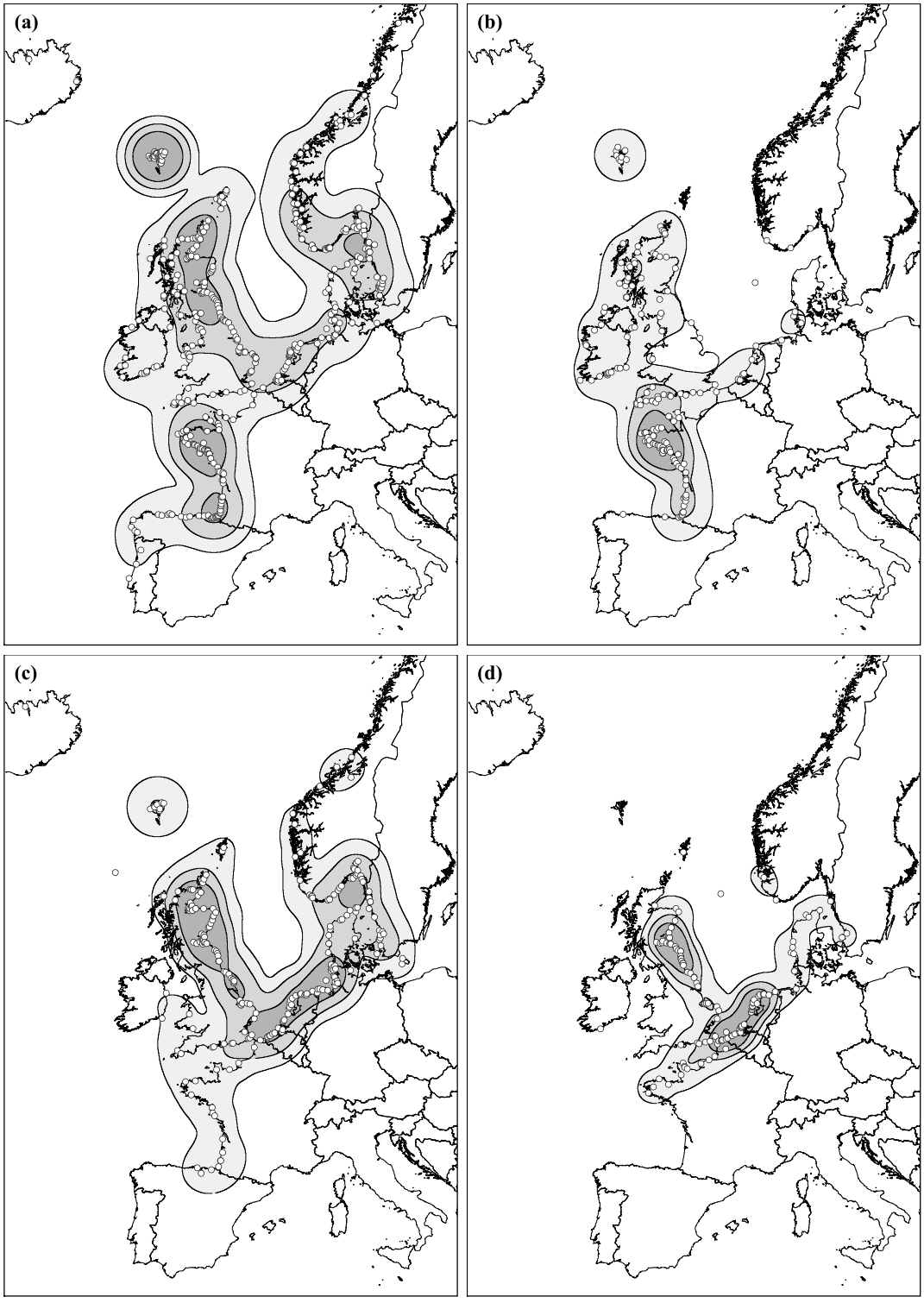

Figure 5.9 Locations of common guillemot ring-recoveries during nonbreeding seasons (October–March) 1983–2006, with 95, 75 and 50% kernel density contours (represented by increasingly dark shades of grey). (a) Age 0, ringed on Canna ($n = 485$); (b) age $\geqslant 4$, ringed on Canna ($n = 185$); (c) age 0, ringed on the Isle of May ($n = 241$); (d) age $\geqslant 4$, ringed on the Isle of May ($n = 139$).

Table 5.4 Results of two-dimensional Kolmogorov-Smirnov tests on pairs of recovery distribution data.

Data pair	D_{KS} statistic	p-value
Canna age 0 / Canna age 4^+	0.378	2.77e−12
Isle of May age 0 / Isle of May age 4^+	0.348	3.43e−07
Canna age 0 / Isle of May age 0	0.289	1.12e−08
Canna age 4^+ / Isle of May age 4^+	0.743	1.67e−28
Canna age 0 / Isle of May age 4^+	0.471	1.85e−15
Isle of May age 0 / Canna age 4^+	0.626	3.42e−26

Table 5.5 Results of pairwise χ^2 tests for differences in recovery frequencies by geographical region, according to age and/or natal colony.

Data pair	χ^2_2 statistic	p-value
Canna age 0 / Canna age 4^+	81.382	<2.20e−16
Isle of May age 0 / Isle of May age 4^+	10.376	5.58e−03
Canna age 0 / Isle of May age 0	58.022	2.52e−13
Canna age 4^+ / Isle of May age 4^+	165.132	<2.20e−16
Canna age 0 / Isle of May age 4^+	62.012	3.42e−14
Isle of May age 0 / Canna age 4^+	177.366	<2.20e−16

Notes: Calculations performed with function '`chisq.test`' in [R]; observed frequencies are provided in Figure 5.2.

tests on recovery distributions are provided in Table 5.4. All p-values are highly significant, indicating that each pair of distributions are significantly different from each other. Results from Monte Carlo tests confirm this, with all $p < 0.001$ (observed D_{KS} were greater than those from all 999 simulated datasets for all pairings).

Results of pairwise χ^2 tests on the frequency of recoveries by geographical region are provided in Table 5.5. As with the two-dimensional K-S test, all p-values are highly significant, implying that none of the age/colony pairings have the same proportion of recoveries by region, even at this very coarse scale.

5.4 Discussion

Survival rates of wild animal species commonly vary over both time and space, with important consequences for multi-population dynamics (Ozgul et al. 2006). The identification of patterns of age-dependent temporal and spatial variation in survival, and how these are related to features of the environment, is therefore of prime importance to conservation ecology. However, due to the requirement for detailed data at large spatial and temporal scales, published studies of spa-

tiotemporal variation in age-specific survival are scarce (but see Ringsby et al. 1999, Schaub et al. 2005, Ozgul et al. 2006, Baker & Thompson 2007). Using mark-recapture and ring-recovery data obtained from long-running field studies at three widely separated colonies, we were able to show that spatiotemporal patterns of variation in survival between different age classes and colonies of common guillemots are consistent with differences in distribution outside the breeding season. Although we still cannot point to the exact aspect of winter environment which drives interannual variation in survival, these results support the notion that spatial variation in winter conditions can have a strong influence on population dynamics on a large scale.

Isle of May survival rates have been analysed in previous chapters and in a number of other studies. The estimates provided here are very similar to those provided by Harris et al. (2007b) (first-year survival) and Crespin et al. (2006b) (adult survival), and we refer the reader to these papers for detailed discussions of the various factors that may affect the survival of Isle of May guillemots. First-year and adult survival were strongly correlated over time ($\rho_{\phi^{iom}_{0,t},\phi^{iom}_{a,t}} = 0.79$) and, with the exception of an agglomeration of first-year recoveries in the Skaggerak, the two groups also had a high degree of overlap in core (within 50% kernel density contours) ring-recovery distributions. Taking the distributions of recovery locations, which by default are restricted to coastlines, as representative of at-sea wintering areas, we can therefore assume that Isle of May first-years and adults winter mainly together in the southern and western North Sea, where they are exposed to similar environmental conditions.

Adult survival of Canna guillemots was previously analysed for years 1983–1995 by Harris et al. (2000). Here we present adult survival estimates for a much longer time period, and by combining data from birds ringed as chicks and incorporating information on dead recoveries we produce more precise, time-specific estimates for the earlier years. We also provide the first estimates of first-year and immature survival for Canna guillemots. Unlike Isle of May guillemots, first-year and adult survival of Canna birds were not significantly correlated ($\rho_{\phi^{can}_{0,t},\phi^{can}_{a,t}} = 0.27$, 95% CI includes zero) and this is reflected in only a small degree of overlap in core wintering areas: Canna adults appear to winter, or at least die, mainly in a relatively small area off Brittany, and while first-years also use this area, large numbers enter the North Sea where they mix extensively with Isle of May birds, particularly first-years. The high correspondence between Isle of May and Canna first-year wintering areas almost certainly explains the strong correlation in survival between these two groups ($\rho_{\phi^{iom}_{0,t},\phi^{can}_{0,t}} = 0.85$). Conversely, the lack of any overlap in core winter distributions of Isle of May

Table 5.6 Results of post hoc Spearman's rank correlation tests of first-year and adult survival between Skomer and Isle of May/Canna guillemots. Values are correlation coefficients, r_s, with p-values in parentheses.

	$\phi^{sko}_{a,t}$	$\phi^{iom}_{0,t}$	$\phi^{iom}_{a,t}$	$\phi^{can}_{0,t}$	$\phi^{can}_{a,t}$
$\phi^{sko}_{0-1,t}$	0.36 (0.304)	0.44 (0.198)	0.25 (0.487)	0.60 (0.070)	0.19 (0.590)
$\phi^{sko}_{a,t}$	–	0.20 (0.425)	0.30 (0.220)	0.30 (0.226)	0.23 (0.362)

and Canna adults probably explains the lack of correlation in survival between them ($\rho_{\phi^{iom}_{a,t},\,\phi^{can}_{a,t}} = 0.23$, 95% CI includes zero).

Due to data limitations, it was not possible to obtain time-specific survival estimates for Colonsay adult guillemots, nor investigate their winter distribution. The constant survival estimate of 0.955 for all years except 2004 was very much in line with mean adult survival on both the Isle of May and Canna (Table 5.3). Survival in 2004 was considerably reduced on Colonsay, and was also the lowest on record at the other two colonies: a reduction of a similar magnitude to Colonsay was observed for Canna adults, and although less extreme on the Isle of May, 2004 survival was nevertheless considerably lower than all other years of the study (the 95% CI only included one other posterior mean).

Survival rates have also been previously published for a fourth UK guillemot colony, on Skomer Island, southwest Wales. Skomer is located more than 400 km from the nearest of our three Scottish colonies (see Figure 5.1), and is therefore effectively isolated during the breeding season, but there is some small degree of overlap among wintering distributions. Votier et al. (2008) provide juvenile survival estimates for years 1985–1998 (excluding 1991–1994; estimates are two-year compound survival to age 2), together with maps of nonbreeding season ring-recovery distributions for guillemots ringed at southern Irish Sea colonies. Adult survival rates for 1985–2002 are provided by Votier et al. (2005).

Juvenile and adult survival of Skomer guillemots were not correlated during the ten years of concurrent estimates, and neither were survival of these two groups significantly correlated with any of first-year or adult survival at either the Isle of May or Canna (see Table 5.6). Younger guillemots from Skomer were widely dispersed, with core recovery areas within southwest England, southeast Ireland and the Bay of Biscay, whereas older birds had a far more restricted range with a single, small core area off southeast Ireland (see Votier et al. 2008, figure 2). The correspondence between these wintering areas and those of Isle of May and Canna birds was also generally low. It is perhaps surprising that survival of Skomer juveniles and Canna adults were not more similar, as these groups have a reasonable overlap in core and overall (within 95% kernel den-

sity contours) recovery areas, but this appeared to be the least correlated of all pairs. The closest to statistical significance, with a reasonably high correlation coefficient of 0.60 ($p = 0.070$), were Skomer and Canna juveniles, both of which appear to have a large presence in Biscay; however, unlike Canna very few Skomer birds enter the North Sea, where conditions are potentially quite different. Despite the lack of any temporal correlations with other colonies, the mean adult survival rate of Skomer guillemots, at 0.955, was very similar to those at the three Scottish colonies (provided in Table 5.3). Assuming a second-year survival rate equal to that of Isle of May and Canna birds (~ 0.78), we calculated mean first-year survival at Skomer to be approximately 0.623, which is somewhat higher than the means for Isle of May and Canna over the same 10-year period (0.510 and 0.504, respectively). Survival estimates for birds aged 2 and 3 years were 0.953 and 0.874, which are, respectively, slightly higher and lower than the equivalent estimates for the Isle of May and Canna (Table 5.3).

The available information for Skomer is thus generally consistent with our findings from the Isle of May, Canna and Colonsay, that: (1) as predicted, survival was highly correlated over time for 'groups' sharing wintering areas, and essentially uncorrelated for those with separate, or only partially overlapping, wintering areas; and (2) despite widely varying degrees of temporal correlation, mean age-dependent survival rates were remarkably consistent across colonies. These results strongly suggest that some aspect of winter environment is responsible for interannual variation in survival of British guillemots. The differences in temporal patterns of survival observed between groups of birds with separate winter distributions point towards environmental features that, within years, vary on a smaller spatial scale than the dispersal range of the guillemot colonies studied, thus providing different conditions for annual survival in, for example, the North Sea, Irish Sea and Bay of Biscay. However, the fact that there was no obvious latitudinal or longitudinal variation in mean survival rates among the four colonies suggests that 'average' environmental conditions were similar across the entire range of winter distributions from Spain to Norway. Furthermore, all correlations between pairs of time-specific survival estimates—including nonsignificant correlations between groups with widely separated wintering areas—were positive (Tables 5.2 and 5.6), implying that the environmental drivers of survival are also correlated, albeit loosely, on a large scale. Finally, adult survival in 2004 was similarly low for both east and west coast Scottish colonies (no 2004 estimate was available for Skomer), indicating the effect of an extreme large-scale or spatially correlated climatic event that year. In fact, the poor survival in 2004 was associated with a sub-

stantial wreck of seabirds in northwest Scotland during late August–September of that year, of which the majority of Canna guillemots recovered were adults of breeding age (Swann 2004). The apparent cause of the wreck was low availability of suitable prey, exacerbated by a period of stormy weather (Swann 2006). The low availability of prey may have been relatively localised, but a prolonged series of Atlantic depressions has the potential to affect wintering guillemots from all British colonies.

It therefore seems likely that spatiotemporal variation in survival of British guillemots is driven by a combination of large-scale environmental factors and more localised features: large-scale variables (for example the number of deep winter depressions crossing northern Europe, or spatially correlated sea surface temperatures) create similar conditions over a wide area, and thus act to synchronise survival rates between distant colonies; meanwhile, smaller-scale phenomena (for example local variations in prey density, or oil spills) appear to reduce the strength of temporal correlations by creating within-year variability in conditions between regions. The influence of spatial variation in environmental conditions on survival is further complicated by variation in the degree of nonbreeding season mixing between colonies and age classes, leading to the observed correlations among birds from different regions (e.g. Isle of May and Canna first-years), or different temporal trends for birds from the same colony (e.g. Canna first-years and adults).

In long-lived species with low reproductive output and delayed maturity survival is an important driver of population growth rate, and hence population dynamics (Heppell et al. 2000, Sæther & Bakke 2000, Oli & Dobson 2003). The spatiotemporal variation in survival found among four British guillemot colonies therefore has important multi-population dynamics consequences for the species. In particular, positive correlations of survival rates among age classes within a colony (e.g. Isle of May first-years and adults) will tend to increase variation in the population growth rate of that colony (Coulson et al. 2005). Furthermore, covariation of survival between multiple widely separated colonies, whether due to overlap in winter distribution or the influence of correlated environmental conditions, could synchronise the growth rate of the whole metapopulation (Schaub et al. 2005, Jenouvrier et al. 2009b), potentially reducing its persistence (Palmqvist & Lundberg 1998). Population growth rate is most sensitive to adult survival in long-lived avian species (Lebreton & Clobert 1991, Sæther & Bakke 2000), so synchronised reductions in adult survival over a wide geographic area, such as that observed for guillemots in 2004, are particularly harmful to metapopulation dynamics. Regarding the two apparent

causes for low survival in 2004, climate forecasts predict an increase in the frequency of 'deep' winter depressions crossing the UK (Hulme et al. 2002), and ongoing changes in marine foodwebs of the northeast Atlantic are drastically affecting the availability of suitable prey species for seabirds (e.g. Mavor et al. 2005, 2006, 2008, Harris et al. 2007a). Therefore, it seems likely that the frequency and severity of such extreme survival years will increase in the future, with potential serious consequences for common guillemots and other colonial seabird populations.

In summary, the results of this study indicate that conditions in wintering areas have a strong impact on guillemot demography and population dynamics, and thus exemplifies how the identification of spatial patterns in demography can lead to insights into the factors driving population change. In the current context of environmental change, such large-scale studies provide a useful tool for identifying vulnerable life-history traits, or important geographical regions, and thus aid decisions on appropriate conservation strategies.

Chapter 6

General discussion

6.1 Thesis overview

Within the preceding chapters we have demonstrated how related ecological datasets may be advantageously combined in integrated analyses, under a Bayesian framework, to gain maximum benefit from those data. The particular application involved a number of datasets relating to the UK's most abundant breeding seabird species, the common guillemot *Uria aalge*.

The thesis follows a natural progression, beginning with the separate analyses of multiple guillemot datasets from a single colony; these data are then combined to form an integrated population model; this model is extended to make future population predictions for the colony; and finally, the spatial aspect of the analysis is extended to consider data from other UK guillemot colonies. In so doing, it performs two main functions: it adds to and extends the growing body of literature on integrated modelling, and it provides an important application to seabird data in a time of much uncertainty about the future of the UK's seabird populations.

6.2 An integrated model of a seabird colony

In Chapter 2, we presented three separate analyses of datasets relating to the abundance, survival and productivity, respectively, of a single population of guillemots breeding on the Isle of May, southeast Scotland. However, we note that while abundance data most obviously contain direct information on the size of a population, they also contain information about the underlying processes that drive the observed changes in population size—its vital rates. As we demonstrated though, the independent analysis of abundance data provides relatively little information about the individual vital rates, because there is

usually only one data point per year; in this case, it is only possible to say whether the population had a good or bad year, but not which vital rate(s) were responsible for the changes. Note that this is not always the case: data obtained from multiple counts in a single season, such as under the British Trust for Ornithology's Constant Effort Sites scheme, can be used to estimate both abundance and productivity (as well as survival from recaptures recorded during the same visits; see, e.g., Cave et al. 2009); alternatively, multivariate time series of counts, in which different age-classes are recorded separately, can also help in this respect (Tavecchia et al. 2009). We also highlighted that analysing data independently can produce inconsistent results, which may be due to genuine inconsistencies in the data, or as a consequence of incorrect/inadequate model specification for some or all of the datasets. Most notably, estimates of guillemot survival derived from mark-recapture data were not consistent with the population counts; additionally, adult survival estimates differed considerably between two different mark-recapture datasets containing information on essentially the same members of the population (breeding adults).

The observation that different datasets from the same population often contain information about common parameters, and the piecemeal nature of many ecological analyses where comparisons between datasets are made on an ad hoc basis, were the primary motivations behind the development of integrated population modelling (Besbeas et al. 2002, 2005). This is where a model for abundance data (usually a state-space model) is combined with one or more models for demographic data under a joint likelihood to obtain simultaneous estimates of population size and vital rates. The Isle of May guillemot data were ideally suited to such an approach, with a number of parameters shared between two, or even three, different datasets. Furthermore, there were questions relating to the dynamics of the colony that the individual datasets on their own were unable to answer, the foremost of these being: 'What proportion of young Isle of May birds emigrate from the colony?' The natural solution was to develop an integrated population model for the Isle of May data, which was the focus of Chapter 3. With this model we were able to account explicitly for the emigration of prebreeder guillemots, using the strength of the combined data to disentangle the effects of emigration from those of ring loss and reduced visibility of breeding birds.

As noted in Section 3.5, the estimates of survival and productivity from the integrated model compared closely to those obtained from separate analyses of the mark-recapture-recovery and productivity data, using the same model structures. This is in contrast to Chapter 2, where there were inconsistencies

between the datasets, but these results were based on different model structures. In fact, preliminary attempts at the integrated model (not included in this thesis) using similar models to those in Chapter 2 also performed poorly, providing an unsatisfactory fit to the data. This highlights that integrated population modelling is not an instant miracle cure to resolve inconsistencies between datasets, and neither does it cover up for mis-specification of the underlying model structure. Rather, it can provide insight into the possible reasons for any problems, and thereby suggest what adjustments to the model might be made to improve the fit. Here, the observation error variance can reflect, in part, a measure of model fit, and may be used to guide model construction (Tavecchia et al. 2009). Integrated modelling may also help to identify where additional data-collection efforts could be focused to provide the most useful information on parameters of interest.

Although the dynamics of guillemot colonies are complex—due to delayed maturity, individual and interannual variability in the age of first breeding, and immigration/emigration of prebreeders—the Isle of May population model was kept relatively parsimonious by defining only two age-classes and specifying a number of simplifying assumptions. It could be argued that the model was not realistic enough to properly capture the dynamics of the population. Nevertheless, it achieved a close fit to the data and appeared robust to changes in the major assumptions, such as age of first breeding.

A necessary assumption when combining likelihoods is that of independence of the different surveys. However, in studies of wild populations—particularly those living on islands, or colonially-nesting species such as seabirds—this assumption will often not be met (Besbeas et al. 2008). This is because demographic information for such spatially confined populations is generally gathered on a subset of the population being surveyed for abundance data. In the case of the Isle of May guillemot study, for example, adult mark-recapture and productivity data were largely collected on the same sample of individuals nesting in the easily observed study plots; the group of birds ringed as chicks contributed to both live-recapture and ring-recovery data; and individuals in both these groups were included in the total colony counts. Besbeas et al. (2008) showed, using simulated data, that violation of the independence assumption can lead to biased parameter estimates; however, they used an extreme case where the entire censused population was marked. Conversely, in a test using real data, Cave et al. (2009) found no evidence of bias when ignoring the issue of independence. Given that the Isle of May demographic data was gathered on a relatively small subset of the total colony, the effect of any dependence on the

parameter estimates was probably very small (see also Tavecchia et al. 2009), although this is an issue that may warrant further investigation. The most likely source of any dependence would be among the productivity and adult survival estimates, which could be tested by splitting these datasets into their individual study plots and using separate sets of plots to estimate survival and productivity.

Pre-recruitment emigration among the Isle of May guillemot colony was estimated at 19.5% per cohort, which is lower than previously published estimates, these ranging from 24 to 33% (Harris et al. 1996a, Crespin et al. 2006a, Harris et al. 2007b). This difference is possibly because our estimate also reflected immigration of prebreeders from other colonies recruiting into the Isle of May breeding population, which is known to occur (Halley & Harris 1993) but which for simplicity we did not explicitly allow for in the model. However, the emigration parameter ψ could not truly reflect net movement because it was a probability, and consequently restricted to the interval [0,1]. Therefore, the assumption of no immigration is likely to be an unrealistic one, and may have implications for our estimates of other parameters in the model, particularly the emigration rate. Knowledge of immigration comes from resightings on the Isle of May of guillemots ringed at other colonies (Halley & Harris 1993) but there are far too few of these observations to be of any use for estimating immigration. It is difficult to see how other data might be collected to better estimate immigration rates, as the few sightings of birds from other colonies resulted from several years of very labour intensive fieldwork. Increased ringing of guillemots at nearby colonies would provide a larger source population for observations, but this would be costly, and even then would give little indication of numbers of birds coming from further afield. It may, however, be possible to incorporate immigration in the model quite simply by, for example, specifying a constant or time-specific number of immigrants per year in the process model, which would be an extension to the model well worth investigating.

We approached this analysis from a Bayesian perspective, using MCMC to obtain samples from the posterior distribution. We could equally have used sequential importance sampling (SIS; Doucet et al. 2001) as an alternative to MCMC. There is little to choose between the two methods, each having its own advantages (and disadvantages): Newman et al. (2009) suggest that SIS is 'a more automatic procedure' that is easier and quicker to programme than MCMC, and performs comparably where data are relatively uninformative; on the other hand, they note that a careful implementation of MCMC with informative data (as we had) produces posterior distributions with considerably

less Monte Carlo variation than SIS for the same computing time; in particular, standard SIS algorithms become very inefficient for random effects models (L. Thomas pers. comm.). Computing time is often an important consideration with complex Bayesian analyses, and given that our MCMC simulations took upwards of 60 hours to run, a suitable SIS implementation may have proven prohibitively time consuming. On the other hand, an advantage of SIS is that it easily handles the incorporation of new time points at the end of the series (Newman et al. 2009), so that as new data become available each year the model can simply be updated, whereas the MCMC algorithm would need re-running for the full time series.

A further alternative would be a classical analysis using the Kalman filter (see, e.g., Besbeas et al. 2002). Traditionally, this approach relies on the use of potentially restrictive normal approximations to discrete distributions and a linear model structure. However, analyses based on the normality assumption have been shown to be robust, at least with large population sizes (Brooks et al. 2004). Furthermore, recent work by Besbeas et al. (2008) into methods for initialising the Kalman filter for ecological time series, and accounting for nonlinearities, have improved and extended the usability of the Kalman filter such that it would be a viable alternative. This does not avoid the fact that the Bayesian approach naturally deals with those situations for which the Kalman filter essentially has 'workarounds', thereby providing a more flexible analysis framework (Millar & Meyer 2000, Jamieson & Brooks 2004). Therefore, in this case, the Bayesian approach using MCMC was the preferred choice.

6.3 Integrated population predictions

Increases in sea surface temperatures in UK coastal waters have already been correlated with reductions in seabird productivity and survival, presumably mediated through changes in prey abundance (e.g. Frederiksen et al. 2004b, Harris et al. 2005, Sandvik et al. 2005). With UK climate-change scenarios predicting further increases in sea surface temperature in the future (Lowe et al. 2009), serious pressures will potentially be placed on seabird populations. The frequency of extreme weather events is also expected to increase (Solomon et al. 2007), likely leading to further reductions in population growth rates through increased variability in demographic parameters (Frederiksen et al. 2008). The recent widespread breeding failures at many UK seabird colonies (e.g. Mavor et al. 2005, 2008) may already reflect the state of things to come, and the

ability to reliably predict the population consequences of recent and possible future changes in demographic rates is thus vital for the proper planning of management and conservation strategies.

In Chapter 4, we implemented a modified version of the integrated population model to produce population predictions for the Isle of May guillemot colony. An advantage of the integrated approach over the standard types of predictive model is the way in which the predictions simultaneously reflect both abundance and demographic data, thereby making full use of the available information and, potentially, resulting in more accurate, precise and reliable predictions. Also, the future projection period was essentially treated as part of the estimation model, and in this way posterior distributions for the predicted states (breeder and prebreeder population sizes) were obtained as part of the model output, rather than performing stochastic projections (Maunder et al. 2006).

Here, again, the Bayesian approach was key, and to be preferred over a classical analysis. With the Bayesian analysis, we were easily able to incorporate most major sources of uncertainty into the projections, including uncertainty in the parameter and population estimates, and in the underlying demographic process. Had we been selecting between competing models, we could also have accounted for model uncertainty by using reversible jump MCMC (Green 1995, King & Brooks 2002, King et al. 2009). But possibly the biggest advantage of a Bayesian approach over a classical approach in the present context is in the form of the statistical output. The posterior probability distributions yielded by Bayesian analyses are simple to explain and present to managers and policy makers, and automatically include the uncertainty of the estimates (Wade 2000). And the potential of posterior distributions extends beyond obtaining simple summary statistics. Once posterior samples are generated, they (or functions of them) may be queried for a large number of biologically important questions (e.g. Taylor et al. 1996, Brooks et al. 2008), or used by managers in a decision analysis to evaluate the consequences of different conservation decisions (Berger 1985, Taylor et al. 1996, Wade 2000). For example, we were able to obtain posterior estimates of the 10-year probabilities of population decline below a range of different thresholds, providing simple statistics for comparison between scenarios.

One source of uncertainty that could not be formally incorporated in the model framework was future uncertainty. By modelling a number of scenarios we anticipated a range of possible outcomes, but without a means to assign probabilities to these outcomes there is no way to know which, if any, is most

likely. A formal way to include future uncertainty would be to use the probabilities associated with climate prediction scenarios, but this depends first on a model relating demographic parameters or population growth to an environmental variable, and second that future climate models for this variable are available. For example, Jenouvrier et al. (2009a) projected emperor penguin *Aptenodytes forsteri* population responses to future sea ice changes, using Intergovernmental Panel on Climate Change (IPCC) projections of sea ice extent. However, previous studies of the Isle of May guillemots did not identify any environmental covariates that adequately explained variation in survival (Crespin et al. 2006a, Harris et al. 2007b). Although not detailed earlier in the thesis, we also conducted our own exploratory analysis of a range of possible environmental covariates for survival and productivity: the covariates tested were the NAO index, local and regional winter sea surface temperatures, and one- and two-year lagged versions of each of these, none of which appeared to be significantly correlated with any of the demographic parameters. However, it should be noted that these were only tested on an ad hoc basis by estimating the Spearman's rank correlation between covariates and parameter point estimates, and did not take into account the sampling variability of the parameters. Thus, there may be some profit in exploring these covariates further in a more rigorous logistic regression framework, with random effects to cope with any temporal variability not explained by the covariates (see, e.g., Gimenez et al. 2008), and with the benefit of several years of additional data.

In the absence of alternative information, we restricted our analysis to assuming that future conditions for each demographic rate mirrored either recent or long-term historical conditions. Given the recent decline in demographic performance, its probable links with environmental factors, and the predictions of future environmental change, the 'worst-case' scenario (i.e., productivity and survival continue at post-2000 levels) may well be the most realistic of the five scenarios tested. Under this scenario, the model predicted an expected decline in population size of 31% over 10 years. While this figure is in itself important, of greater interest, particularly for policy makers, is the variation in population trajectories, as this gives an indication of how confident we can be in our predictions. For example, the 95% credible interval of the 10-year proportional change for the above scenario ranged from an 8% to a 53% decrease, indicating that there is a lot of uncertainty in the final outcome. However, the fact that the upper limit was well below zero provides a very high degree of certainty that there will be some decline in population size over this period.

6.4 Spatiotemporal variation in survival

Although no environmental covariates have so far been found that explain interannual variation in survival of Isle of May guillemots, evidence suggests that the main mortality occurs during the nonbreeding season, which points towards some aspect of winter environment. We provided strong evidence for this in Chapter 5, with the finding that survival of guillemots from three widely separated UK colonies was highly correlated for groups with overlapping wintering areas, and essentially uncorrelated for those with little or no overlap. This suggests that the main environmental drivers of UK guillemot survival act at a regional scale (e.g. North Sea, Irish Sea, Bay of Biscay). However, there was some evidence that larger-scale environmental phenomena also influence survival over a much wider geographic area (see, for example, discussion on 2004 adult survival rates in Section 5.4, page 118).

Spatiotemporal correlations in survival can have important consequences for the population dynamics of a species (e.g. Schaub et al. 2005, Ozgul et al. 2006, Jenouvrier et al. 2009b), potentially resulting in higher species extinction risk (Palmqvist & Lundberg 1998). Of particular concern for long-lived species like the common guillemot are large-scale reductions in adult survival caused by extreme climate conditions, such as storms (Jenouvrier et al. 2009b). We found generally low levels of synchrony in adult survival of guillemots from widely separated UK colonies, presumably because they had nonoverlapping wintering distributions and were, therefore, subject to different environmental conditions. However, there was evidence of an extreme climatic effect in 2004, when survival of adult guillemots from both the east and west coasts was the lowest on record. We highlighted in Chapter 4 that even relatively small decreases in adult survival can have large consequences for guillemot population growth. If, as predicted, extreme weather events become more common in the future (Hulme et al. 2002, Solomon et al. 2007), exacerbating the effects of continued food shortages, the future of the entire UK guillemot population has the potential to be severely threatened, along with other long-lived seabird species.

The search for suitable environmental covariates of survival described in the previous section was also extended to this analysis, and included Canna survival rates. In particular, here we considered regional winter sea surface temperatures corresponding to the core wintering areas of each group of birds, as defined by their ring-recovery distributions. As before, although our search was unsuccessful, future studies may benefit from including such covariates within the analysis framework.

The conclusions of this chapter could potentially be strengthened by incorporating data from other UK guillemot colonies, particularly from different regions not covered here (e.g. east coast of England, north Scotland and Northern Isles). There are a number of other colonies at which ringing takes place, but unfortunately there are no other large guillemot mark-recapture-recovery datasets from the UK that would have sufficient numbers of birds ringed for this type of analysis. There are a few datasets with recoveries only, but only Fair Isle (between Orkney and Shetland) and Great Saltee (southeast Ireland, quite near to Skomer) would have enough recoveries to be worth looking at that span a reasonably long period. However, it is believed that they ring almost entirely chicks at these colonies, so it would not be possible to derive reliable estimates of adult survival or winter distribution.

A meaningful comparison of ring-recovery locations of the different populations and age-classes of guillemots in this analysis was not possible using the two-dimensional Kolmogorov-Smirnov test, which is perhaps unsurprising given this tests for whether two distributions are exactly the same—an extremely unlikely outcome in this context. We therefore relied upon a visual comparison of kernel density plots; yet a more formal statistical comparison of winter distributions would greatly enhance the robustness and interpretation of the results. A potential approach would be to calculate the overlap of kernel density regions among the different groups, to produce a percentage similarity, for example. Such a calculation does not appear to be possible with the output of ArcView GIS 3.2; however, the statistics software [R] has a number of packages available for computing kernel density estimates that may be useful.

We also draw attention to the potential problems of using ring-recovery distributions as a proxy for wintering distributions of live guillemots. First, the effect of wind and currents may cause corpses to drift some distance from the location of death before being washed ashore, potentially resulting in systematic bias due to prevailing conditions. Second, the occurrence of recoveries varies spatially, and temporally, because of variation in reporting probabilities due to non-uniform search effort (Siriwardena et al. 2004). Over half of all guillemot recoveries have details of the cause of death, which include high proportions of birds drowned in fishing nets (usually inshore), oiled individuals, and those shot for human consumption (Harris & Swann 2002). The distribution of recoveries is therefore heavily biased towards areas of high fishing activity (notably southern Scandinavia and Ireland), pollution (the Netherlands, Germany and Channel Islands) and human predation (Faeroe Islands), and biased away from remote, sparsely populated regions (e.g. northwest Scotland). Furthermore, Harris &

Swann (2002) note that birds in their first year of life are much more likely to be shot or caught in nets than adults, which will exaggerate the bias in estimated distribution of this age class. They also note that ring-recoveries underestimate the true marine range of seabirds, with consequences outside the relatively enclosed areas of the North and Irish Seas; in particular, they deduce that guillemots are much more numerous off west Britain and Ireland than the recoveries suggest. All these factors highlight the need for caution when drawing conclusions about winter ranges of live birds derived from geographic distributions of ring-recoveries.

The use of Program MARK to conduct the analyses in Chapter 5 represented a deviation from previous chapters, where bespoke Fortran code was written to implement MCMC simulations. The main reason for using MARK was to speed up and simplify the process of model selection for the individual colony data, by using maximum likelihood estimation with AIC. This is perhaps one area where a classical analysis is to be preferred over a Bayesian one: we were using standard mark-recapture-recovery models with well-tested, prewritten software; we had no prior information to include, other than a set of candidate models; and lastly, maximum likelihood with AIC has a more rigorous framework than the equivalent process using MCMC and DIC (also available in MARK), as well as being faster and accommodating goodness-of-fit testing.

We then used the MCMC module in MARK to test for process correlations between pairs of survival rates. A simple extension to this analysis would be to test whether correlated sets of parameters could be modelled more parsimoniously by assuming the same survival rates for both, or even multiple, groups, perhaps with an additive effect (on the logit scale). For example, an obvious model to try would be

$$\text{logit}(\phi_{0,t}^{can}) = \text{logit}(\phi_{0,t}^{iom}) + k_1 = \text{logit}(\phi_{a,t}^{iom}) + k_2,$$

where k_1 and k_2 represent additive constants and are parameters to be estimated. This approach might be particularly beneficial for the Colonsay data, which was not detailed enough to obtain time-specific estimates but, due to its proximity, is likely to have similar adult survival rates to Canna.

Clearly, with three colonies and multiple age-classes there would be a large number of combinations to test, and the model selection approach in MARK would be tedious and time-consuming, particularly given the size of the combined dataset. Here, then, a Bayesian reversible jump MCMC framework could have significant benefits for efficiently exploring the model space and rigorously

selecting between competing models (see, e.g., King & Brooks 2002). This framework is very flexible and could also, if desired, easily incorporate extensions such as covariates and/or random effects. On the other hand, reversible jump MCMC would be considerably more difficult to implement than a MARK analysis, although advances in Bayesian analysis software such as WinBUGS have already simplified the process considerably (see Gimenez et al. 2008) and will most likely become even more user-friendly and powerful in the future.

6.5 Future directions

In light of the findings contained herein, particularly those relating to the future of the Isle of May guillemot colony—combined with the results of other published studies detailing the actual or potential effects of environmental change on seabird populations—there is a clear need for continued gathering and analysis of seabird data from UK colonies. Integrated analyses present a particularly promising direction for seabird data, because collection of abundance and demographic data routinely takes place at a number of UK colonies as part of JNCC's Seabird Monitoring Programme (see JNCC 2009). Annual estimates of population size and breeding success are available for many UK colonies. More detailed monitoring to provide data on survival rates, among other things, is conducted at a few geographically dispersed 'key sites': Isle of May (southeast Scotland), Fair Isle (Shetland), Canna (west Scotland) and Skomer (Wales). In addition, three complete censuses of breeding seabirds have been conducted in Britain and Ireland, during 1969–70, 1985–88, and 1998–2002.

A natural extension would be to perform integrated analyses of common guillemot data from the other well-studied colonies, comparing estimates of demographic parameters and emigration rates with those of the Isle of May birds. The state-space model of Chapter 3 could also be easily adapted for the analysis of abundance and demographic data from other, similar, seabird species, for example razorbill *Alca torda* and Atlantic puffin *Fratercula arctica*. These models could then be projected in the same way as we did for the Isle of May guillemots in Chapter 4. There is also the possibility to incorporate other forms of data, where available. A relevant example is data on the incidence of nonbreeding on the Isle of May: this occurs at relatively low levels, but possibly has significance for colonial dynamics, so these data could be included as an additional binomial likelihood of the same form as the productivity model.

Seabird colonies are not closed units, and by far the most interesting direc-

tion would be to develop an integrated metapopulation model using the entire UK guillemot time series, with the aim to simultaneously model the dynamics of all colonies or regions and movement between them. Similar models have already been developed for grey seal *Halichoerus grypus* metapopulation dynamics (see Thomas et al. 2005, Harrison et al. 2006, Newman et al. 2009), providing a useful starting point; indeed, the similarity between the grey seal and guillemot model structures is striking! In a guillemot metapopulation model, information from the well-studied colonies could be used to specify informative prior distributions for demographic parameters at neighbouring colonies where only annual abundance and/or productivity data are collected. The three whole-UK counts would provide supplementary abundance information, particularly important for colonies not covered by the Seabird Monitoring Programme or other studies.

Using such a model, it would be interesting to see if emigration from some colonies—the Isle of May, for example—is complemented by substantial immigration at nearby colonies. It is possible that some larger colonies act as source populations, while smaller colonies, and those near range limits, act as sinks. Thus, it may be that migration is density dependent, and probably also regulated by intercolony distance, both of which can easily be accounted for with appropriate models (see, e.g., Thomas et al. 2005).

Finally, a predictive integrated metapopulation model would provide a powerful management and conservation tool, providing advanced warning of UK-wide population declines and indication of regions where restoration efforts should be focused.

Appendix A

Prior specification for random effects variance parameters

A.1 The random effects model

Consider an individual random effects model on resighting probability p_i, having the form

$$\text{logit}(p_i) = \mu + \epsilon_i, \qquad i = 1, \ldots, n. \tag{A.1}$$

Here p_i is the probability of resighting individual i, μ represents the underlying resighting probability in the absence of any individual effects, and ϵ_i denotes individual random effects. The ϵ_i are assumed to come from an underlying normal distribution,

$$\epsilon_i \sim \text{N}(0, \sigma_\epsilon^2), \tag{A.2}$$

where σ_ϵ^2, the random effects variance, is a parameter to be estimated.

Under a Bayesian analysis, priors need to be specified on parameters μ and σ_ϵ^2. Assuming a lack of any prior knowledge, we require noninformative priors: a suitable noninformative prior placed directly on p_i would be a $\text{U}(0, 1)$ distribution, so ideally we would like the priors placed on μ and σ_ϵ^2 to exactly or most closely replicate this under the inverse-logit transformation.

A.2 Prior for underlying resighting probability

For the underlying resighting probability μ, we specify a prior with probability density function

$$f(\mu) = \frac{\exp(\mu)}{(1 + \exp(\mu))^2}. \tag{A.3}$$

This is a logistic distribution with a mean of zero and variance $\frac{1}{3}\pi^2$, and it has the desirable property of exactly inducing a $\mathrm{U}(0,1)$ prior on the resighting probability in the absence of any individual effects, i.e., when $\epsilon_i = 0$ (King & Brooks 2008).

A.3 Prior for random effects variance

For the random effects variance σ^2_ϵ, we specify a prior of the form

$$\sigma^2_\epsilon \sim \Gamma^{-1}(\alpha, \beta), \tag{A.4}$$

for which $\mathbb{E}(\sigma^2_\epsilon) = \beta/(\alpha - 1)$ and $\mathrm{Var}(\sigma^2_\epsilon) = \beta^2/((\alpha-1)^2(\alpha-2))$. It has been common practice in Bayesian analyses of models containing random effects to use the above inverse-gamma prior with parameters $\alpha = \beta = 0.001$, under the impression that this is suitably noninformative on σ^2. However, King & Brooks (2008) point out that this specification produces an undesirable distribution on the probability parameter being modelled (in this case p_i) with all the prior mass on values very close to 0, 0.5 and 1, and very little support elsewhere (see Figure A.1h). Furtheremore Gelman (2006), confirmed by Royle (2008), showed that this prior can have problems, particularly for datasets in which low values of σ^2 are possible, and recommends the use of a noninformative uniform prior on the standard deviation. Instead of this, we follow the same reasoning as the prior on μ; i.e., we attempt to find the parameters α and β that most closely induce a $\mathrm{U}(0,1)$ distribution on p_i, under the condition when $\mu = 0$. We begin below with a simple simulation study, using trial-and-error to find suitable values for α and β, and then investigate the parameterisation further using several analytical approaches.

A.3.1 Simulation study

We know that a logistic distribution on ϵ_i with mean equal to 0 and variance of $\frac{1}{3}\pi^2$ (~ 3.29) would exactly induce a $\mathrm{U}(0,1)$ prior on p_i; we therefore seek to approximate this distribution with our choice of prior parameters, α and β. Trial-and-error simulations carried out in the statistics package [R] (R Development Core Team 2008) showed that the integer values $\alpha = 3$ and $\beta = 7$ reproduce the required distribution on ϵ_i very closely, with a variance of 3.49, and thus result in an approximately $\mathrm{U}(0,1)$ distribution on p_i (Figure A.1a, b; 95% of the distribution of p_i lies between 0.023 and 0.977). Importantly, the

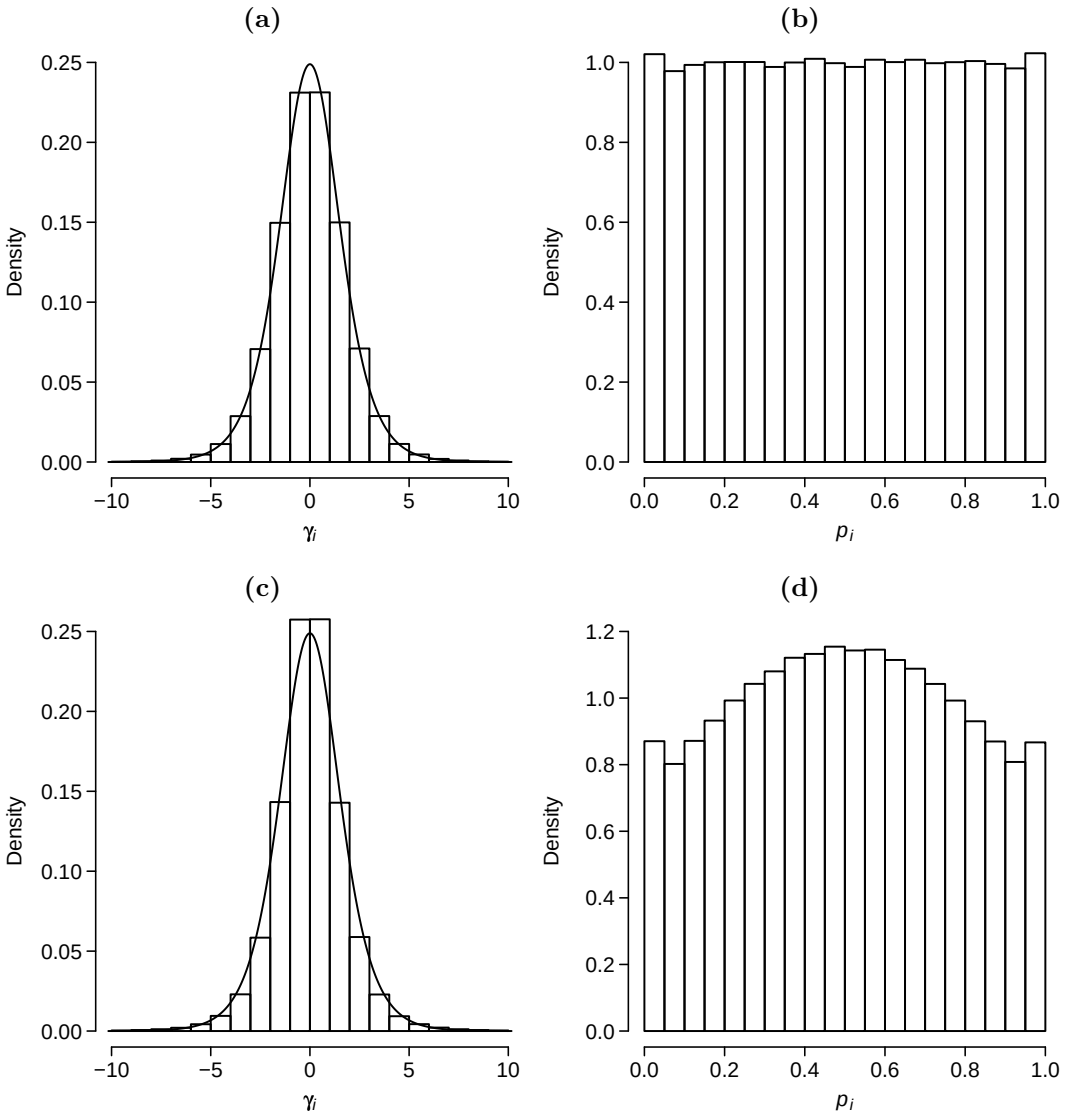

Figure A.1 Prior distributions induced on ϵ_i (histograms (a), (c), (e), (g)), and correspondingly on p_i following an inverse-logit transformation ((b), (d), (f), (h)), by a selection of inverse-gamma priors on the random effects variance σ^2_ϵ: (a) and (b) inverse-gamma parameters $\alpha = 3$, $\beta = 7$; (c) and (d) $\alpha = 2$, $\beta = 3.4$; (continued on page 136)

inverse-gamma prior on σ^2_ϵ specified by these parameter values is also suitably vague, having a mean of 3.5 and variance 12.25.

Many other combinations of α and β can be found that result in a variance close to 3.29 for ϵ_i, but $\alpha = 3$, $\beta = 7$ seem to reproduce the shape of the logistic distribution most closely. When α and β are smaller, the prior on ϵ_i is narrower with longer tails, and vice versa for larger values of α and β; the respective distributions induced on p_i have greater mass at the centre or at the tails (see Figures A.1c, d and A.1e, f, for examples where $\alpha = 2$, $\beta = 3.4$ and $\alpha = 10$, $\beta = 30$). The commonly-used inverse-gamma parameters $\alpha = \beta = 0.001$ induce

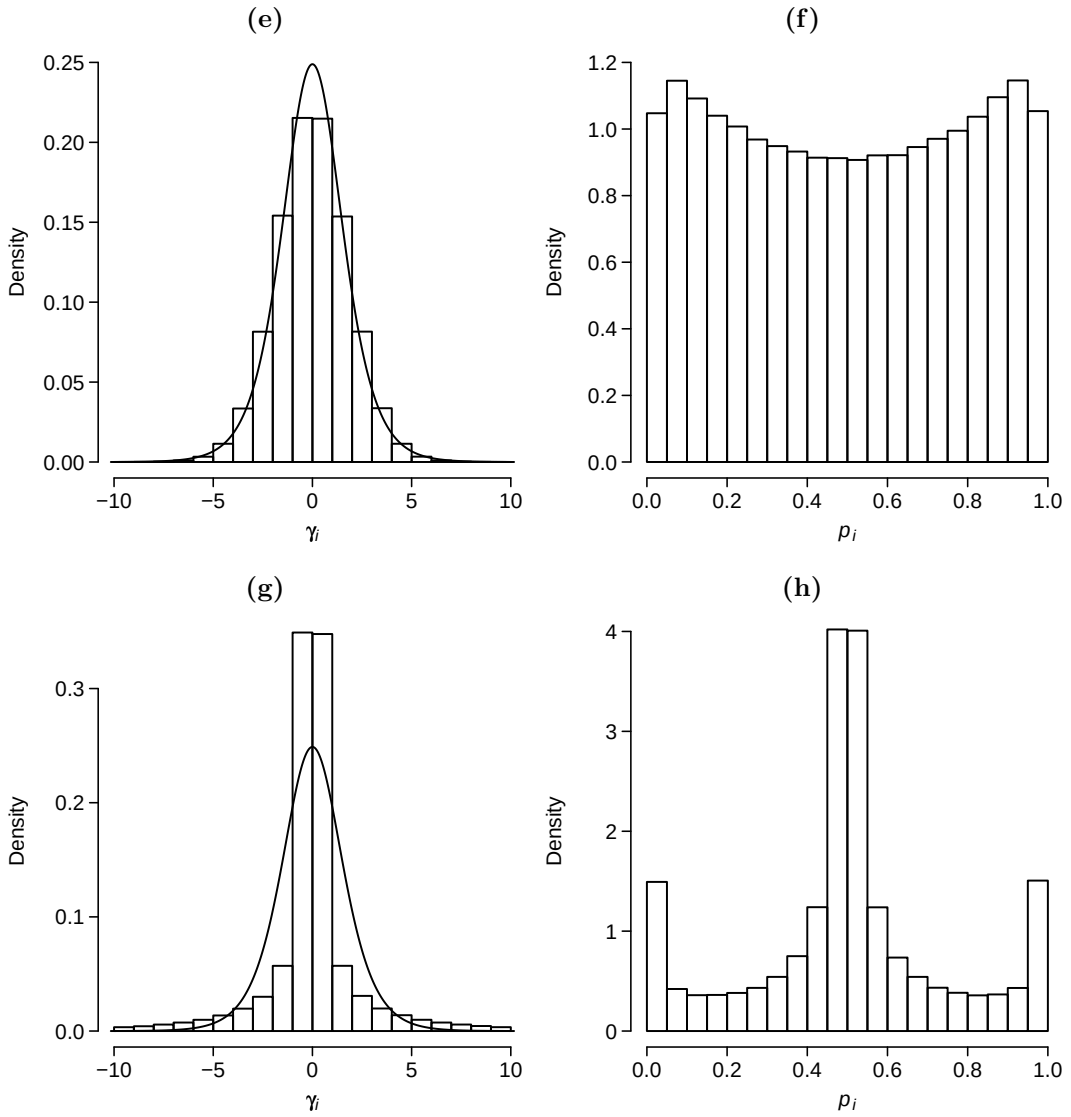

Figure A.1 (continued) (e) and (f) $\alpha = 10$, $\beta = 30$; (g) and (h) $\alpha = \beta = 0.001$. The solid lines in (a), (c), (e) and (g) are equivalent to the logistic prior specified for μ (equation (A.3)) and are thus the distribution that would exactly induce a $\mathrm{U}(0, 1)$ prior on p_i. Histograms are based on 10^6 samples per distribution.

a very heavy-tailed distribution on ϵ_i with a variance of 9.09 and, as previously mentioned, a distinctly non-uniform prior on p_i (Figure A.1g, h).

A.3.2 Analytical methods

While we have shown by simulation that the parameters $\alpha = 3$, $\beta = 7$ induce an approximately uniform prior on p_i, a more rigorous method is necessary in order to find the combination of these parameters that result in the most uniform prior distribution. In this section we describe a number of analytical approaches to this problem. For the sake of simplicity and clarity, in the following calculations

p_i is replaced by p, and ϵ_i by ϵ. The computer algebra system Maple™ 9.5 (Maple 9.51 2004) was used to solve some of the calculations.

We begin by deriving the probability density function of the distribution induced on p by the hyper-prior on σ_ϵ^2, in terms of the parameters α and β. Recall that we are interested in the model

$$\text{logit}(p) = \epsilon,$$

where

$$\epsilon \mid \sigma_\epsilon^2 \sim \text{N}(0, \sigma_\epsilon^2); \qquad \sigma_\epsilon^2 \sim \Gamma^{-1}(\alpha, \beta).$$

First we need to derive $f(\epsilon)$, which is given by

$$\begin{aligned} f(\epsilon) &= \int_0^\infty f(\epsilon \mid \sigma_\epsilon^2) f(\sigma_\epsilon^2)\, d\sigma_\epsilon^2 \\ &= \int_0^\infty \frac{1}{\sqrt{2\pi\sigma_\epsilon^2}} \exp\left(-\frac{\epsilon^2}{2\sigma_\epsilon^2}\right) \cdot \frac{\beta^\alpha}{\Gamma(\alpha)} (\sigma_\epsilon^2)^{-(\alpha+1)} \exp\left(-\frac{\beta}{\sigma_\epsilon^2}\right) d\sigma_\epsilon^2 \\ &= \frac{1}{\sqrt{2\pi}} \frac{\beta^\alpha}{\Gamma(\alpha)} \int_0^\infty (\sigma_\epsilon^2)^{-(\alpha+\frac{3}{2})} \exp\left(-\frac{\epsilon^2 + 2\beta}{2\sigma_\epsilon^2}\right) d\sigma_\epsilon^2 \\ &= \frac{2^\alpha \beta^\alpha (\epsilon^2 + 2\beta)^{-(\alpha+\frac{1}{2})}\, \Gamma(\alpha + \frac{1}{2})}{\Gamma(\alpha)\sqrt{\pi}}. \end{aligned} \tag{A.5}$$

Then, to find the distribution in terms of p, we use the formula

$$f_P(p) = f_E(g^{-1}(p)) \left| \frac{d}{dp} g^{-1}(p) \right|,$$

where

$$g^{-1}(p) = \log\left(\frac{p}{1-p}\right),$$

and

$$\frac{d}{dp} g^{-1}(p) = \frac{1}{p(1-p)}.$$

Therefore, we have that

$$f_P(p) = \frac{2^\alpha \beta^\alpha \left(\left(\log\left(\frac{p}{1-p}\right)\right)^2 + 2\beta\right)^{-(\alpha+\frac{1}{2})} \Gamma(\alpha + \frac{1}{2})}{\Gamma(\alpha)\sqrt{\pi}\, p(1-p)}, \qquad 0 < p < 1. \tag{A.6}$$

To further investigate the shape of this distribution we need to locate the stationary point(s), for which we require the conditions that satisfy $\frac{df_P(p)}{dp} = 0$,

i.e.,

$$\frac{-\left(2\log(\frac{p}{1-p})\alpha+\log(\frac{p}{1-p})+\log(\frac{p}{1-p})^2+2\beta-2p\log(\frac{p}{1-p})^2-4p\beta\right)2^\alpha\beta^\alpha\left(\log(\frac{p}{1-p})^2+2\beta\right)^{-(\alpha+\frac{3}{2})}\Gamma(\alpha+\frac{1}{2})}{(-1+p)^2\sqrt{\pi}p^2\Gamma(\alpha)}=0. \tag{A.7}$$

By inspection, we can see that $p = 0.5$ satisfies $\frac{df_P(p)}{dp} = 0$ for all values of α and $\beta > 0$, so there always exists a stationary point at the mid-point of p's range. To induce a distribution on p which is as close to uniform as possible, we would like the second derivative of $f_P(p)$ at this point to equal zero, indicating that the distribution is completely flat at the midpoint (i.e., not a maximum or minimum). The second derivative of $f_P(p)$ is given by

$$\begin{aligned}\frac{d^2f_P(p)}{dp^2} = &-\left(8\beta^2-24p\beta^2+24p^2\beta^2-24p\log(\tfrac{p}{1-p})^2\beta+6\log(\tfrac{p}{1-p})\beta+8\log(\tfrac{p}{1-p})^2\beta-2\beta+24p^2\log(\tfrac{p}{1-p})^2\beta\right.\\
&+12\log(\tfrac{p}{1-p})\alpha\beta-4\alpha\beta-12\log(\tfrac{p}{1-p})p\beta-24\log(\tfrac{p}{1-p})\alpha p\beta+3\log(\tfrac{p}{1-p})^3-6p\log(\tfrac{p}{1-p})^4+2\log(\tfrac{p}{1-p})^4\\
&+6\log(\tfrac{p}{1-p})^3\alpha-6\log(\tfrac{p}{1-p})^3p+4\alpha^2\log(\tfrac{p}{1-p})^2+2\log(\tfrac{p}{1-p})^2-12\log(\tfrac{p}{1-p})^3\alpha p+6p^2\log(\tfrac{p}{1-p})^4\\
&\left.+6\alpha\log(\tfrac{p}{1-p})^2\right)2^\alpha\beta^\alpha\left(\log(\tfrac{p}{1-p})^2+2\beta\right)^{-(\alpha+\frac{5}{2})}\Gamma(\alpha+\tfrac{1}{2})\,/\left(p^3\sqrt{\pi}(-1+p)^3\Gamma(\alpha)\right),\end{aligned} \tag{A.8}$$

and setting $\frac{d^2f_P(p)}{dp^2}\Big|_{p=0.5} = 0$ gives

$$\begin{aligned}&8\beta^2-12\beta^2+6\beta^2-2\beta-4\alpha\beta=0\\
&\qquad\Rightarrow\quad \beta=2\alpha+1,\qquad \alpha,\beta>0.\end{aligned} \tag{A.9}$$

Therefore, it appears that any values of α and β satisfying this equality will induce a perfectly flat distribution on p at the mid-point, $p = 0.5$. However, this does not imply that the distribution will be uniform across the entire range of p, as illustrated in Figure A.2, although note that the parameters obtained from the simulation study ($\alpha = 3$, $\beta = 7$) seem to offer a reasonable solution. Therefore, we also need a way to measure, and subsequently minimise, the deviation of $f_P(p)$ from uniform across the range $p = (0, 1)$.

Minimising the maximum first derivative

The first solution to finding the 'flattest' distribution involves finding the value of α (and hence β, given $\beta = 2\alpha + 1$) that minimises the maximum gradient of $f_P(p)$, i.e., $\min\limits_{\alpha\geqslant 1}\left(\max\limits_{0<p<1}\frac{df_P(p)}{dp}\right)$. However, due to the behaviour of $f_P(p)$ at values of p close to 0 and 1, where the density and gradient approach infinity (see Figure A.2), this is not a reliable indicator of the gradient over the majority of the distribution and the result is biased towards higher values of α (Figure A.3).

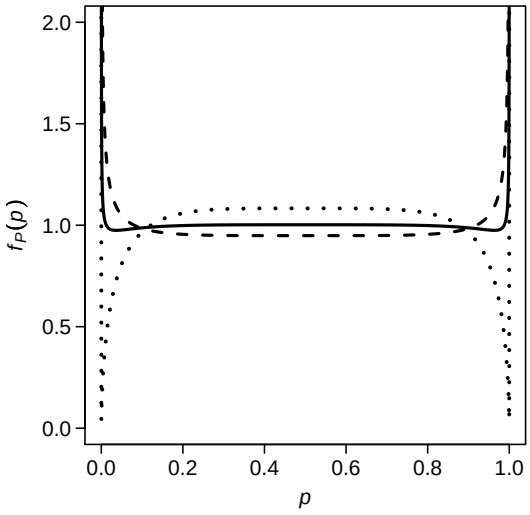

Figure A.2 Distributions of p induced by three combinations of parameters α and β for the inverse-gamma prior on σ^2_ϵ: $\alpha = 2$, $\beta = 5$ (dashed line); $\alpha = 3$, $\beta = 7$ (solid line); $\alpha = 9$, $\beta = 19$ (dotted line). All three distributions are exactly uniform at the mid-point, $p = 0.5$, but deviate to varying degrees towards the limits of the distribution.

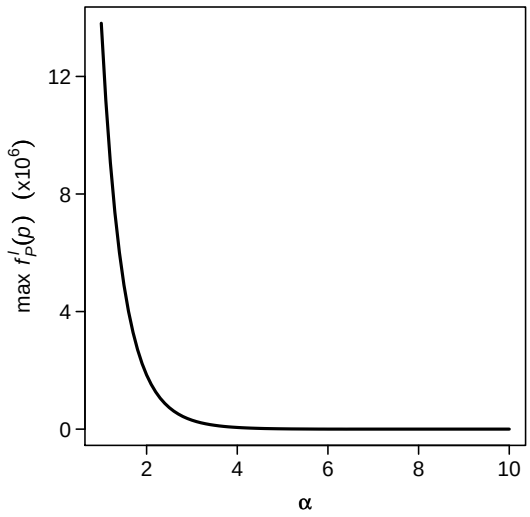

Figure A.3 Maximum first derivative of $f_P(p)$ versus inverse-gamma parameter α, calculated over the range $p = (0.00001, 0.99999)$.

Minimising the mean/median first derivative

A similar solution to that above, but one that should reduce the influence of extreme gradients, is to minimise the expected value of the absolute first derivative of $f_P(p)$, i.e., $\min_{\alpha \geqslant 1} \mathbb{E}\left(\left|\frac{df_P(p)}{dp}\right|\right)$. However, the result is highly sensitive to the range of p over which the statistic is calculated: there is a clear minimum at $\alpha \approx 3.62$ for $p = (0.001, 0.999)$ (Figure A.4a) but the result approaches that of the previous method as the limits of p approach 0 and 1 more closely (Figure A.4b).

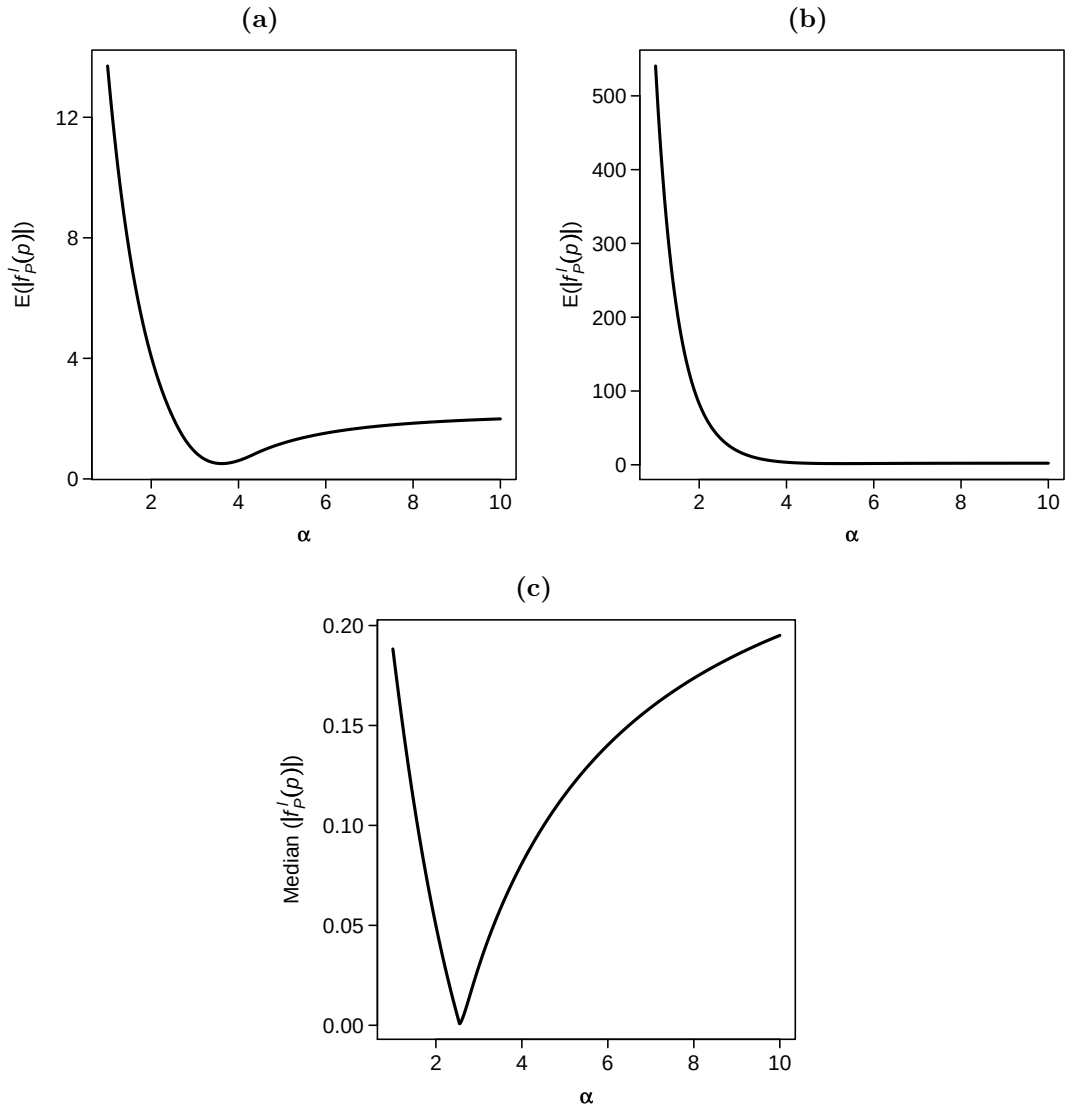

Figure A.4 (a), (b) Expected value of the absolute first derivative of $f_P(p)$ versus inverse-gamma parameter α, calculated over the ranges: (a) $p = (0.001, 0.999)$; (b) $p = (0.00001, 0.99999)$. (c) Median of the absolute first derivative of $f_P(p)$ versus α, calculated over $p = (0.00001, 0.99999)$; the result is essentially identical given various limits of p.

As an alternative to the expected value we can take the median of the absolute first derivative, which is a better way to reduce the influence of extreme gradients at the limits of p. Consistent results are achieved despite changes in the endpoints of the calculation and the statistic is minimised at $\alpha \approx 2.55$ (Figure A.4c).

Minimising the deviation of the function from unity

A U$(0, 1)$ distribution has a density of 1 across its entire range; thus, minimising the expected absolute deviation of the function $f_P(p)$ from 1 over $p = (0, 1)$, i.e.,

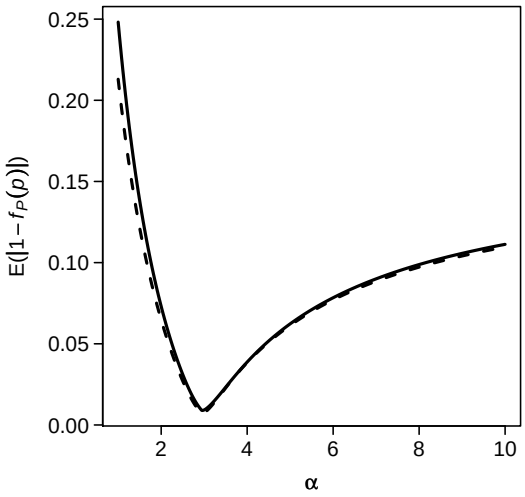

Figure A.5 Expected absolute value of $(1 - f_P(p))$ versus inverse-gamma parameter α, calculated for $p = (0.001, 0.999)$ (dashed line) and $p = (0.00001, 0.99999)$ (solid line).

$\min_{\alpha \geqslant 1} \mathbb{E}\big(\big|1 - f_P(p)\big|\big)$, forms another criterion for determining a suitable value for α. This solution also appears to be relatively insensitive to changes in the limits of p (Figure A.5), but results in a slightly different optimum value of α to the median first derivative method: $\alpha \approx 2.96$; calculated for $p = (0.00001, 0.99999)$.

A.4 Summary

In choosing a suitable prior for use with random effects variance parameters, we have taken the approach of finding a distribution such that the corresponding induced prior on the untransformed variable is approximately uniform on the interval $(0, 1)$, in the absence of any other effects in the model. Using an inverse-gamma distribution for the variance, σ_ϵ^2, we showed that the combination of parameters $\beta = 2\alpha + 1$ induce a distribution $f_P(p)$ on the untransformed parameter p that is perfectly flat at its midpoint, $p = 0.5$. Beyond this, no single approach described in Section A.3.2 gave the same 'best' value of α, and hence β, to achieve our objective.

Because $f_P(p)$ is undefined at 0 and 1, and its density tends to infinity as these limits are approached, the outcome of all approaches depend to some extent over what range of p calculations are performed, which in turn is limited by computational constraints. However, the 'median first derivative' and 'deviation from unity' methods were relatively insensitive to the limits used, and gave consistent results down to $p = 10^{-8}$. Of these, the latter is probably the more suitable approach: because this statistic is based on a mean value, rather than a median, it provides a better compromise between achieving over-

all 'uniformness' and reducing the influence of undesirable spikes in the density. Therefore, based on the deviation from unity method and the results of the initial trial-and-error simulations, the inverse-gamma parameters $\alpha = 3$ and $\beta = 7$ are considered suitable for inducing an approximately uniform prior on the untransformed parameter, before considering any fixed or other effects in the model. Nevertheless, this distribution should be used with caution where small values of the variance are expected, as it has little support for values less than around 0.5. This highlights the need to always conduct a thorough prior sensitivity analysis.

References

Arnott, S. A. & Ruxton, G. D. (2002). Sandeel recruitment in the North Sea: Demographic, climatic and trophic effects. *Marine Ecology Progress Series* **238**, 199–210.

Asbjørnsen, E. J., Sæther, B.-E., Linnell, J. D. C., Engen, S., Andersen, R. & Bretten, T. (2005). Predicting the growth of a small introduced muskox population using population prediction intervals. *Journal of Animal Ecology* **74**, 612–618.

Ashbrook, K., Wanless, S., Harris, M. P. & Hamer, K. C. (2008). Hitting the buffers: Conspecific aggression undermines benefits of colonial breeding under adverse conditions. *Biology Letters* **4**, 630–633.

Baillie, S. R. & Green, R. E. (1987). The importance of variation in recovery rates when estimating survival rates from ringing recoveries. *Acta Ornithologica* **23**, 41–60.

Baker, J. D. & Thompson, P. M. (2007). Temporal and spatial variation in age-specific survival rates of a long-lived mammal, the Hawaiian monk seal. *Proceedings of the Royal Society of London: Series B* **274**, 407–415.

Barry, S. C., Brooks, S. P., Catchpole, E. A. & Morgan, B. J. T. (2003). The analysis of ring-recovery data using random effects. *Biometrics* **59**, 54–65.

Bayes, T. (1763). An essay towards solving a problem in the doctrine of chances. By the late Rev. Mr. Bayes, F. R. S. communicated by Mr. Price, in a letter to John Canton, M. A. and F. R. S. *Philosophical Transactions of the Royal Society of London* **53**, 370–418.

Beissinger, S. R. & McCullough, D. R. (eds.) (2002). *Population Viability Analysis*. Chicago: University of Chicago Press.

Berger, J. O. (1985). *Statistical Decision Theory and Bayesian Analysis*. New York: Springer-Verlag.

Besbeas, P., Borysiewicz, R. S. & Morgan, B. J. T. (2008). Completing the ecological jigsaw. In *Modeling Demographic Processes in Marked Populations*, vol. 3 of *Environmental and Ecological Statistics Series*, eds. D. L. Thomson, E. G. Cooch & M. J. Conroy, pp. 515–542.

Besbeas, P. & Freeman, S. N. (2006). Methods for joint inference from panel survey and demographic data. *Ecology* **87**, 1138–1145.

Besbeas, P., Freeman, S. N. & Morgan, B. J. T. (2005). The potential of integrated population modelling. *Australian and New Zealand Journal of Statistics* **47**, 35–48.

Besbeas, P., Freeman, S. N., Morgan, B. J. T. & Catchpole, E. A. (2002). Integrating mark-recapture-recovery and census data to estimate animal abundance and demographic parameters. *Biometrics* **58**, 540–547.

Bjørnstad, O. N., Ims, R. A. & Lambin, X. (1999). Spatial population dynamics: Analyzing patterns and processes of population synchrony. *Trends in Ecology and Evolution* **14**, 427–432.

Bonner, S. J. & Schwarz, C. J. (2004). Continuous time-dependent individual covariates and the Cormack-Jolly-Seber model. *Animal Biodiversity and Conservation* **27.1**, 149–155.

Borysiewicz, R. S., Morgan, B. J. T., Hénaux, V., Bregnballe, T., Lebreton, J.-D. & Gimenez, O. (2008). An integrated analysis of multisite recruitment, mark-recapture-recovery and multisite census data. In *Modeling Demographic Processes in Marked Populations*, vol. 3 of *Environmental and Ecological Statistics Series*, eds. D. L. Thomson, E. G. Cooch & M. J. Conroy, pp. 581–596.

Brooks, S. P. (1998). Markov chain Monte Carlo method and its application. *Journal of the Royal Statistical Society: Series D* **47**, 69–100.

Brooks, S. P., Freeman, S. N., Greenwood, J. J. D., King, R. & Mazzetta, C. (2008). Quantifying conservation concern – Bayesian statistics, birds and the red lists. *Biological Conservation* **141**, 1436–1441.

Brooks, S. P. & Gelman, A. (1998). General methods for monitoring convergence of iterative simulations. *Journal of Computational and Graphical Statistics* **7**, 434–455.

Brooks, S. P., King, R. & Morgan, B. J. T. (2004). A Bayesian approach to combining animal abundance and demographic data. *Animal Biodiversity and Conservation* **27.1**, 515–529.

Brownie, C., Anderson, D. R., Burnham, K. P. & Robson, D. S. (1985). *Statistical Inference from Band-Recovery Data – A Handbook*. 2nd edn. Washington, DC: US Fish and Wildlife Service, Resource Publication 156.

Buckland, S. T., Newman, K. B., Thomas, L. & Koesters, N. B. (2004). State-space models for the dynamics of wild animal populations. *Ecological Modelling* **171**, 157–175.

Burnham, K. P. (1993). A theory for combined analysis of ring recovery and recapture data. In *Marked Individuals in the Study of Bird Population*, eds. J.-D. Lebreton & P. M. North, pp. 199–213. Basel: Birkhäuser Verlag.

Burnham, K. P. & Anderson, D. R. (2002). *Model Selection and Multi-Model Inference: A Practical Information-Theoretic Approach*. 2nd edn. New York: Springer-Verlag.

Burnham, K. P., Anderson, D. R., White, G. C., Brownie, C. & Pollock, K. H. (1987). *Design and Analysis Methods for Fish Survival Experiments Based on Release-Recapture*. American Fisheries Society Monograph 5. Bethesda, Maryland: American Fisheries Society.

Casella, G. & George, E. I. (1992). Explaining the Gibbs sampler. *The American Statistician* **46**, 167–174.

Caswell, H. (2000). Prospective and retrospective perturbation analyses: Their roles in conservation biology. *Ecology* **83**, 619–627.

Caswell, H. (2001). *Matrix Population Models: Construction, Analysis and Interpretation*. 2nd edn. Sunderland, Massachusetts: Sinauer Associates.

Caswell, H. (2005). Sensitivity analysis of the stochastic growth rate: Three extensions. *Australian and New Zealand Journal of Statistics* **47**, 75–85.

Catchpole, E. A., Freeman, S. N., Morgan, B. J. T. & Harris, M. P. (1998). Integrated recovery/recapture data analysis. *Biometrics* **54**, 33–46.

Catchpole, E. A., Morgan, B. J. T., Coulson, T., Freeman, S. N. & Albon, S. D. (2000). Factors influencing Soay sheep survival. *Journal of the Royal Statistical Society: Series C* **49**, 453–472.

Catchpole, E. A., Morgan, B. J. T., Freeman, S. N. & Peach, K. (1999). Modelling the survival of British lapwings *Vanellus vanellus* using ring-recovery data and weather covariates. *Bird Study* **46** (Supplement), 5–13.

Cave, V. M., King, R. & Freeman, S. N. (2009). An integrated population model from constant effort bird-ringing data. Accepted for publication in the *Journal of Agricultural, Biological and Environmental Statistics* .

Centre for Ecology and Hydrology (2009). Isle of May long-term study (IMLOTS) [online]. Accessed 02 October 2009 at http://www.ceh.ac.uk/sci_programmes/IsleofMayLong-TermStudy.html.

Chib, S. & Greenberg, E. (1995). Understanding the Metropolis-Hastings algorithm. *The American Statistician* **49**, 327–335.

Clark, J. A., Robinson, R. A., Balmer, D. E., Blackburn, J. R., Grantham, M. J., Griffin, B. M., Marchant, J. H., Risely, K. & Adams, S. Y. (2005). Bird ringing in Britain and Ireland in 2004. *Ringing & Migration* **22**, 213–253.

Cohen, J. E., Christensen, S. W. & Goodyear, C. P. (1983). A stochastic age-structured population model of striped bass (*Morone saxatilis*) in the Potomac River. *Canadian Journal of Fisheries and Aquatic Sciences* **40**, 2170–2183.

Cooch, E. G., Rockwell, R. F. & Brault, S. (2001). Retrospective analysis of demographic responses to environmental change: A lesser snow goose example. *Ecological Monographs* **71**, 377–400.

Cormack, R. M. (1964). Estimates of survival from the sighting of marked animals. *Biometrika* **51**, 429–438.

Coull, B. A. & Agresti, A. (1999). The use of mixed logit models to reflect heterogeneity in capture-recapture studies. *Biometrics* **55**, 294–301.

Coulson, T., Gaillard, J.-M. & Festa-Bianchet, M. (2005). Decomposing the variation in population growth into contributions from multiple demographic rates. *Journal of Animal Ecology* **74**, 789–801.

Coulson, T., Mace, G. M., Hudson, E. & Possingham, H. (2001). The use and abuse of population viability analysis. *Trends in Ecology and Evolution* **16**, 219–221.

Crespin, L., Harris, M. P., Lebreton, J.-D., Frederiksen, M. & Wanless, S. (2006a). Recruitment to a seabird population depends on environmental factors and on population size. *Journal of Animal Ecology* **75**, 228–238.

Crespin, L., Harris, M. P., Lebreton, J.-D. & Wanless, S. (2006b). Increased adult mortality and reduced breeding success with age in a population of common guillemot *Uria aalge* using marked birds of unknown age. *Journal of Avian Biology* **37**, 273–282.

Croxall, J. P. & Rothery, P. (1991). Population regulation of seabirds: Implications of their demography for conservation. In *Bird Population Studies: Relevance to Conservation and Management*, eds. C. M. Perrins, J.-D. Lebreton & G. J. M. Hirons, pp. 272–296. Oxford: Oxford University Press.

de Valpine, P. & Hastings, A. (2002). Fitting population models incorporating process noise and observation error. *Ecological Monographs* **72**, 57–76.

Dennis, B. (1996). Discussion: Should ecologists become Bayesians? *Ecological Applications* **6**, 1095–1103.

Dhondt, A. A. (2001). Trade-offs between reproduction and survival in tits. *Ardea* **89**, 155–166.

Dickey, M. H., Gauthier, G. & Cadieux, M. C. (2008). Climatic effects on the breeding phenology and reproductive success of an Arctic-nesting goose species. *Global Change Biology* **14**, 1973–1985.

Doherty, P. F., Jr., Schreiber, E. A., Nichols, J. D., Hines, J. E., Link, W. A., Schenk, G. A. & Schreiber, R. W. (2004). Testing life history predictions in a long-live seabird: A population matrix approach with improved parameter estimation. *Oikos* **105**, 606–618.

Dorazio, R. M. & Royle, J. A. (2003). Mixture models for estimating the size of a closed population when capture rates vary among individuals. *Biometrics* **59**, 351–364.

Doucet, A., de Freitas, N. & Gordon, N. (eds.) (2001). *Sequential Monte Carlo Methods in Practice*. New York: Springer-Verlag.

Eaton, J. W., Bateman, D. & Hauberg, S. (2008a). *GNU Octave Manual Version 3*. Network Theory Limited.
http://www.octave.org

Eaton, M. A., Austin, G. E., Banks, A. N., Conway, G. J., Douse, A., Grice, P. V., Hearn, R. D., Hilton, G. M., Hoccom, D., Musgrove, A. J., Noble, D. G., Ratcliffe, N., Rehfisch, M. M., Worden, J. & Wotton, S. (2007). *The State of the UK's Birds 2006*. Sandy, Bedfordshire: RSPB, BTO, WWT, CCW, EHS, NE and SNH.

Eaton, M. A., Balmer, D. E., Burton, N., Grice, P. V., Musgrove, A. J., Hearn, R. D., Hilton, G. M., Leech, D., Noble, D. G., Ratcliffe, N., Rehfisch, M. M., Whitehead, S. & Wotton, S. (2008b). *The State of the UK's Birds 2007*. Sandy, Bedfordshire: RSPB, BTO, WWT, CCW, EHS, NE and SNH.

Eaton, M. A., Balmer, D. E., Conway, G. J., Gillings, S., Grice, P. V., Hall, C., Hearn, R. D., Musgrove, A. J., Risely, K. & Wotton, S. (2009). *The State of the UK's Birds 2008*. Sandy, Bedfordshire: RSPB, BTO, WWT, CCW, NIEA, JNCC, NE and SNH.

Eaton, M. A., Noble, D. G., Hearn, R. D., Grice, P. V., Gregory, R. D., Wotton, S., Ratcliffe, N., Hilton, G. M., Rehfisch, M. M., Crick, H. Q. P. & Hughes, J. (2005). *The State of the UK's Birds 2004*. Sandy, Bedfordshire: BTO, RSPB, WWT, CCW, EN, EHS and SNH.

Ellison, A. M. (1996). An introduction to Bayesian inference for ecological research and environmental decision-making. *Ecological Applications* **6**, 1036–1046.

Ellison, A. M. (2004). Bayesian inference in ecology. *Ecology Letters* **7**, 509–520.

Fasano, G. & Franceschini, A. (1987). A multidimensional version of the Kolmogorov-Smirnov test. *Monthly Notices of the Royal Astronomical Society* **225**, 155–170.

Frederiksen, M. & Bregnballe, T. (2000). Evidence for density-dependent survival in adult cormorants from a combined analysis of recoveries and resightings. *Journal of Animal Ecology* **69**, 737–752.

Frederiksen, M., Daunt, F., Harris, M. P. & Wanless, S. (2008). The demographic impact of extreme events: Stochastic weather drives survival and population dynamics in a long-lived seabird. *Journal of Animal Ecology* **77**, 1020–1029.

Frederiksen, M., Harris, M. P. & Wanless, S. (2005). Inter-population variation in demographic parameters: A neglected subject? *Oikos* **111**, 209–214.

Frederiksen, M., Hearn, R. D., Mitchell, C., Sigfússon, A., Swann, R. L. & Fox, A. D. (2004a). The dynamics of hunted Icelandic goose populations: A reassessment of the evidence. *Journal of Applied Ecology* **41**, 315–334.

Frederiksen, M., Wanless, S., Harris, M. P., Rothery, P. & Wilson, L. J. (2004b). The role of industrial fisheries and oceanographic change in the decline of North Sea black-legged kittiwakes. *Journal of Applied Ecology* **41**, 1129–1139.

Freeman, S. N. & Crick, H. Q. P. (2003). The decline of the spotted flycatcher *Muscicapa striata* in the UK: An integrated population model. *Ibis* **145**, 400–412.

Freeman, S. N., Robinson, R. A., Clark, J. A., Griffin, B. M. & Adams, S. Y. (2007). Changing demography and population decline in the common starling *Sturnus vulgaris*: A multisite approach to integrated population monitoring. *Ibis* **149**, 587–596.

Gaillard, J.-M., Festa-Bianchet, M. & Yoccoz, N. G. (1998). Population dynamics of large herbivores: Variable recruitment with constant adult survival. *Trends in Ecology and Evolution* **13**, 58–63.

Gaillard, J.-M., Festa-Bianchet, M., Yoccoz, N. G., Loison, A. & Toïgo, C. (2000). Temporal variation in fitness components and population dynamics of large herbivores. *Annual Review of Ecology and Systematics* **31**, 367–393.

Gaillard, J.-M. & Yoccoz, N. G. (2003). Temporal variation in survival of mammals: A case of environmental canalization? *Ecology* **84**, 3294–3306.

Gaston, A. J. & Smith, J. L. (2001). Changes in oceanographic conditions off northern British Columbia (1983-1999) and the reproduction of a marine bird, the ancient murrelet (*Synthliboramphus antiquus*). *Canadian Journal of Zoology* **79**, 1735–1742.

Gauthier, G., Besbeas, P., Lebreton, J.-D. & Morgan, B. J. T. (2007). Population growth in snow geese: A modeling approach integrating demographic and survey information. *Ecology* **88**, 1420–1429.

Gelman, A. (1996). Inference and monitoring convergence. In *Markov Chain Monte Carlo in Practice*, eds. W. R. Gilks, S. Richardson & D. J. Spiegelhalter, pp. 131–143. Boca Raton, Florida: Chapman & Hall/CRC.

Gelman, A. (2006). Prior distributions for variance parameters in hierarchical models. *Bayesian Analysis* **1**, 515–534.

Gelman, A., Carlin, J. B., Stern, H. S. & Rubin, D. B. (2003). *Bayesian Data Analysis*. 2nd edn. London: Chapman & Hall/CRC.

Gelman, A., Roberts, G. O. & Gilks, W. R. (1996). Efficient Metropolis jumping rules. In *Bayesian Statistics 5*, eds. J. M. Bernado, J. O. Berger, A. P. Dawid & A. F. M. Smith, pp. 599–608. New York: Oxford University Press.

Gelman, A. & Rubin, D. B. (1992). Inference from iterative simulation using multiple sequences. *Statistical Science* **7**, 457–472.

Gimenez, O., Bonner, S. J., King, R., Parker, R. A., Brooks, S. P., Jamieson, L. E., Grosbois, V., Morgan, B. J. T. & Thomas, L. (2008). WinBUGS for population ecologists: Bayesian modeling using Markov chain Monte Carlo. In *Modeling Demographic Processes in Marked Populations*, vol. 3 of *Environmental and Ecological Statistics Series*, eds. D. L. Thomson, E. G. Cooch & M. J. Conroy, pp. 885–918.

Goodman, D. (2004). Methods for joint inference from multiple data sources for improved estimates of population size and survival rates. *Marine Mammal Science* **20**, 401–423.

Gould, W. R. & Nichols, J. D. (1998). Estimation of temporal variability in survival in animal populations. *Ecology* **79**, 2531–2538.

Green, P. J. (1995). Reversible jump Markov chain Monte Carlo computation and Bayesian model determination. *Biometrika* **82**, 711–732.

Grosbois, V., Gimenez, O., Gaillard, J.-M., Pradel, R., Barbraud, C., Clobert, J., Møller, A. P. & Weimerskirch, H. (2008). Assessing the impact of climate variation on survival in vertebrate populations. *Biological Reviews* **83**, 357–399.

Grosbois, V., Harris, M. P., Anker-Nilssen, T., McCleery, R. H., Shaw, D. N., Morgan, B. J. T. & Gimenez, O. (2009). Modelling survival at multi-population scales using mark-recapture data. *Ecology* **90**, 2922–2932.

Grosbois, V., Henry, P.-Y., Blondel, J., Perret, P., Lebreton, J.-D., Thomas, D. W. & Lambrechts, M. M. (2006). Climate impacts on mediterranean blue tit survival: An investigation across seasons and spatial scales. *Global Change Biology* **12**, 2235–2249.

Grøtan, V., Sæther, B.-E., Engen, S., Solberg, E. J., Linnell, J. D. C., Andersen, R., Brøseth, H. & Lund, E. (2005). Climate causes large-scale spatial synchrony in population fluctuations of a temperate herbivore. *Ecology* **86**, 1472–1482.

Halley, D. J. & Harris, M. P. (1993). Intercolony movement and behaviour of immature guillemots *Uria aalge*. *Ibis* **135**, 264–270.

Halley, D. J., Harris, M. P. & Wanless, S. (1995). Colony attendance patterns and recruitment in immature common murres (*Uria aalge*). *The Auk* **112**, 947–957.

Harris, M. P. (1989). Variation in the correction factor used for converting counts of individual guillemots *Uria aalge* into breeding pairs. *Ibis* **131**, 85–93.

Harris, M. P., Anker-Nilssen, T., McCleery, R. H., Erikstad, K. E., Shaw, D. N. & Grosbois, V. (2005). Effect of wintering area and climate on the survival of adult Atlantic puffins *Fratercula arctica* in the eastern Atlantic. *Marine Ecology Progress Series* **297**, 283–296.

Harris, M. P., Beare, D., Toresen, R., Nøttestad, L., Kloppmann, M., Dörner, H., Peach, K., Rushton, D. R. A., Foster-Smith, J. & Wanless, S. (2007a). A major increase in snake pipefish *Entelurus aequoreus* in northern European seas since 2003: Potential implications for seabird breeding success. *Marine Biology* **151**, 973–983.

Harris, M. P., Frederiksen, M. & Wanless, S. (2007b). Within- and between-year variation in the juvenile survival of common guillemots *Uria aalge*. *Ibis* **149**, 472–481.

Harris, M. P., Halley, D. J. & Swann, R. L. (1994). Age of first breeding in common murres. *The Auk* **111**, 207–209.

Harris, M. P., Halley, D. J. & Wanless, S. (1996a). Philopatry in the common guillemot *Uria aalge*. *Bird Study* **43**, 134–137.

Harris, M. P. & Swann, R. L. (2002). Common guillemot (guillemot) *Uria aalge*. In *The Migration Atlas: Movements of the Birds of Britain and Ireland*, eds. C. V. Wernham, M. P. Toms, J. H. Marchant, J. A. Clark, G. M. Siriwardena & S. R. Baillie, pp. 397–400. London: T & A. D. Poyser.

Harris, M. P. & Wanless, S. (1995). Survival and non-breeding of adult common guillemots *Uria aalge*. *Ibis* **137**, 192–197.

Harris, M. P. & Wanless, S. (2004). Common guillemot *Uria aalge*. In *Seabird Populations of Britain and Ireland: Results of the Seabird 2000 Census (1998–2002)*, eds. P. I. Mitchell, S. F. Newton, N. Ratcliffe & T. E. Dunn, pp. 350–363. London: T & A. D. Poyser.

Harris, M. P., Wanless, S. & Barton, T. R. (1996b). Site use and fidelity in the common guillemot *Uria aalge*. *Ibis* **138**, 399–404.

Harris, M. P., Wanless, S., Rothery, P., Swann, R. L. & Jardine, D. C. (2000). Survival of adult common guillemots *Uria aalge* at three Scottish colonies. *Bird Study* **47**, 1–7.

Harrison, P. J., Buckland, S. T., Thomas, L., Harris, R., Pomeroy, P. P. & Harwood, J. (2006). Incorporating movement into models of grey seal population dynamics. *Journal of Animal Ecology* **75**, 634–645.

Harwood, J. & Stokes, K. (2003). Coping with uncertainty in ecological advice: Lessons from fisheries. *Trends in Ecology and Evolution* **18**, 617–622.

Hastings, W. K. (1970). Monte Carlo sampling methods using Markov chains and their applications. *Biometrika* **57**, 97–109.

Heath, M., Edwards, M., Furness, R., Pinnegar, J. & Wanless, S. (2009). A view from above: Changing seas, seabirds and food sources. In *Marine Climate Change Ecosystem Linkages Report Card 2009*, eds. J. M. Baxter, P. J. Buckley & M. T. Frost, Online Science Reviews. Lowestoft: MCCIP. http://www.mccip.org.uk/elr/view

Heppell, S. S., Caswell, H. & Crowder, L. B. (2000). Life histories and elasticity patterns: Perturbation analysis for species with minimal demographic data. *Ecology* **81**, 654–665.

Heubeck, M. (2004). Black-legged kittiwake *Rissa tridactyla*. In *Seabird Populations of Britain and Ireland: Results of the Seabird 2000 Census (1998–2002)*, eds. P. I. Mitchell, S. F. Newton, N. Ratcliffe & T. E. Dunn, pp. 277–290. London: T & A. D. Poyser.

Hilborn, R. & Mangel, M. (1997). *The Ecological Detective*. Princeton: Princeton University Press.

Holliday, N. P., Kennedy, J., Kent, E. C., Marsh, R., Hughes, S. L., Sherwin, T. & Berry, D. I. (2008). Sea temperature. In *Marine Climate Change Impacts Annual Report Card 2007–2008*, eds. J. M. Baxter, P. J. Buckley & C. J. Wallace, Online Scientific Reviews. Lowestoft: MCCIP.
http://www.mccip.org.uk/arc/2007/Temperature.htm

Hooge, P. N., Eichenlaub, W. & Solomon, E. K. (1999). *Animal Movement Extension to ArcView, Version 2.04 Beta*. Alaska Science Center – Biological Science Office, US Geological Survey, Anchorage, Alaska.
http://www.absc.usgs.gov/glba/gistools

Hulme, M., Jenkins, G. L., Lu, X., Turnpenny, J. R., Mitchell, T. D., Jones, R. G., Lowe, J. A., Murphy, J. M., Hassell, D., Boorman, P. M., McDonald, R. & Hill, S. (2002). *Climate Change Scenarios for the United Kingdom: The UKCIP02 Scientific Report*. School of Environmental Sciences, University of East Anglia, Norwich: Tyndall Centre for Climate Change Research.

Hurrell, J. W., Kushnir, Y., Ottersen, G. & Visbeck, M. (eds.) (2003). *The North Atlantic Oscillation: Climatic Significance and Environmental Impact*. Geophysical Monograph 134. Washington, DC: American Geophysical Union.

Jamieson, L. E. & Brooks, S. P. (2004). Density dependence in North American ducks. *Animal Biodiversity and Conservation* **27.1**, 113–128.

Jardine, D. C., How, J., Clarke, J. & Clarke, P. M. (2002). Seabirds on Colonsay and Oronsay, Inner Hebrides. *Scottish Birds* **23**, 1–9.

Jenouvrier, S., Caswell, H., Barbraud, C., Holland, M., Strœve, J. & Weimerskirch, H. (2009a). Demographic models and IPCC climate projections predict the decline of an emperor penguin population. *Proceedings of the National Academy of Sciences, USA* **106**, 1844–1847.

Jenouvrier, S., Thibault, J.-C., Viallefont, A., Vidal, P., Ristow, D., Mougin, J.-L., Brichetti, P., Borg, J. J. & Bretagnolle, V. (2009b). Global climate patterns explain range-wide synchronicity in survival of a migratory seabird. *Global Change Biology* **15**, 268–279.

JNCC (2009). UK seabirds in 2008: Results from the UK Seabird Monitoring Programme.
http://www.jncc.gov.uk/page-4555

Jolly, G. M. (1965). Explicit estimates from capture-recapture data with both death and immigration-stochastic model. *Biometrika* **52**, 225–247.

Jüssi, M., Härkönen, T., Helle, E. & Jüssi, I. (2008). Decreasing ice coverage will reduce the breeding success of Baltic grey seal (*Halichoerus grypus*) females. *Ambio* **37**, 80–85.

Kalman, R. E. (1960). A new approach to linear filtering and prediction problems. *Transactions of the ASME–Journal of Basic Engineering* **82**, 35–45.

King, R. & Brooks, S. P. (2002). Model selection for integrated recovery/recapture data. *Biometrics* **58**, 841–851.

King, R. & Brooks, S. P. (2008). On the Bayesian estimation of a closed population size in the presence of heterogeneity and model uncertainty. *Biometrics* **64**, 816–824.

King, R., Brooks, S. P. & Coulson, T. (2008a). Analysing complex capture-recapture data in the presence of individual and temporal covariates and model uncertainty. *Biometrics* **64**, 1187–1195.

King, R., Brooks, S. P., Mazzetta, C., Freeman, S. N. & Morgan, B. J. T. (2008b). Identifying and diagnosing population declines: A Bayesian assessment of lapwings in the UK. *Journal of the Royal Statistical Society: Series C* **57**, 609–632.

King, R., Brooks, S. P., Morgan, B. J. T. & Coulson, T. (2006). Factors influencing Soay sheep survival: A Bayesian analysis. *Biometrics* **62**, 211–220.

King, R., Morgan, B. J. T., Gimenez, O. & Brooks, S. P. (2009). *Bayesian Analysis for Population Ecology.* London: Chapman & Hall/CRC.

Koenig, W. D. (1999). Spatial autocorrelation of ecological phenomena. *Trends in Ecology and Evolution* **14**, 22–26.

Koons, D. N., Grand, J. B. & Arnold, J. M. (2006). Population momentum across vertebrate life histories. *Ecological Modelling* **197**, 418–430.

Lebreton, J.-D., Burnham, K. P., Clobert, J. & Anderson, D. R. (1992). Modeling survival and testing biological hypotheses using marked animals: A unified approach with case studies. *Ecological Monographs* **62**, 67–118.

Lebreton, J.-D. & Clobert, J. (1991). Bird population dynamics, management, and conservation: The role of mathematical modelling. In *Bird Population Studies: Relevance to Conservation and Management*, eds. C. M. Perrins, J.-D. Lebreton & G. J. M. Hirons, pp. 105–125. Oxford: Oxford University Press.

Liebhold, A., Koenig, W. D. & Bjørnstad, O. N. (2004). Spatial synchrony in population dynamics. *Annual Review of Ecology, Evolution, and Systematics* **35**, 467–490.

Link, W. A. & Barker, R. J. (2004). Hierarchical mark-recapture models: A framework for inference about demographic processes. *Animal Biodiversity and Conservation* **27.1**, 441–449.

Link, W. A. & Barker, R. J. (2006). Model weights and the foundations of multimodel inference. *Ecology* **87**, 2626–2635.

Link, W. A. & Barker, R. J. (2009). *Bayesian Inference with Ecological Applications*. San Diego: Academic Press.

Loison, A., Sæther, B.-E., Jerstad, K. & Røstad, O. W. (2002). Disentangling the sources of variation in the survival of the European dipper. *Journal of Applied Statistics* **29**, 289–304.

Lowe, J. A., Howard, T. P., Pardaens, A., Tinker, J., Holt, J., Wakelin, S., Milne, G., Leake, J., Wolf, J., Horsburgh, K., Reeder, T., Jenkins, G. L., Ridley, J., Dye, S. & Bradley, S. (2009). *UK Climate Projections Science Report: Marine and Coastal Projections*. Exeter, UK: Met Office Hadley Centre.

MacArthur, R. H. & Wilson, E. O. (1967). *The Theory of Island Biogeography*. Princeton: Princeton University Press.

Maple 9.51 (2004). Maplesoft, a division of Waterloo Maple Inc., Waterloo, Ontario.
http://www.maplesoft.com

Maunder, M. N., Harley, S. J. & Hampton, J. (2006). Including parameter uncertainty in forward projections of computationally intensive statistical population dynamic models. *ICES Journal of Marine Science* **63**, 969–979.

Mavor, R. A., Heubeck, M., Schmitt, S. & Parsons, M. (2008). *Seabird Numbers and Breeding Success in Britain and Ireland, 2006*. Peterborough: Joint Nature Conservation Committee. (UK Nature Conservation, No. 31).

Mavor, R. A., Parsons, M., Heubeck, M. & Schmitt, S. (2005). *Seabird Numbers and Breeding Success in Britain and Ireland, 2004*. Peterborough: Joint Nature Conservation Committee. (UK Nature Conservation, No. 29).

Mavor, R. A., Parsons, M., Heubeck, M. & Schmitt, S. (2006). *Seabird Numbers and Breeding Success in Britain and Ireland, 2005*. Peterborough: Joint Nature Conservation Committee. (UK Nature Conservation, No. 30).

MCCIP (2009). Summary report. In *Marine Climate Change Ecosystem Linkages Report Card 2009*, eds. J. M. Baxter, P. J. Buckley & M. T. Frost. Lowestoft: MCCIP.
http://www.mccip.org.uk/elr

Metropolis, N., Rosenbluth, A. W., Rosenbluth, M. N., Teller, A. H. & Teller, E. (1953). Equation of state calculations by fast computing machines. *The Journal of Chemical Physics* **21**, 1087–1092.

Millar, R. B. (2004). Sensitivity of Bayes estimators to hyper-parameters with an application to maximum yield from fisheries. *Biometrics* **60**, 536–542.

Millar, R. B. & Meyer, R. (2000). Non-linear state space modelling of fisheries biomass dynamics by using Metropolis Hastings within-Gibbs sampling. *Journal of the Royal Statistical Society: Series C* **49**, 327–342.

Newman, K. B. (1998). State-space modeling of animal movement and mortality with application to salmon. *Biometrics* **54**, 1290–1314.

Newman, K. B., Fernández, C., Thomas, L. & Buckland, S. T. (2009). Monte Carlo inference for state-space models of wild animal populations. *Biometrics* **65**, 572–583.

Newton, I. (1995). Relationship between breeding and wintering ranges in Palearctic-African migrants. *Ibis* **137**, 241–249.

Newton, I. (1998). *Population Limitation in Birds*. London: Academic Press.

Nur, N., Ford, R. G. & Ainley, D. G. (1994). *Computer Model of Farallon Seabird Populations. Final Report to Gulf of the Farallones National Marine*

Sanctuary. San Fransisco: US National Oceanic and Atmospheric Administration.
http://www.prbo.org/cms/525

Nur, N. & Sydeman, W. J. (1999). Demographic processes and population dynamic models of seabirds: Implications for conservation and restoration. In *Current Ornithology*, vol. 15, eds. V. Nolan, Jr., E. D. Ketterson & C. F. Thompson, pp. 149–188. New York: Plenum Press.

Oli, M. K. & Dobson, F. S. (2003). The relative importance of life-history variables to population growth rate in mammals: Cole's prediction revisited. *The American Naturalist* **161**, 422–440.

Ozgul, A., Armitage, K. B., Blumstein, D. T. & Oli, M. K. (2006). Spatiotemporal variation in survival rates: Implications for population dynamics of yellow-bellied marmots. *Ecology* **87**, 1027–1037.

Palmqvist, E. & Lundberg, P. (1998). Population extinctions in correlated environments. *Oikos* **83**, 359–367.

Paradis, E., Baillie, S. R., Sutherland, W. J., Dudley, C., Crick, H. Q. P. & Gregory, R. D. (2000). Large-scale spatial variation in the breeding performance of song thrushes *Turdus philomelos* and blackbirds *T. merula* in Britain. *Journal of Applied Ecology* **37** (Supplement 1), 73–87.

Parsons, M., Mitchell, I., Butler, A., Ratcliffe, N., Frederiksen, M., Foster, S. & Reid, J. B. (2008). Seabirds as indicators of the marine environment. *ICES Journal of Marine Science* **65**, 1520–1526.

Peach, W. J., Siriwardena, G. M. & Gregory, R. D. (1999). Long-term changes in over-winter survival rates explain the decline of reed buntings *Emberiza schoeniclus* in Britain. *Journal of Applied Ecology* **36**, 798–811.

Peacock, J. A. (1983). Two-dimensional goodness-of-fit testing in astronomy. *Monthly Notices of the Royal Astronomical Society* **202**, 615–627.

Pledger, S., Pollock, K. H. & Norris, J. L. (2003). Open capture-recapture models with heterogeneity: I. Cormack-Jolly-Seber model. *Biometrics* **59**, 786–794.

Post, E. & Forchhammer, M. C. (2002). Synchronization of animal population dynamics by large-scale climate. *Nature* **420**, 168–171.

Press, W. H., Teukolsky, S. A., Vetterling, W. T. & Flannery, B. P. (1994). *Numerical Recipes in FORTRAN: The Art of Scientific Computing*. 2nd edn. New York: Cambridge University Press.

Punt, A. E. & Hilborn, R. (1997). Fisheries stock assessment and decision analysis: The Bayesian approach. *Reviews in Fish Biology and Fisheries* **7**, 35–63.

R Development Core Team (2008). *R: A Language and Environment for Statistical Computing*. R Foundation for Statistical Computing, Vienna, Austria. http://www.R-project.org

Reid, J. M., Bignal, E. M., Bignal, S., McCracken, D. I. & Monaghan, P. (2004). Identifying the demographic determinants of population growth rate: A case study of red-billed choughs *Pyrrhocorax pyrrhocorax*. *Journal of Animal Ecology* **73**, 777–788.

Reynolds, T. J., King, R., Harwood, J., Frederiksen, M., Harris, M. P. & Wanless, S. (2009). Integrated data analysis in the presence of emigration and mark loss. *Journal of Agricultural, Biological and Environmental Statistics* **14**, 411–431.

Ringsby, T. H., Sæther, B.-E., Altwegg, R. & Solberg, E. J. (1999). Temporal and spatial variation in survival rates of a house sparrow, *Passer domesticus*, metapopulation. *Oikos* **85**, 419–425.

Ringsby, T. H., Sæther, B.-E., Tufto, J., Jensen, H. & Solberg, E. J. (2002). Asynchronous spatiotemporal demography of a house sparrow metapopulation in a correlated environment. *Ecology* **83**, 561–569.

Robinson, R. A. (2005). *BirdFacts: Profiles of Birds Occuring in Britain and Ireland (v1.24, June 2009)*. BTO Research Report No 407. Thetford: BTO. http://www.bto.org/birdfacts

Robinson, R. A., Green, R. E., Baillie, S. R., Peach, W. J. & Thomson, D. L. (2004). Demographic mechanisms of the population decline of the song thrush *Turdus philomelos* in Britain. *Journal of Animal Ecology* **73**, 670–682.

Rockwell, R. F., Cooch, E. G. & Brault, S. (1997). Dynamics of the mid-continent population of lesser snow geese: Projected impacts of reductions in survival and fertility on population growth rate. In *Arctic Ecosystems in Peril: Report of the Arctic Goose Habitat Working Group*, ed. B. D. J. Batt,

pp. 73–100. Washington, DC: US Fish and Wildlife Service. http://www.fws.gov/migratorybirds/CurrentBirdIssues/Management/arcgoose/tblconts.html

Rockwood, L. L. (2006). *Introduction to Population Ecology*. Oxford: Blackwell.

Rodriguez, C. & Bustamante, J. (2003). The effect of weather on lesser kestrel breeding success: Can climate change explain historical population declines? *Journal of Animal Ecology* **72**, 793–810.

Royle, J. A. (2008). Modeling individual effects in the Cormack-Jolly-Seber model: A state-space formulation. *Biometrics* **64**, 364–370.

Royle, J. A. & Dorazio, R. M. (2008). *Hierarchical Modeling and Inference in Ecology: The Analysis of Data from Populations, Metapopulations, and Communities*. San Diego: Academic Press.

Royle, J. A. & Link, W. A. (2002). Random effects and shrinkage estimation in capture-recapture models. *Journal of Applied Statistics* **29**, 329–351.

Sæther, B.-E. & Bakke, Ø. (2000). Avian life history variation and contribution of demographic traits to the population growth rate. *Ecology* **81**, 642–653.

Sæther, B.-E. & Engen, S. (2002). Including uncertainties in population viability analysis using population prediction intervals. In *Population Viability Analysis*, eds. S. R. Beissinger & D. R. McCullough, pp. 191–212. Chicago: University of Chicago Press.

Sæther, B.-E., Engen, S., Islam, A., McCleery, R. H. & Perrins, C. (1998). Environmental stochasticity and extinction risk in a population of small songbird, the great tit. *The American Naturalist* **151**, 441–450.

Sæther, B.-E., Grøtan, V., Engen, S., Noble, D. G. & Freckleton, R. P. (2009). Critical parameters for predicting population fluctuations of some British passerines. *Journal of Animal Ecology* **78**, 1063–1075.

Sæther, B.-E., Grøtan, V., Tryjanowski, P., Barbraud, C., Engen, S. & Fulin, M. (2006). Climate and spatio-temporal variation in the population dynamics of a long distance migrant, the white stork. *Journal of Animal Ecology* **75**, 80–90.

Sæther, B.-E., Lillegård, M., Grøtan, V., Filli, F. & Engen, S. (2007). Predicting fluctuations of reintroduced ibex populations: The importance of density-dependence, environmental stochasticity and uncertain population estimates. *Journal of Animal Ecology* **76**, 326–336.

Sandvik, H., Erikstad, K. E., Barrett, R. T. & Yoccoz, N. G. (2005). The effect of climate on adult survival in five species of North Atlantic seabirds. *Journal of Animal Ecology* **74**, 817–831.

Schaub, M., Gimenez, O., Sierro, A. & Arlettaz, R. (2007). Use of integrated modeling to enhance estimates of population dynamics obtained from limited data. *Conservation Biology* **21**, 945–955.

Schaub, M., Kania, W. & Köppen, U. (2005). Variation of primary production during winter induces synchrony in survival rates in migratory white storks *Ciconia ciconia*. *Journal of Animal Ecology* **74**, 656–666.

Schwarz, C. J. & Seber, G. A. F. (1999). Estimating animal abundance: Review III. *Statistical Science* **14**, 427–456.

Scottish Natural Heritage (2006). Isle of May National Nature Reserve: Seabirds [online]. Accessed 02 October 2009 at `http://www.snh.org.uk/VirtualTours/IsleOfMay/main.html`.

Seber, G. A. F. (1965). A note on the multiple recapture census. *Biometrika* **52**, 249–259.

Siriwardena, G. M., Wernham, C. V. & Baillie, S. R. (2004). Quantifying variation in migratory strategies using ring-recoveries. *Animal Biodiversity and Conservation* **27.1**, 299–317.

Skalski, J. R., Hoffman, A. & Smith, S. G. (1993). Testing the significance of individual and cohort level covariates in animal survival studies. In *Marked Individuals in the Study of Bird Population*, eds. J.-D. Lebreton & P. M. North. Basle: Birkhäuser Verlag.

Smith, G. C., Parrott, D. & Robertson, P. A. (2008). Managing wildlife populations with uncertainty: Cormorants *Phalacrocorax carbo*. *Journal of Applied Ecology* **45**, 1675–1682.

Solomon, S., Qin, D., Manning, M., Chen, Z., Marquis, M., Averyt, K. B., Tignor, M. & Miller, H. L. (eds.) (2007). *Climate Change 2007: The Physical*

Science Basis. Contribution of Working Group I to the Fourth Assessment Report of the Intergovernmental Panel on Climate Change. Cambridge and New York: Cambridge University Press.

Spiegelhalter, D. J., Thomas, A., Best, N. G. & Lunn, D. (2007). *WinBUGS User Manual, Version 1.4.3*. MRC Biostatistics Unit, Cambridge. http://www.mrc-bsu.cam.ac.uk/bugs

Stenseth, N. C., Ottersen, G., Hurrell, J. W., Mysterud, A., Lima, M., Chan, K.-S., Yoccoz, N. G. & Ådlandsvik, B. (2003). Studying climate effects on ecology through the use of climate indices: The North Atlantic Oscillation, El Niño Southern Oscillation and beyond. *Proceedings of the Royal Society of London: Series B* **270**, 2087–2096.

Stephens, P. A., Frey-Roos, F., Arnold, W. & Sutherland, W. J. (2002). Model complexity and population predictions. The alpine marmot as a case study. *Journal of Animal Ecology* **71**, 343–361.

Swann, R. L. (2004). Seabird wreck, north west Scotland late summer 2004. *The Seabird Group Newsletter* **98**, 12–13.

Swann, R. L. (2005). *Canna Seabird Studies 2005*. Unpublished report to JNCC.

Swann, R. L. (2006). *Canna Seabird Studies 2004*. Peterborough: Joint Nature Conservation Committee. (JNCC Report No. 376). http://www.jncc.gov.uk/default.aspx?page=3637

Tavecchia, G., Besbeas, P., Coulson, T., Morgan, B. J. T. & Clutton-Brock, T. H. (2009). Estimating population size and hidden demographic parameters with state-space modeling. *The American Naturalist* **173**, 722–733.

Taylor, B. L., Wade, P. R., Stehn, R. A. & Cochrane, J. F. (1996). A Bayesian approach to classification criteria for spectacled eiders. *Ecological Applications* **6**, 1077–1089.

Thomas, L., Buckland, S. T., Newman, K. B. & Harwood, J. (2005). A unified framework for modelling wildlife population dynamics. *Australian and New Zealand Journal of Statistics* **47**, 19–34.

Trenkel, V. M., Elston, D. A. & Buckland, S. T. (2000). Fitting population dynamics models to count and cull data using sequential importance sampling. *Journal of the American Statistical Association* **95**, 363–374.

Tuljapurkar, S. (1990). *Population Dynamics in Variable Environments*. New York: Springer-Verlag.

Turchin, P. (2003). *Complex Population Dynamics: A Theoretical/Empirical Synthesis*. Princeton: Princeton University Press.

Véran, S. & Lebreton, J.-D. (2008). The potential of integrated modelling in conservation biology: A case study of the black-footed albatross (*Phoebastria nigripes*). *The Canadian Journal of Statistics* **36**, 85–98.

Votier, S. C., Birkhead, T. R., Oro, D., Trinder, M., Grantham, M. J., Clark, J. A., McCleery, R. H. & Hatchwell, B. J. (2008). Recruitment and survival of immature seabirds in relation to oil spills and climate variability. *Journal of Animal Ecology* **77**, 974–983.

Votier, S. C., Hatchwell, B. J., Beckerman, A., McCleery, R. H., Hunter, F. M., Pellatt, J., Trinder, M. & Birkhead, T. R. (2005). Oil pollution and climate have wide-scale impacts on seabird demographics. *Ecology Letters* **8**, 1157–1164.

Wade, P. R. (2000). Bayesian methods in conservation biology. *Conservation Biology* **14**, 1308–1316.

Wanless, S., Harris, M. P., Redman, P. & Speakman, J. R. (2005). Low energy values of fish as a probable cause of a major seabird breeding failure in the North Sea. *Marine Ecology Progress Series* **294**, 1–8.

White, G. C. & Burnham, K. P. (1999). Program MARK: Survival estimation from populations of marked animals. *Bird Study* **46** (Supplement), 120–138.

Williams, B. K., Nichols, J. D. & Conroy, M. J. (2002). *Analysis and Management of Animal Populations*. San Diego: Academic Press.